MONASH University

Adaptive Reception-Transmission Scheduling in Wireless Networks

Mohsen Mohammadkhani Razlighi
M. Sci., Sharif University, 2012
B. Sci., Zanjan University, 2010

A thesis submitted for the degree of *Doctor of Philosophy* at
Monash University in 2020
Department of Electrical and Computer System Engineering

Copyright Notice

Notice 1

Abstract

In a general network comprised of many nodes, a node can either receive, transmit, or simultaneously receive and transmit. In this research, we aim to find the optimal state of each node (receive, transmit, or simultaneously receive and transmit), based on knowledge of global/local fading channel gains, such that the performance of the network is optimized. The problem that this research aims to tackle is very difficult in general. As a result, to gain insight, we first investigate a simple three-node network. This three-node network can represent a source, a relay, and a destination, or two mobile users with a base stations (BS). For the considered three-node network, we propose optimal adaptive reception-transmission scheduling of the nodes which maximizes the performance of the considered three-node network. Next, we turn to the general network comprised of many nodes and propose optimal adaptive reception-transmission scheduling of the nodes which maximizes the performance of the network. Our numerical results show that significant performance gains are achieved using the proposed scheduling schemes compared to existing schemes.

Publications During Enrolment

The following publications have arisen from the research reported in this thesis.

1 M. Mohammadkhani Razlighi and N. Zlatanov, "Buffer-Aided Relaying For The Two-Hop Full-Duplex Relay Channel With Self-Interference," in IEEE Transactions on Wireless Communications, vol. 17, no. 1, pp. 477-491, Jan. 2018.

2 M. M. Razlighi, N. Zlatanov and P. Popovski, "Dynamic Time-Frequency Division Duplex," in IEEE Transactions on Wireless Communications, vol. 19, no. 5, pp. 3118-3132, May 2020.

3 M. M. Razlighi, N. Zlatanov, S. R. Pokhrel and P. Popovski, "Optimal Centralized Dynamic-Time-Division-Duplex," in IEEE Transactions on Wireless Communications, doi: 10.1109/TWC.2020.3022990.

4 M. M. Razlighi and N. Zlatanov, "On Buffer-Aided Relaying for the Two-Hop Full Duplex Relay Channel with Self-Interference," GLOBECOM 2017 - 2017 IEEE Global Communications Conference, Singapore, 2017, pp. 1-7.

5 M. M. Razlighi, N. Zlatanov and P. Popovski, "On Distributed Dynamic-TDD Schemes for Base Stations with Decoupled Uplink-Downlink Transmissions," 2018 IEEE International Conference on Communications Workshops (ICC Workshops), Kansas City, MO, 2018, pp. 1-6.

6 M. M. Razlighi, N. Zlatanov and P. Popovski, "Optimal Centralized Dynamic-TDD Scheduling Scheme for a General Network of Half-Duplex Nodes,"

2019 IEEE Wireless Communications and Networking Conference (WCNC), Marrakesh, Morocco, 2019, pp. 1-6.

Thesis Including Published Works Declaration

This thesis includes 3 original papers published in peer reviewed journals. The ideas, development and writing up of all the papers in the thesis were the principal responsibility of myself, the student, working within the Department of Electrical and Computer Systems Engineering under the supervision of Dr. Nikola Zlatanov.

The inclusion of co-authors reflects the fact that the work came from active collaboration between researchers and acknowledges input into team-based research.

My contribution to the work involved the following:

Thesis Chapter	Publication Title	Status (published, in press, accepted or returned for revision, submitted)	Nature and % of student contribution	Co-author name(s) Nature and % of Co-author's contribution	Co-author(s), Monash student Y/N
2	Buffer-Aided Relaying For The Two-Hop Full-Duplex Relay Channel With Self-Interference	Published	75 %. Deriving the results, numerical evaluation of the results, and writing the paper.	Nikola Zlatanov, input into the system model and the manuscript 25 %	N
3	Dynamic Time-Frequency Division Duplex	Published	75 %. Deriving the results, numerical evaluation of the results, and writing the paper.	Nikola Zlatanov, input into the system model and the manuscript 20 %; Petar Popovski, input into manuscript 5 %	N; N

4	Optimal centralized dynamic-time-division-duplex transmission-reception scheduling scheme for a general network of half-duplex nodes	Published	75 %. Defining the system model, deriving the results, numerical evaluation of the results, writing the paper.	Nikola Zlatanov, input into the system model and the manuscript 15 %; Petar Popovski, input into manuscript 5 %; Shiva Pekhrol, input into manuscript 5 %,	N; N; N

I have not renumbered sections of published papers in order to generate a consistent presentation within the thesis.

Student name: Mohsen Mohammadkhani Razlighi

Student signature: **Date:**

I hereby certify that the above declaration correctly reflects the nature and extent of the student's and co-authors' contributions to this work. In instances where I am not the responsible author I have consulted with the responsible author to agree on the respective contributions of the authors.

Main Supervisor name: Dr. Nikola Zlatanov

Main Supervisor signature: **Date:**

Acknowledgements

First and foremost I wish to thank my supervisor, Dr. Nikola Zlatanov. He gave me kind support and help in many areas, discussed several ideas with me, and prevented many wrong turns. And secondly, but importantly, to my wife, Fatemeh, who has stood by my side as always all the way from Iran to here, Australia. She gave me love, support, and happiness. I would also thank my father Vali, my mother Soraya, who taught me how to live and succeed. Thanks also to all my friends at ECSE of Monash University.

To my wife Fatemeh.

Table of Contents

Chapter 1

Introduction

In a general network comprised of many nodes, a node can either receive, transmit, or simultaneously receive and transmit. In this research, we aim to find the optimal state of each node (receive, transmit, or simultaneously receive and transmit), based on knowledge of global/local fading channel gains, such that the performance of the network is optimized. The problem that this research aims to tackle is very difficult in general. As a result, to gain insight, we first investigate a simple three-node network. This three-node network can represent a source, a relay, and a destination, or two mobile users with a base stations (BS). For the considered three-node network, we propose optimal adaptive reception-transmission scheduling of the nodes which maximizes the performance of the considered three-node network. Next, we turn to the general network comprised of many nodes and propose optimal adaptive reception-transmission scheduling of the nodes which maximizes the performance of the network.

Network nodes which can receive, transmit, or simultaneously receive and transmit in the same frequency band are known to operate in the full-duplex (FD) mode. However, due to the in-band simultaneous reception-transmission, FD nodes are impaired by self-interference (SI), which occurs due to leakage of energy from the transmitter-end into the receiver-end of the FD node. The self-interference impairs the decoding of the received information signal significantly. On the other hand, a node which cannot simultaneously transmit and receive in the same frequency band, and can either transmit or receive is known to operate in the half-

duplex (HD) mode. HD nodes avoid the creation of SI.

Using the HD and FD terms, in this research we will investigate the following networks:
-an HD source (S), an FD relay, and an HD destination (D);
-two HD mobile users (U1 and U2) with an HD base stations (BS1);
-general network comprised of many HD nodes;

1.1 Full-Duplex Buffer-Aided Relaying

Relays play an important role in wireless communications for increasing the data rate between a source and a destination [1]. Therefore, one of the first immediate applications of FD technology is expected to be in the deployment of FD relays which would provide support to HD BSs. In particular, the idea is to deploy FD relays around HD BSs, which will relay information from the HD BSs to users that are at significant distances from the base stations. The system model resulting from such a scenario is the two-hop FD relay channel, which is comprised of a source, an FD relay, and a destination, where a direct source-destination link does not exist due to the assumed large distance between the source and the destination.

The two-hop relay channel with and without fading has been extensively investigated in the literature both for HD relaying as well as FD relaying with and without SI [2, 3], where the reception and transmission scheduling was performed in a prefixed manner. On the other hand, [4] proposed a buffer-aided relaying scheme where, in each time slot, the HD relay selects to either receive or transmit based on the qualities of the receiving and transmitting channels, showing that buffers improve the performance of HD relays. However, for two-hop FD relay channel, only the capacity with an idealized FD relay without SI was derived in [1], and achievable rates for the two-hop FD relay channel with SI and fading are known for only certain special cases, such as an SI channel not impaired by fading, see [5, 6].

Motivated by the lack of advanced schemes for the general two-hop FD relay channel with SI and fading, in chapter 2, we investigate this channel and propose novel achievable rates/throughputs. The novel rates/throughputs are achieved using buffer-aided relaying. Thereby, similar to HD relays, we show that buffers

also improve the performance of FD relays with SI. This means that buffer-aided relaying should become an integral part of FD relaying systems around HD base stations in order to increase their performance significantly.

1.2 Dynamic Time-Frequency Division Duplex

Traditionally, a half-duplex (HD) base station (BS) operates in either the time-division duplex (TDD) mode or the frequency-division duplex (FDD) mode in order to receive and transmit information from/to its users. In the TDD mode, a user uses the same frequency band for uplink and downlink, while uplink and downlink transmissions occur in different time slots [7]. On the other hand, in the FDD mode, a user is allocated two frequency bands, one dedicated for uplink and the other one for downlink, where the uplink and downlink transmissions occur simultaneously [7].

The duplexing mode, either TDD or FDD between a BS and its users can be static or dynamic. In static duplexing, the time-frequency resources in which the BS performs uplink receptions and downlink transmissions from/to the user are prefixed and unchangeable over time [8]. On the other hand, in dynamic duplexing schemes, each time-frequency resource unit can be dynamically allocated either for uplink-reception or for downlink-transmission based on the instantaneous channel state information (CSI). As a result, dynamic duplexing schemes achieve a much better performance compared to static duplexing schemes [9, 10], and thereby have attracted significant research interest [9–13].

A dynamic duplexing scheme can be implemented in either centralized or distributed fashion [11]. In centralized dynamic duplexing schemes, the decision for allocating the time-frequency resource for uplink-reception or for downlink-transmission is performed at a central node, which then informs all BSs about the decision. In this way, the uplink receptions and the downlink transmissions between neighbouring cells can be synchronized in order to minimize inter-cell interference (ICI) [12–22]. However, centralized dynamic duplexing schemes cost a large amount of signaling information to be exchanged between the central node and all other network nodes, which makes it infeasible in practice for most cases.

In chapter 3, we introduce dynamic time-frequency-division duplex (D-TFDD),

which is a novel duplexing scheme. In D-TFDD, a user receives from the BS on the downlink in one frequency band and transmits to the BS on the uplink in another frequency band, as in FDD. Next, the user shares the uplink (downlink) transmission (reception) on the corresponding frequency band with the downlink (uplink) reception (transmission) of another user in a D-TDD fashion. Hence, in a given frequency band, the BS receives on the uplink from user 1 in one time slot and transmits to user 2 in a different time slot. We propose optimal distributed D-TFDD schemes for the cases when the ICI is known and unknown at the receiving nodes. For both cases, the proposed D-TFDD schemes increase the uplink-downlink throughput region of the BS/users and significantly decrease the outage probabilities on both the uplink and downlink channels. Most importantly, the proposed D-TFDD schemes double the diversity gain on both the uplink and downlink channels compared to the diversity gain of existing D-TDD schemes, which results in significant performance gains. Besides, one of the prominent aspects of fifth generation (5G) mobile networks is having a flexible physical layer design. In one hand, this capability facilitates implementing challenging physical layer protocols, and on the other hand opens the door for unconventional schemes to be implemented on the physical layer. Such a flexible hardware-software design can easily accommodate our D-TFDD scheme and thereby improve the performance of 5G networks [23]. In addition, distributed resource allocation for dense heterogeneous wireless networks is in one of the main scopes of 5G [23], which also fits well with our D-TFDD scheme. Moreover, proposed scheme is applicable to multi-tier multi-cell systems, which is another feature of 5G networks.

1.3 Adaptive Reception-Transmission Schedule at Network Nodes of a General Network

In a general network comprised of HD and FD nodes, we aim to find the optimal state of the nodes (receive or transmit or simultaneously receive and transmit), based on the local/global CSI knowledge, such that the performance of the network is optimized. Given a general network of many nodes causes severe interference on the receiver nodes. However, considering the full-CSI knowledge of the general network can be used to devise the optimum policy for assigning nodes of the net-

work to work optimally either in downlink or in the uplink in each time slot, which has been gained interest recently [10, 24–28].

The distributed scheme investigated in chapter 3 does not maximize the overall network performance. In Chapter 4, we investigate a centralized D-TDD scheme, which induces excessive overhead and thus not practical for implementation. However, knowing the performance of the optimal centralized D-TDD scheme is highly valuable since it serves as an upper bound and thus an (unattainable) benchmark for any practical TDD scheme. The optimal centralized D-TDD scheme for a general network is an open problem. Motivated by this, in Chapter 4 we derive the optimal centralized D-TDD scheme for a general network.

Centralized D-TDD schemes are investigated in [12, 13, 16, 29–31]. The works in [29–31] propose non-optimal heuristic centralized scheduling schemes. The work in [13] proposes a centralized D-TDD scheme for a general network where the decisions for transmission and reception at the nodes are chosen from a finite and predefined set of configurations, which is not optimal in general and may limit the network performance. A network comprised of two-way links is investigated in [16], where each link can be used either for transmission or reception in a given time slot, with the aim of optimising the direction of the two-way links in each time slot. However, the difficulty of the problem in [16] also leads to a sub-optimal solution being proposed. The work in [12] investigates a general network, where the nodes can select to transmit, receive, or be silent in a given time slot. However, the proposed solution in [12] is again sub-optimal due to the difficulty of the investigated problem. On the other hand, [21, 32] investigate centralized D-TDD schemes for a general network comprised of FD nodes, which both have proposed a non-optimal solution due to the complexity of the problem.

To the best of our knowledge, the optimal centralized D-TDD scheme for a general network comprised of FD or HD nodes is an open problem in the literature. As a result, in Chapter 4 , we derive the optimal centralized D-TDD scheme for a general network comprised of FD nodes. In particular, we derive the optimal scheduling of the reception, transmission, simultaneous reception and transmission, or silence at every FD node in a given time slot such that the rate-region of the network is maximized. In addition, as a special case, we also derive the optimal centralized D-TDD scheme for a network comprised of HD nodes. Our numeri-

cal results show that the proposed optimal centralized D-TDD scheme achieves significant gains over existing centralized D-TDD schemes.

Chapter 2

Buffer-Aided Relaying For The Two-Hop Full-Duplex Relay Channel With Self-Interference

The preliminary results have been published in the IEEE GLOBECOM, Singapore, 2017.

- M. M. Razlighi and N. Zlatanov, "On Buffer-Aided Relaying for the Two-Hop Full Duplex Relay Channel with Self-Interference," IEEE GLOBECOM, Singapore, 2017.

The complete research, which includes detailed theorems and their proofs have been published in the IEEE Transactions on Wireless Communications, vol. 17, no. 1, pp. 477-491, Jan. 2018., which included in this chapter.

- M. Mohammadkhani Razlighi and N. Zlatanov, "Buffer-Aided Relaying For The Two-Hop Full-Duplex Relay Channel With Self-Interference," in IEEE Transactions on Wireless Communications, vol. 17, no. 1, pp. 477-491, Jan. 2018.

Buffer-Aided Relaying For The Two-Hop Full-Duplex Relay Channel With Self-Interference

Mohsen Mohammadkhani Razlighi, *Student Member, IEEE*, and Nikola Zlatanov, *Member, IEEE*

***Abstract*— In this paper, we investigate the fading two-hop full-duplex (FD) relay channel with self-interference, which is comprised of a source, an FD relay impaired by self-interference, and a destination, where a direct source-destination link does not exist. For this channel, we propose three buffer-aided relaying schemes with adaptive reception-transmission at the FD relay for the cases when the source and the relay both perform continuous-rate transmission with adaptive-power allocation, continuous-rate transmission with fixed-power allocation, and discrete-rate transmission, respectively. The proposed buffer-aided relaying schemes enable the FD relay to adaptively select to either receive, transmit, or simultaneously receive and transmit in a given time slot based on the qualities of the receiving, transmitting, and self-interference channels, a degree-of-freedom unavailable without buffer-aided relaying. Our numerical results show that significant performance gains are achieved using the proposed buffer-aided relaying schemes compared with conventional FD relaying, where the FD relay is forced to always simultaneously receive and transmit, and to buffer-aided half-duplex relaying, where the half-duplex relay cannot simultaneously receive and transmit. The main implication of this paper is that FD relaying systems without buffer-aided relaying miss-out on significant performance gains.**

***Index Terms*— Buffer-aided relaying, full-duplex, self-interference.**

I. Introduction

RELAYS play an important role in wireless communications for increasing the data rate and/or the reliability between a source and a destination [1]. In general, the relay can operate in two different modes, namely, full-duplex (FD) mode and half-duplex (HD) mode. In the FD mode, transmission and reception at the FD relay can occur simultaneously and in the same frequency band. However, due to the in-band simultaneous reception and transmission, FD relays are impaired by self-interference (SI), which occurs due to leakage of energy from the transmitter-end into the receiver-end of the FD relay. Currently, there are advanced hardware designs which can suppress the SI by about 110 dB in certain scenarios, see [2]. Because of this, FD relaying with SI is gaining considerable research interest [2], [3]. On the other hand, in the HD mode, transmission and reception take place in the same frequency band but in different time slots, or in the same time slot but in different frequency bands. As a result, HD relays avoid the creation of SI. However, since an FD relay uses twice the resources compared to an HD relay, the achievable data rates of an FD relaying system may be significantly higher than that of an HD relaying system.

One of the first immediate applications of FD relaying is expected to be in providing support to HD base stations. In particular, the idea is to deploy FD relays around HD base stations, which will relay information from the HD base stations to users that are at significant distances from the base stations. The system model resulting from such a scenario is the two-hop FD relay channel, which is comprised of a source, an FD relay, and a destination, where a direct source-destination link does not exist due to the assumed large distance between the source and the destination. In this paper, we will investigate new achievable rates/throughputs for this system model, i.e, for the two-hop FD relay channel with SI and links impaired by fading.

The two-hop relay channel with and without fading has been extensively investigated in the literature both for HD relaying as well as FD relaying with and without SI. In particular, the capacity of the two-hop HD relay channel without fading was derived in [4]. On the other hand, for the two-hop HD relay channel with fading, [5] proposed a conventional decode-and-forward (DF) relaying scheme, where the HD relay switches between reception and transmission in a prefixed manner, and [6] proposed a buffer-aided relaying scheme where, in each time slot, the HD relay selects to either receive or transmit based on the qualities of the receiving and transmitting channels. As a result, the rate achieved by the scheme in [6] is larger than the rate achieved by the scheme in [5], showing that buffers improve the performance of HD relays. The capacity of the two-hop FD relay channel with an idealized FD relay without SI was derived in [1] and [5] for the cases with and without fading, respectively. Recently, the capacity of the Gaussian two-hop FD relay channel with SI and without fading was derived in [7]. However, for the two-hop FD relay channel with SI and fading achievable rates are known for only certain special cases, such as an SI channel not impaired by fading, see [8].

Motivated by the lack of advanced schemes for the general two-hop FD relay channel with SI and fading, in this paper,

Manuscript received April 4, 2017; revised August 15, 2017 and October 5, 2017; accepted October 22, 2017. Date of publication November 3, 2017; date of current version January 8, 2018. This paper was presented at the IEEE Globecom 2017. The associate editor coordinating the review of this paper and approving it for publication was C. Lee. *(Corresponding author: Mohsen Mohammadkhani Razlighi.)*

The authors are with the Department of Electrical and Computer Systems Engineering, Monash University, Melbourne, VIC 3800, Australia (e-mail: mohsen.mohammadkhanirazlighi@monash.edu; nikola.zlatanov@monash.edu).

Color versions of one or more of the figures in this paper are available online at http://ieeexplore.ieee.org.

Digital Object Identifier 10.1109/TWC.2017.2767582

we investigate this channel and propose novel achievable rates/throughputs. The novel rates/throughputs are achieved using buffer-aided relaying. Thereby, similar to HD relays, we show that buffers also improve the performance of FD relays with SI. This means that buffer-aided relaying should become an integral part of FD relaying systems, i.e., that FD relaying systems without buffer-aided relaying miss-out on significant performance gains.

The proposed novel buffer-aided relaying schemes for the two-hop FD relay channel with SI and fading enable the FD relay to *select adaptively either to receive, transmit, or simultaneously receive and transmit in a given time slot* based on the qualities of the receiving, transmitting, and SI channels such that the achievable data rate/throughput is maximized. Note that such a degree of freedom is *not available* if a buffer is not employed. Specifically, we propose three buffer-aided relaying schemes with adaptive reception-transmission at the FD relay, for the cases when both the source and the relay perform continuous-rate transmission with adaptive-power allocation, continuous-rate transmission with fixed-power allocation, and discrete-rate transmission, respectively. The proposed buffer-aided schemes significantly improve the achievable rate/throughput of the considered relay channel compared to existing schemes. In particular, our numerical results show that significant performance gains are achieved using the proposed buffer-aided relaying schemes compared to *conventional FD relaying*, where the FD relay is forced to always simultaneously receive and transmit, and to buffer-aided HD relaying, where the HD relay cannot simultaneously receive and transmit.

Buffer-aided relaying schemes are widely investigated in [6], [8]–[29] and references therein. Most of these works investigate only HD buffer-aided relaying systems, see [6], [13], [16]–[28]. From the works related to FD buffer-aided relaying, [11], [12], [14] investigate relay channels with a direct link between the source and the destination. However, the proposed FD buffer-aided relaying schemes in [11], [12], [14] transform to the conventional FD relaying scheme if the direct link between the source and the destination becomes unavailable. Hence, the proposed FD buffer-aided schemes in in [11], [12], and [14] are not optimal. On the other hand, [15] proposes FD buffer-aided schemes for relaying systems with multiple antennas. However, the proposed FD buffer-aided schemes in [15] are also not optimal.

Optimal FD buffer-aided relaying schemes were in [9], [10], and [29]. However, the authors in [9] assumed that the SI at the FD relay is neglectable, which may not be a realistic model in practice. Similarly, the work in [10] investigates a FD relay channel where the SI channel is not impaired by fading (i.e., does not vary with time), which also may not be an accurate model of the SI channel. In particular, in practical wireless communications, due to the movement of objects/reflections, the SI channel is impaired by fading and thereby varies with time. As a result, the proposed FD buffer-aided relaying schemes in [10] are not optimal to the practical scenario when the SI channel is impaired by fading and therefore perform very poorly for that scenario. Contrary to [10], in this paper, the SI channel is assumed to be impaired by fading, and thereby the proposed FD buffer-aided relaying schemes in this paper significantly outperform the FD buffer-aided relaying schemes proposed in [10]. On the other hand, the authors in [29] propose an optimal FD buffer-aided relaying scheme for the case when the source and the relay transmit with a single fixed-rate. However, in practice, wireless transmitters do not usually transmit with a single rate nor with a continuous-rate, but rather select their rate adaptively from a set of discrete-rates. To investigate this practical discrete-rate scenario, in this paper, we propose optimal FD buffer-aided relaying schemes for the case when both the source and the relay select their transmission rates from sets of discrete rates.

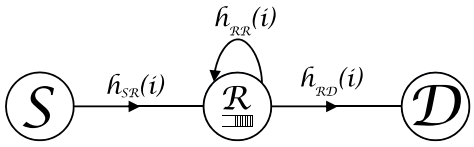

Fig. 1. Relaying system, comprised of a source, S, an FD relay impaired by SI, R, and a destination, D, where a direct S-D link is not available.

This paper is organized as follows. In Section II, we present the system and channel models. In Section III, we formulate a general FD buffer-aided relaying scheme with adaptive reception-transmission at the FD relay. In Section IV, we propose optimal buffer-aided relaying schemes for the cases when both the source and the relay transmit with continuous-rates, and with adaptive- and fixed-power allocation. Optimal buffer-aided relaying schemes for the considered relay channel with discrete-rate transmission is derived in Section V. Simulation and numerical results are provided in Section VI, and the conclusions are drawn in Section VII.

II. System and Channel Models

We consider the two-hop FD relay channel, which is comprised of a source, S, an FD relay impaired by SI, R, and a destination, D, where a direct S-D link does not exist, cf. Fig. 1. In addition, we assume that the FD relay is a DF relay equipped with a sufficiently large buffer in which it can store incoming data and from which it can extract data for transmission to the destination.

A. Channel Model

We assume that the S-R and R-D links are complex-valued additive white Gaussian noise (AWGN) channels impaired by slow fading. Furthermore, similar to the majority of related papers [30], [31], we also assume that the SI channel is impaired by slow fading. Thereby, the SI channel also varies with time. We assume that the transmission time is divided into $N \to \infty$ time slots. Furthermore, we assume that the fading is constant during one time slot and changes from one time slot to the next. Let $h_{SR}(i)$ and $h_{RD}(i)$ denote the complex-valued fading gains of the S-R and R-D channels in time slot i, respectively, and let $h_{RR}(i)$ denote the complex-valued fading gain of the SI channel in time slot

i. Moreover, let $\sigma^2_{n_R}$ and $\sigma^2_{n_D}$ denote the variances of the complex-valued AWGNs at the relay and the destination, respectively. For convenience, and without loss of generality, we define normalized squared fading gains for the S-R, R-D, and SI channels as $\gamma_{SR}(i) = |h_{SR}(i)|^2/\sigma^2_{n_R}$, $\gamma_{RD}(i) = |h_{RD}(i)|^2/\sigma^2_{n_D}$, and $\gamma_{RR}(i) = |h_{RR}(i)|^2/\sigma^2_{n_R}$, respectively. Let $P_S(i)$ and $P_R(i)$ denote the transmit powers of the source and the relay in time slot i, respectively. We assume that the SI, which is received via the SI channel in any symbol interval of time slot i, is independent and identically distributed (i.i.d.) according to the zero-mean Gaussian distribution with variance $P_R(i)|h_{RR}(i)|^2$, an assumption similar to the majority of related works [30]–[33]. This assumption is realistic due to the combined effect of various sources of imperfections in the SI cancellation process, and can also be considered as the worst-case scenario of SI [34]. As a result, in time slot i, the S-R channel is a complex-valued AWGN channel with channel gain $h_{SR}(i)$ and noise variance $P_R(i)|h_{RR}(i)|^2 + \sigma^2_{n_R}$. Hence, the capacity of this channel in time slot i is obtained as

$$C_{SR}(i) = \log_2\left(1 + \frac{P_S(i)\gamma_{SR}(i)}{P_R(i)\gamma_{RR}(i) + 1}\right). \tag{1}$$

On the other hand, in time slot i, the R-D channel is also a complex-valued AWGN channel with channel gain $h_{RD}(i)$ and noise variance $\sigma^2_{n_D}$. Hence, the capacity of this channel in time slot i is obtained as

$$C_{RD}(i) = \log_2\left(1 + P_R(i)\gamma_{RD}(i)\right). \tag{2}$$

In time slot i, we assume that the source and the relay transmit codewords encoded with a capacity achieving code, i.e., codewords comprised of $n \to \infty$ symbols that are generated independently from complex-valued zero-mean Gaussian distributions with variances $P_S(i)$ and $P_R(i)$, respectively. The data rates of the codewords transmitted from the source and the relay in time slot i are denoted by $R_{SR}(i)$ and $R_{RD}(i)$, respectively. The values of $R_{SR}(i)$ and $R_{RD}(i)$ will be defined later on.

III. General FD Buffer-Aided Relying

In this section, we formulate a general FD buffer-aided relaying scheme with adaptive reception-transmission at the FD relay.

A. Problem Formulation

Depending on whether the source and/or the relay are silent, we have four different states for the considered two-hop FD relay channel with SI in each time slot:

- *State 0:* S and R are both silent.
- *State 1:* S transmits and R receives without transmitting.
- *State 2:* R transmits and S is silent.
- *State 3:* S transmits and R simultaneously receives and transmits.

To model these four states, we define three binary variables for time slot i, $q_1(i)$, $q_2(i)$, and $q_3(i)$, as

$$q_1(i) = \begin{cases} 1 & \text{if S transmits and R receives without} \\ & \text{transmitting in time slot } i \\ 0 & \text{otherwise,} \end{cases} \tag{3}$$

$$q_2(i) = \begin{cases} 1 & \text{if R transmits and S is silent in time} \\ & \text{slot } i \\ 0 & \text{otherwise,} \end{cases} \tag{4}$$

$$q_3(i) = \begin{cases} 1 & \text{if S transmits and R simultaneously} \\ & \text{receives and transmits in time slot } i \\ 0 & \text{otherwise.} \end{cases} \tag{5}$$

Since the two-hop FD relay channel can be in one and only one of the four states in time slot i, the following has to hold

$$q_1(i) + q_2(i) + q_3(i) \in \{0, 1\}, \tag{6}$$

where if $q_1(i) + q_2(i) + q_3(i) = 0$ occurs, it means that the system is in State 0, i.e., both S and R are silent in time slot i.

To generalize the FD buffer-aided relaying scheme even further, we assume different transmit powers at the source and the relay during the different states. In particular, let $P_S^{(1)}(i)$ and $P_S^{(3)}(i)$ denote the powers of the source when $q_1(i) = 1$ and $q_3(i) = 1$, respectively, and let $P_R^{(2)}(i)$ and $P_R^{(3)}(i)$ denote the powers of the relay when $q_2(i) = 1$ and $q_3(i) = 1$, respectively. Obviously, $P_S^{(1)}(i) = 0$, $P_R^{(2)}(i) = 0$, and $P_S^{(3)}(i) = P_R^{(3)}(i) = 0$ when $q_1(i) = 0$, $q_2(i) = 0$, and $q_3(i) = 0$ hold, respectively.

In the following sections, we provide the optimal values for the state selection variables $q_k(i)$, $\forall k$, which maximize the achievable rate and the throughput of the considered relay channel. To this end, we define the following auxiliary optimal state selection scheme

$$\text{Optimal Scheme} = \begin{cases} q_1(i) = 1 & \text{if } \Lambda_1(i) > \Lambda_3(i) \\ & \text{and } \Lambda_1 \geq \Lambda_2(i) \\ q_2(i) = 1 & \text{if } \Lambda_2(i) > \Lambda_3(i) \\ & \text{and } \Lambda_2 > \Lambda_1(i) \\ q_3(i) = 1 & \text{if } \Lambda_3(i) \geq \Lambda_1(i) \\ & \text{and } \Lambda_3 \geq \Lambda_2(i), \end{cases} \tag{7}$$

where $\Lambda_1(i)$, $\Lambda_2(i)$, and $\Lambda_3(i)$ will be defined later on, cf. Theorems 1 to 3.

IV. Buffer-Aided Relaying With Continuous-Rate Transmission

In this section, we provide buffer-aided relaying schemes for the case when both the source and the relay are able to adapt their transmission rates to the underlying channels in each time slot without any limitation on the values of the transmission rates. Thereby, we provide two buffer-aided relaying schemes with continuous-rate transmission; one in which both the source and the relay also adapt their transmit powers to the underlying channels in each time slot, and the other one in which both the source and the relay transmit with fixed-powers in each time slot.

A. Problem Formulation for Buffer-Aided Relaying With Continuous-Rate Transmission

Using the state selection variables $q_k(i)$, $\forall k$, and the transmit powers of the source and the relay for each possible state, we can write the capacities of the S-R and R-D channels in time slot i, $C_{SR}(i)$ and $C_{RD}(i)$, as

$$C_{SR}(i) = q_1(i)\log_2\left(1+P_S^{(1)}(i)\gamma_{SR}(i)\right) + q_3(i)\log_2\left(1+\frac{P_S^{(3)}(i)\gamma_{SR}(i)}{P_R^{(3)}(i)\gamma_{RR}(i)+1}\right), \quad (8)$$

$$C_{RD}(i) = q_2(i)\log_2\left(1+P_R^{(2)}(i)\gamma_{RD}(i)\right) + q_3(i)\log_2\left(1+P_R^{(3)}(i)\gamma_{RD}(i)\right). \quad (9)$$

Now, since the source is assumed to be backlogged, we can set the transmission rate at the source in time slot i, $R_{SR}(i)$, to $R_{SR}(i) = C_{SR}(i)$, where $C_{SR}(i)$ is given by (8). As a result, the achievable rate on the S-R channel during $N \to \infty$ time slots, denoted by $\bar{R}_{SR}$, is obtained as

$$\bar{R}_{SR} = \lim_{N\to\infty}\frac{1}{N}\sum_{i=1}^{N} R_{SR}(i) = \lim_{N\to\infty}\frac{1}{N}\sum_{i=1}^{N}\left[q_1(i)\log_2\left(1+P_S^{(1)}(i)\gamma_{SR}(i)\right) + q_3(i)\log_2\left(1+\frac{P_S^{(3)}(i)\gamma_{SR}(i)}{P_R^{(3)}(i)\gamma_{RR}(i)+1}\right)\right]. \quad (10)$$

On the other hand, the relay can transmit only if it has information stored in its buffer. Let $Q(i)$, denote the amount of (normalized) information in bits/symbol in the buffer of the relay at the end (beginning) of time slot i (time slot $i+1$). Then, we can set the transmission rate at the relay in time slot i, $R_{RD}(i)$, to $R_{RD}(i) = \min\{Q(i-1), C_{RD}(i)\}$, where $C_{RD}(i)$ is given by (9). As a result, the achievable rate on the R-D channel during $N \to \infty$ time slots, denoted by $\bar{R}_{RD}$, is obtained as

$$\bar{R}_{RD} = \lim_{N\to\infty}\frac{1}{N}\sum_{i=1}^{N} R_{RD}(i) = \lim_{N\to\infty}\frac{1}{N}\sum_{i=1}^{N}\left[\min\left\{Q(i-1), q_2(i)\log_2\left(1+P_R^{(2)}(i)\gamma_{RD}(i)\right) + q_3(i)\log_2\left(1+P_R^{(3)}(i)\gamma_{RD}(i)\right)\right\}\right], \quad (11)$$

where $Q(i)$ is obtained recursively as

$$Q(i) = Q(i-1) + R_{SR}(i) - R_{RD}(i). \quad (12)$$

Our task in this section is to maximize the achievable rate of the considered relay channel given by (11). To this end, we use the following Lemma from [6, Th. 1].

Lemma 1: The data rate extracted from the buffer of the relay and transmitted to the destination during $N \to \infty$ time slots, $\bar{R}_{RD}$, is maximized when the following condition holds

$$\lim_{N\to\infty}\frac{1}{N}\sum_{i=1}^{N}\left[q_1(i)\log_2\left(1+P_S^{(1)}(i)\gamma_{SR}(i)\right) + q_3(i)\log_2\left(1+\frac{P_S^{(3)}(i)\gamma_{SR}(i)}{P_R^{(3)}(i)\gamma_{RR}(i)+1}\right)\right] = \lim_{N\to\infty}\frac{1}{N}\sum_{i=1}^{N}\left[q_2(i)\log_2\left(1+P_R^{(2)}(i)\gamma_{RD}(i)\right) + q_3(i)\log_2\left(1+P_R^{(3)}(i)\gamma_{RD}(i)\right)\right]. \quad (13)$$

Moreover, when condition (1) holds, the rate, $\bar{R}_{RD}$, given by (11), simplifies to

$$\bar{R}_{RD} = \lim_{N\to\infty}\frac{1}{N}\sum_{i=1}^{N}\left[q_2(i)\log_2\left(1+P_R^{(2)}(i)\gamma_{RD}(i)\right) + q_3(i)\log_2\left(1+P_R^{(3)}(i)\gamma_{RD}(i)\right)\right]. \quad (14)$$

Proof: See [6, Th. 1] for the proof. ∎

Lemma 1 is very convenient since it provides an expression for the maximum data rate, $\bar{R}_{RD}$, which is independent of the state of the buffer $Q(i)$. This is because, when condition (1) holds, the number of time slots for which $R_{RD}(i) = \min\{Q(i-1), C_{RD}(i)\} = Q(i-1)$ occurs is negligible compared to the number of time slots for which $R_{RD}(i) = \min\{Q(i-1), C_{RD}(i)\} = C_{RD}(i)$ occurs when $N \to \infty$, see [6]. In other words, when condition (1) holds, we can consider that the buffer at the relay has enough information almost always.

B. Buffer-Aided Relaying With Continuous-Rate Transmission and Adaptive-Power Allocation

In this subsection, we assume that the source and the relay can also adapt their transmit powers in each time slot such that a long-term average power constraint P is satisfied. More precisely, $P_S^{(1)}(i)$, $P_S^{(3)}(i)$, $P_R^{(2)}(i)$, and $P_R^{(3)}(i)$ have to satisfy the following constraint

$$\lim_{N\to\infty}\frac{1}{N}\sum_{i=1}^{N}\left[q_1(i)P_S^{(1)}(i) + q_2(i)P_S^{(3)}(i)\right] + \lim_{N\to\infty}\frac{1}{N}\sum_{i=1}^{N}\left[q_2(i)P_R^{(2)}(i) + q_3(i)P_R^{(3)}(i)\right] \le P. \quad (15)$$

Now, employing Lemma 1, we devise the optimization problem for maximizing the rate, $\bar{R}_{RD}$, when $N \to \infty$, in (16), where constraint C1 ensures that (1) holds, C2 constrains the values that $q_k(i)$, $\forall k, i$, can assume, C3 ensures no more than one state is active at a given time slot i, C4 ensures the joint source-relay power constraint in (15) holds, and constraint C5 ensure that the transmit powers are non-negative.

In the following theorem, we provide the solution of problem (16), as shown at the top of this page, which maximizes the achievable rate of the considered buffer-aided FD

$$\begin{aligned}
&\underset{q_k(i),P_S^{(k)}(i),P_R^{(k)}(i),\forall i,k}{\text{Maximize:}} \ \frac{1}{N}\sum_{i=1}^{N}\Big[q_2(i)\log_2\Big(1+P_R^{(2)}(i)\gamma_{RD}(i)\Big)+q_3(i)\log_2\Big(1+P_R^{(3)}(i)\gamma_{RD}(i)\Big)\Big]\\
&\text{Subject to}: \ \text{C1}: \ \frac{1}{N}\sum_{i=1}^{N}\left[q_1(i)\log_2\Big(1+P_S^{(1)}(i)\gamma_{SR}(i)\Big)+q_3(i)\log_2\left(1+\frac{P_S^{(3)}(i)\gamma_{SR}(i)}{P_R^{(3)}(i)\gamma_{RR}(i)+1}\right)\right]\\
&\qquad\qquad =\frac{1}{N}\sum_{i=1}^{N}\Big[q_2(i)\log_2\Big(1+P_R^{(2)}(i)\gamma_{RD}(i)\Big)+q_3(i)\log_2\Big(1+P_R^{(3)}(i)\gamma_{RD}(i)\Big)\Big]\\
&\qquad \text{C2}: \ q_k(i)\in\{0,1\}, \quad \text{for } k=1,2,3\\
&\qquad \text{C3}: \ q_1(i)+q_2(i)+q_3(i)\in\{0,1\}\\
&\qquad \text{C4}: \ \frac{1}{N}\sum_{i=1}^{N}\Big[q_1(i)P_S^{(1)}(i)+q_2(i)P_S^{(3)}(i)\Big]+\frac{1}{N}\sum_{i=1}^{N}\Big[q_2(i)P_R^{(2)}(i)+q_3(i)P_R^{(3)}(i)\Big]\le P\\
&\qquad \text{C5}: \ P_S^{(k)}(i)\ge 0, P_R^{(k)}(i)\ge 0, \quad \forall k,
\end{aligned} \tag{16}$$

relay channel with SI for continuous-rate transmission with adaptive-power allocation.

Theorem 1: The optimal state selection variables $q_k(i)$, $\forall k,i$, found as the solution of (16), are given in (7), where $\Lambda_1(i)$, $\Lambda_2(i)$, and $\Lambda_3(i)$ are defined as

$$\Lambda_1(i)=\mu\log_2\Big(1+P_S^{(1)}(i)\gamma_{SR}(i)\Big)-\zeta P_S^{(1)}(i), \tag{17}$$

$$\Lambda_2(i)=(1-\mu)\log_2\Big(1+P_R^{(2)}(i)\gamma_{RD}(i)\Big)-\zeta P_R^{(2)}(i), \tag{18}$$

$$\begin{aligned}\Lambda_3(i)=&\mu\log_2\left(1+\frac{P_S^{(3)}(i)\gamma_{SR}(i)}{P_R^{(3)}(i)\gamma_{RR}(i)+1}\right)-\zeta P_S^{(3)}(i)\\&+(1-\mu)\log_2\Big(1+P_R^{(3)}(i)\gamma_{RD}(i)\Big)-\zeta P_R^{(3)}(i).\end{aligned} \tag{19}$$

Moreover, the optimal $P_S^{(1)}(i)$ and $P_R^{(2)}(i)$, found as the solution of (16), are given by

$$P_S^{(1)}(i)=\begin{cases}\frac{\rho}{\eta}-\frac{1}{\gamma_{SR}(i)} & \text{if } \gamma_{SR}(i)>\eta/\rho\\ 0 & \text{otherwise,}\end{cases} \tag{20}$$

$$P_R^{(2)}(i)=\begin{cases}\frac{1}{\eta}-\frac{1}{\eta_{RD}(i)} & \text{if } \gamma_{RD}(i)>\eta\\ 0 & \text{otherwise,}\end{cases} \tag{21}$$

where $\eta\triangleq\frac{\zeta\ln(2)}{1-\mu}$ and $\rho\triangleq\frac{\mu}{1-\mu}$. Whereas, the optimal $P_S^{(3)}(i)$ and $P_R^{(3)}(i)$ are obtained as the solution of the following system of two equations

$$\begin{aligned}&\frac{-\mu\gamma_{RR}(i)\gamma_{SR}(i)P_S^{(3)}(i)}{(1+P_R^{(3)}(i)\gamma_{RR}(i))(1+P_R^{(3)}(i)\gamma_{RR}(i)+P_S^{(3)}(i)\gamma_{SR}(i))}\\&\quad+\frac{(1-\mu)\gamma_{RD}(i)}{(1+P_R^{(3)}(i)\gamma_{RD}(i))}-\ln(2)\zeta=0,\end{aligned} \tag{22}$$

$$\frac{\mu\gamma_{SR}(i)}{(1+P_R^{(3)}(i)\gamma_{RR}(i)+P_S^{(3)}(i)\gamma_{SR}(i))}-\ln(2)\zeta=0. \tag{23}$$

In (22)-(23), μ and ζ are constants found such that C1 and C4 in (16) are satisfied, respectively.

Proof: Please refer to Appendix A for the proof. ■

C. Buffer-Aided Relaying With Continuous-Rate Transmission and Fixed-Power Allocation

In this subsection, we assume that the powers at the source and the relay cannot be adapted to the underlaying channels in each time slot. As a result $P_S^{(1)}(i)=P_S^{(1)}$, $P_R^{(2)}(i)=P_R^{(2)}$, $P_S^{(3)}(i)=P_S^{(3)}$, and $P_R^{(3)}(i)=P_R^{(3)}$ hold $\forall i$.

The maximum achievable rate for this case can be found from (16) by setting $P_S^{(1)}(i)=P_S^{(1)}$, $P_R^{(2)}(i)=P_R^{(2)}$, $P_S^{(3)}(i)=P_S^{(3)}$, and $P_R^{(3)}(i)=P_R^{(3)}$, $\forall i$, in (16). As a result, we do not need to optimize in (16) with respect to these powers. Consequently, the constraints C4 and C5 in (16) can be removed. Thereby, we get a new optimization problem for fixed-power allocation whose solutions are provided in the following theorem.

Theorem 2: The state selection variables $q_k(i)$, $\forall k,i$, maximizing the achievable rate of the considered buffer-aided FD relay channel with SI for continuous-rate transmission with fixed-power allocation (i.e., found as the solution of (16) with $P_S^{(1)}(i)=P_S^{(1)}$, $P_R^{(2)}(i)=P_R^{(2)}$, $P_S^{(3)}(i)=P_S^{(3)}$, and $P_R^{(3)}(i)=P_R^{(3)}$, $\forall i$, and constraints C4-C5 removed) are given in (7), where $\Lambda_1(i)$, $\Lambda_2(i)$, and $\Lambda_3(i)$ are defined as

$$\Lambda_1(i)=\mu\log_2\Big(1+P_S^{(1)}\gamma_{SR}(i)\Big), \tag{24}$$

$$\Lambda_2(i)=(1-\mu)\log_2\Big(1+P_R^{(2)}\gamma_{RD}(i)\Big), \tag{25}$$

$$\begin{aligned}\Lambda_3(i)=&\mu\log_2\left(1+\frac{P_S^{(3)}\gamma_{SR}(i)}{P_R^{(3)}\gamma_{RR}(i)+1}\right)\\&+(1-\mu)\log_2\Big(1+P_R^{(3)}\gamma_{RD}(i)\Big).\end{aligned} \tag{26}$$

In (24)-(26), μ is a constant found such that constraint C1 in (16) holds.

Proof: Since the fixed-power allocation problem is a special case of (16), when $P_S^{(1)}(i)=P_S^{(1)}$, $P_R^{(2)}(i)=P_R^{(2)}$, $P_S^{(3)}(i)=P_S^{(3)}$, and $P_R^{(3)}(i)=P_R^{(3)}$, $\forall i$, and when C4 and C5 are removed, we get the same solution as in (17)-(19), but with ζ set to $\zeta=0$. This completes the proof. ■

Remark 1: We note that in the extreme cases when $\gamma_{RR}(i)\to\infty$ and $\gamma_{RR}(i)\to 0$ hold, i.e., the communication

schemes provided in Theorems 1 and 2 converge to the corresponding schemes in [6] and [5], respectively. In other words, in the extreme cases when we have infinite and zero SI, the proposed buffer-aided schemes work as buffer-aided HD relaying and ideal FD relaying, respectively.

D. Practical Estimation of the Necessary Parameters

The proposed state selection scheme, given in (7), requires the computation of $\Lambda_1(i)$, $\Lambda_2(i)$, and $\Lambda_3(i)$ in each time slot. For the two proposed buffer-aided schemes, these parameters can be computed at the FD relay with minimum possible channel state-information (CSI) acquisition overhead. Using $\Lambda_1(i)$, $\Lambda_2(i)$, and $\Lambda_3(i)$, the relay can compute the optimal state selection variables $q_1(i)$, $q_2(i)$, and $q_3(i)$ using (7), and then feedback the optimal state to the source and the destination using two bits of feedback information. On the other hand, the computation of $\Lambda_1(i)$, $\Lambda_2(i)$, and $\Lambda_3(i)$ at the relay requires full CSI of the S-R, R-D, and SI channels, as well as acquisition of the constant μ. Since μ is actually a Lagrange multiplier, in the following, we describe a method for estimating this constant in real-time using only current instantaneous CSI by employing the gradient descent method [35].

In time slot i, we can recursively compute an estimate of the constant μ, denoted by $\mu_e(i)$, as

$$\mu_e(i) = \mu_e(i-1) + \delta(i)\left[\bar{R}^e_{RD}(i) - \bar{R}^e_{SR}(i)\right], \tag{27}$$

where $\bar{R}^e_{RD}(i)$ and $\bar{R}^e_{SR}(i)$ are real time estimates of $\bar{R}_{RD}$ and $\bar{R}_{SR}$, respectively, which can be calculated as

$$\bar{R}^e_{SR}(i) = \frac{i-1}{i}\bar{R}^e_{SR}(i-1) + \frac{1}{i}C_{SR}(i), \tag{28}$$

$$\bar{R}^e_{RD}(i) = \frac{i-1}{i}\bar{R}^e_{RD}(i-1) + \frac{1}{i}C_{RD}(i). \tag{29}$$

The values of $\bar{R}^e_{SR}(0)$ and $\bar{R}^e_{RD}(0)$ are initialized to zero. Moreover, $\delta(i)$ is an adaptive step size which controls the speed of convergence of $\mu_e(i)$ to μ, which can be some properly chosen monotonically decaying function of i with $\delta(1) < 1$.

For the buffer-aided relaying scheme with adaptive-power allocation, proposed in Theorem 1, in addition to μ, the constant ζ found in (17)-(19) has to be acquired as well. This can be conducted in a similar manner as the real-time estimation of μ. In particular, in time slot i, we can recursively compute an estimate of the constant ζ, denoted by $\zeta_e(i)$, as

$$\zeta_e(i) = \zeta_e(i-1) + \delta(i)\left[\bar{P}_e(i) - P\right], \tag{30}$$

where

$$\bar{P}_e(i) = \frac{i-1}{i}\bar{P}_e(i-1) + \frac{1}{i}\Big[q_1(i)P_S^{(1)}(i) + q_2(i)P_R^{(2)}(i) + q_3(i)\left(P_R^{(3)}(i) + P_S^{(3)}(i)\right)\Big], \tag{31}$$

where $P_S^{(1)}(i)$, $P_S^{(3)}(i)$, $P_R^{(2)}(i)$, and $P_R^{(3)}(i)$ are given in Theorem 1.

V. Buffer-Aided Relaying With Discrete-Rate Transmission

In this section, we assume that the transmitting nodes, source and relay, do not have full CSI of their transmit links and/or have some other constraints that limit their ability to vary their transmission rates arbitrarily. As a result, S and R transmit their codewords with rates which are selected from discrete finite sets of date rates, denoted by $\mathcal{R}_S = \{R_S^1, R_S^2, \ldots, R_S^M\}$ and $\mathcal{R}_R = \{R_R^1, R_R^2, \ldots, R_R^L\}$, respectively, where M and L denote the total number of non-zero data rates available for transmission at S and R, respectively. Moreover, we assume $P_S^{(1)}(i) = P_S^{(1)}$, $P_R^{(2)}(i) = P_R^{(2)}$, $P_S^{(3)}(i) = P_S^{(3)}$, and $P_R^{(3)}(i) = P_R^{(3)}$, $\forall i$.

A. Derivation of the Proposed Buffer-Aided Relaying Scheme With Discrete-Rate Transmission

In order to model the receptions and transmissions of the FD relay for discrete data rates in time slot i, we introduce the binary variables $q_1^m(i)$, $q_2^l(i)$, and $q_3^{m,l}(i)$, where m and l are chosen from $m = 1, 2 \ldots, M$ and $l = 1, 2 \ldots, L$, respectively, defined as

$$q_1^m(i) = \begin{cases} 1 & \text{if S transmits with rate } R_S^m \text{ to R} \\ & \text{and R is silent in time slot } i \\ 0 & \text{otherwise,} \end{cases} \tag{32}$$

$$q_2^l(i) = \begin{cases} 1 & \text{if R transmits with rate } R_R^l \text{ to D} \\ & \text{and S is silent in time slot } i \\ 0 & \text{otherwise.} \end{cases} \tag{33}$$

$$q_3^{m,l}(i) = \begin{cases} 1 & \text{if S transmits with rate } R_S^m \text{ to R} \\ & \text{and R transmits with rate } R_R^l \\ & \text{to D in time slot } i \\ 0 & \text{otherwise.} \end{cases} \tag{34}$$

Since the considered network can be in one and only one state in time slot i, the following has to hold

$$\sum_{m=1}^{M} q_1^m(i) + \sum_{l=1}^{L} q_2^l(i) + \sum_{m=1}^{M}\sum_{l=1}^{L} q_3^{m,l}(i) \in \{0, 1\}, \tag{35}$$

where if $\sum_{m=1}^{M} q_1^m(i) + \sum_{l=1}^{L} q_2^l(i) + \sum_{m=1}^{M}\sum_{l=1}^{L} q_3^{m,l}(i) = 0$ holds, then S and R are both silent in time slot i.

Since the available transmission rates at S and R are discrete, outages can occur. An outage occurs if the data rate of the transmitted codeword is larger than the capacity of the underlying channel. To model the outages on the S-R link, we define the following auxiliary binary variables

$$O_{SR,1}^m(i) = \begin{cases} 1 & \text{if } \log_2\left(1 + P_S^{(1)}\gamma_{SR}(i)\right) \geq R_S^m \\ 0 & \text{if } \log_2\left(1 + P_S^{(1)}\gamma_{SR}(i)\right) < R_S^m, \end{cases} \tag{36}$$

$$O_{SR,3}^m(i) = \begin{cases} 1 & \text{if } \log_2\left(1 + \dfrac{P_S^{(3)}\gamma_{SR}(i)}{P_R^{(3)}\gamma_{RR}(i) + 1}\right) \geq R_S^m \\ 0 & \text{if } \log_2\left(1 + \dfrac{P_S^{(3)}\gamma_{SR}(i)}{P_R^{(3)}\gamma_{RR}(i) + 1}\right) < R_S^m. \end{cases} \tag{37}$$

Similarly, to model the outages on the R-D link, we define the following auxiliary binary variables

$$O^l_{RD,2}(i) = \begin{cases} 1 & \text{if } \log_2\left(1+P_R^{(2)}\gamma_{RD}(i)\right) \geq R^l_R \\ 0 & \text{if } \log_2\left(1+P_R^{(2)}\gamma_{RD}(i)\right) < R^l_R, \end{cases} \quad (38)$$

$$O^l_{RD,3}(i) = \begin{cases} 1 & \text{if } \log_2\left(1+P_R^{(3)}\gamma_{RD}(i)\right) \geq R^l_R \\ 0 & \text{if } \log_2\left(1+P_R^{(3)}\gamma_{RD}(i)\right) < R^l_R. \end{cases} \quad (39)$$

Hence, a codeword transmitted by the source in time slot i can be decoded correctly at the relay if and only if (iff) $\sum_{m=1}^{M} q_1^m(i) O^m_{SR,1}(i) + \sum_{m=1}^{M}\sum_{l=1}^{L} q_3^{m,l}(i) O^m_{SR,3}(i) > 0$ holds. Using $O^m_{SR,1}(i)$ and $O^m_{SR,3}(i)$, and the state selection variables $q_1^m(i)$, and $q_3^{m,l}(i)$, we can define the data rate of the source in time slot i, $R_{SR}(i)$, as

$$R_{SR}(i) = \sum_{m=1}^{M} q_1^m(i) O^m_{SR,1}(i) R^m_S + \sum_{m=1}^{M}\sum_{l=1}^{L} q_3^{m,l}(i) O^m_{SR,3}(i) R^m_S. \quad (40)$$

In addition, we can obtain that a codeword transmitted by the relay in time slot i can be decoded correctly at the destination iff $\sum_{l=1}^{L} q_2^l(i) O^l_{RD,2}(i) + \sum_{l=1}^{L}\sum_{m=1}^{M} q_3^{m,l}(i) O^l_{RD,3}(i) > 0$ holds. Similarly, using $O^l_{RD,2}(i)$ and $O^l_{RD,3}(i)$, and the state selection variables $q_2^l(i)$, and $q_3^{m,l}(i)$, we can define the data rate of the relay in time slot i, $R_{RD}(i)$, as

$$R_{RD}(i) = \min\Bigg\{ Q(i-1), \sum_{l=1}^{L} q_2^l(i) O^l_{RD,2}(i) R^l_R + \sum_{l=1}^{L}\sum_{m=1}^{M} q_3^{m,l}(i) O^l_{RD,3}(i) R^l_R \Bigg\}, \quad (41)$$

where

$$Q(i) = Q(i-1) + R_{SR}(i) - R_{RD}(i). \quad (42)$$

The $\min\{\}$ in (41) is because the relay cannot transmit more information than the amount of information in its buffer $Q(i-1)$. Thereby, the throughputs of the S-R and R-D channels during $N \to \infty$ time slots, again denoted by $\bar{R}_{SR}$ and $\bar{R}_{RD}$, can be obtained as

$$\bar{R}_{SR} = \lim_{N\to\infty} \frac{1}{N} \sum_{i=1}^{N} \Bigg[\sum_{m=1}^{M} q_1^m(i) O^m_{SR,1}(i) R^m_S + \sum_{m=1}^{M}\sum_{l=1}^{L} q_3^{m,l}(i) O^m_{SR,3}(i) R^m_S \Bigg], \quad (43)$$

$$\bar{R}_{RD} = \lim_{N\to\infty} \frac{1}{N} \sum_{i=1}^{N} \min\Bigg\{ Q(i-1), \sum_{l=1}^{L} q_2^l(i) O^l_{RD,2}(i) R^l_R + \sum_{l=1}^{L}\sum_{m=1}^{M} q_3^{m,l}(i) O^l_{RD,3}(i) R^l_R \Bigg\}. \quad (44)$$

Our task in this section is to maximize the throughput of the considered relay channel with discrete-rate transmission given by (43) and (44). To this end, we use the following Lemma from [36, Th. 1].

Lemma 2: The throughput $\bar{R}_{RD}$, given by (44), is maximized when the following condition holds

$$\lim_{N\to\infty} \frac{1}{N} \sum_{i=1}^{N} \Bigg[\sum_{m=1}^{M} q_1^m(i) O^m_{SR,1}(i) R^m_S + \sum_{m=1}^{M}\sum_{l=1}^{L} q_3^{m,l}(i) O^m_{SR,3}(i) R^m_S \Bigg] = \lim_{N\to\infty} \frac{1}{N} \sum_{i=1}^{N} \Bigg[\sum_{l=1}^{L} q_2^l(i) O^l_{RD,2}(i) R^l_R + \sum_{l=1}^{L}\sum_{m=1}^{M} q_3^{m,l}(i) O^l_{RD,3}(i) R^l_R \Bigg]. \quad (45)$$

Moreover, when condition (45) holds, the throughput, $\bar{R}_{RD}$, given by (44), simplifies to

$$\bar{R}_{RD} = \lim_{N\to\infty} \frac{1}{N} \sum_{i=1}^{N} \Bigg[\sum_{l=1}^{L} q_2^l(i) O^l_{RD,2}(i) R^l_R + \sum_{l=1}^{L}\sum_{m=1}^{M} q_3^{m,l}(i) O^l_{RD,3}(i) R^l_R \Bigg]. \quad (46)$$

Proof: See [36, Th. 1] for the proof. ∎

Using Lemma 2, we devise the following throughput maximization problem for the considered two-hop FD relay channel with SI and discrete-rate transmission

$$\begin{aligned} \underset{q_1^m(i), q_2^l(i), q_3^{m,l}(i), \forall i,l,m}{\text{Maximize:}} \quad & \frac{1}{N} \sum_{i=1}^{N} \Bigg[\sum_{l=1}^{L} q_2^l(i) O^l_{RD,2}(i) R^l_R + \sum_{l=1}^{L}\sum_{m=1}^{M} q_3^{m,l}(i) O^l_{RD,3}(i) R^l_R \Bigg] \\ \text{Subject to: C1:} \quad & \frac{1}{N} \sum_{i=1}^{N} \Bigg[\sum_{m=1}^{M} q_1^m(i) O^m_{SR,1}(i) R^m_S + \sum_{m=1}^{M}\sum_{l=1}^{L} q_3^{m,l}(i) O^m_{SR,3}(i) R^m_S \Bigg] \\ & = \frac{1}{N} \sum_{i=1}^{N} \Bigg[\sum_{l=1}^{L} q_2^l(i) O^l_{RD,2}(i) R^l_R + \sum_{l=1}^{L}\sum_{m=1}^{M} q_3^{m,l}(i) O^l_{RD,3}(i) R^l_R \Bigg] \\ \text{C2:} \quad & q_1^m(i) \in \{0,1\}, \quad \forall m \\ \text{C3:} \quad & q_2^l(i) \in \{0,1\}, \quad \forall l \\ \text{C4:} \quad & q_3^{m,l}(i) \in \{0,1\}, \quad \forall m, l \\ \text{C5:} \quad & \sum_{m=1}^{M} q_1^m(i) + \sum_{l=1}^{L} q_2^l(i) + \sum_{m=1}^{M}\sum_{l=1}^{L} q_3^{m,l}(i) \in \{0,1\}. \end{aligned} \quad (47)$$

In (47), we maximize the throughput $\bar{R}_{RD}$, given by (46), with respect to the state selection variables $q_1^m(i), q_2^l(i), q_3^{m,l}(i)$, $\forall i, l, m$, when conditions (35) and (45) hold, and when the

state selection variables are binary. The solution of problem (47) leads to the following theorem.

Theorem 3: We define $q_1(i) = q_1^{m^*}(i)$, $q_2(i) = q_2^{l^*}(i)$, and $q_3(i) = q_3^{m^+,l^+}(i)$, where $m^* = \arg\max_m\{R_S^m O_{SR,1}^m(i)\}$, $l^* = \{\arg\max_l\{R_R^l O_{RD,2}^m(i)\}$, and $\{m^+, l^+\} = \left\{\arg\max_m\{R_S^m O_{SR,3}^m(i)\}, \arg\max_l\{R_R^l O_{RD,3}^m(i)\}\right\}$. Then, the optimal state and rate selection variables, $q_1(i)$, $q_2(i)$, and $q_3(i)$ maximizing the throughput of the considered two-hop FD relay channel with SI and discrete-rate transmission, found as the solution of (47), are given in (7), where $\Lambda_1(i)$, $\Lambda_2(i)$, and $\Lambda_3(i)$ are defined as

$$\Lambda_1(i) = \mu R_S^{m^*} O_{SR,1}^{m^*}(i), \tag{48}$$

$$\Lambda_2(i) = (1-\mu) R_R^{l^*} O_{RD,2}^{l^*}(i), \tag{49}$$

$$\Lambda_3(i) = \mu R_S^{m^+} O_{SR,3}^{m^+}(i) + (1-\mu) R_R^{l^+} O_{RD,3}^{l^+}(i), \tag{50}$$

In (48)-(50), μ is a constant found such that constraint C1 in (47) holds.

Proof: Please refer to Appendix B for the proof. ■

B. Practical Estimation of the Necessary Parameters

The discrete-rate transmission scheme, proposed in Theorem 3, requires the calculation of the parameter μ. This parameter can be obtained theoretically by representing constraint C1 in (47) as

$$E\left\{\sum_{m=1}^{M} q_1^m(i) O_{SR,1}^m(i) R_S^m + \sum_{m=1}^{M}\sum_{l=1}^{L} q_3^{m,l}(i) O_{SR,3}^m(i) R_S^m\right\} = E\left\{\sum_{l=1}^{L} q_2^l(i) O_{RD,2}^l(i) R_R^l + \sum_{l=1}^{L}\sum_{m=1}^{M} q_3^{m,l}(i) O_{RD,3}^l(i) R_R^l\right\}, \tag{51}$$

where $E\{.\}$ denotes statistical expectation. Then, using the probability distribution functions (PDFs) of the S-R, R-D, and SI channels, the parameter μ can be found as the solution of (V-B). Note that solving (V-B) requires knowledge of the PDFs of the channels. However, the scheme proposed in Theorem 3 can still operate without any statistical knowledge in the following manner. We apply (27) to obtain an estimate of μ for time slot i, denoted by $\mu_e(i)$, where $C_{SR}(i)$ and $C_{RD}(i)$ in (28) and (29) are replaced by $\sum_{m=1}^{M} q_1^m(i) O_{SR,1}^m(i) R_S^m + \sum_{m=1}^{M}\sum_{l=1}^{L} q_3^{m,l}(i) O_{SR,3}^m(i) R_S^m$ and $\sum_{l=1}^{L} q_2^l(i) O_{RD,2}^l(i) R_R^l + \sum_{l=1}^{L}\sum_{m=1}^{M} q_3^{m,l}(i) O_{RD,3}^l(i) R_R^l$, respectively. We now let $\mu_e(i)$ to take any value in the range $[0, 1]$. Then, when two state selection variables both assume the value one, according to (7), we select one at random with equal probability to assume the value one and set the other state selection variable to zero. For this scheme, we choose $\delta(i)$ to vary with i only during the first several time slots, and then we set it to a constant for the remaining time slots.

VI. Simulation and Numerical Results

In this section, we evaluate the performance of the proposed buffer-aided schemes with adaptive reception-transmission at the FD relay for the two-hop FD relay channel with SI, and compare it to the performance of several benchmark schemes. To this end, we first define the system parameters, then introduce the benchmark schemes and a delay-constrained buffer-aided relaying scheme, and finally present the numerical results.

A. System Parameters

For the presented numerical results, the mean of the channel gains of the S-R and R-D links are calculated using the standard path loss model as

$$E\{|h_L(i)|^2\} = \left(\frac{c}{4\pi f_c}\right)^2 d_L^{-\alpha}, \quad \text{for } L \in \{\text{S-R, R-D}\}, \tag{52}$$

where c is the speed of light, f_c is the carrier frequency, d_L is the distance between the transmitter and the receiver of link L, and α is the path loss exponent. In this section, we set $\alpha = 3$, and $f_c = 2.4$ GHz. Moreover, we assume that the transmit bandwidth is 200 kHz, and the noise power per Hz is -170 dBm. Hence, the total noise power for 200 kHz is obtained as -117 dBm. On the other hand, the value of $E\{|h_{RR}(i)|^2\}$ is set to -133 dB. Note that $E\{|h_{RR}(i)|^2\}$ can be considered as the SI suppression factor of the corresponding SI suppression scheme. Finally, for the numerical examples with discrete-rate schemes, we assume $M = L$ and $R_S^k = R_R^k = kR$, for $k = 1, 2, \ldots, M$, where R is defined differently depending on the corresponding example.

B. Benchmark Schemes

In the following, we introduce three benchmark schemes which will be used for benchmarking the proposed buffer-aided relaying schemes. For the benchmark schemes $P_S(i) = P_S$ and $P_R(i) = P_R$, $\forall i$, is assumed.

Benchmark Scheme 1 (Buffer-Aided HD Relaying With Adaptive Reception-Transmission): The achievable rate of employing an HD relay and using the buffer-aided HD relaying scheme with adaptive reception-transmission proposed in [6], is given in [6, Sec. III-D].

"Benchmark Scheme 2 (Conventional FD Relaying With a Buffer): In conventional FD relaying, the relay simultaneously transmits and receives during all time slots. Hence, there is no adaptive mode selection as in buffer-aided schemes proposed in this paper. Moreover, the power at the source and the relay are set to $P_S = tP$ and $P_R = (1-t)P$, respectively. Because there is a buffer at the FD relay, the received information at the relay can be stored and transmitted in future time slots. As a result the achieved data rate of conventional FD relaying with a buffer during $N \to \infty$ time slots is given by

$$R_{FD,2} = \min\left\{\lim_{N\to\infty}\frac{1}{N}\sum_{i=1}^{N}\log_2\left(1+\frac{tP\gamma_{SR}(i)}{(1-t)P\gamma_{RR}(i)+1}\right), \lim_{N\to\infty}\frac{1}{N}\sum_{i=1}^{N}\log_2\left(1+(1-t)P\gamma_{RD}(i)\right)\right\}. \tag{53}$$

We note that the conventional FD relaying scheme without a buffer achieves a worse performance than the conventional FD relaying scheme with a buffer. As a result, this scheme is not used as a benchmark.

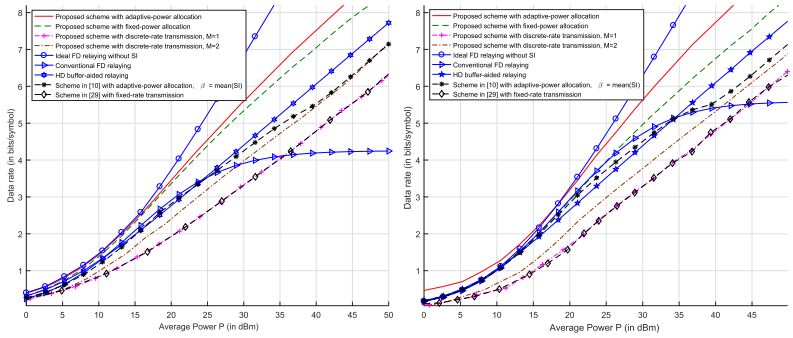

Fig. 2. Data rate vs. average consumed power of the proposed schemes and the benchmark schemes. Left: Symmetric geometry, whith $d_{SR} = d_{RD} = 500$ m. Right: asymmetric geometry, whith $d_{SR} = 700$ m, and $d_{RD} = 300$ m.

Benchmark Scheme 3 (FD Relaying With an Ideal FD Relay Without SI): This is identical to the Benchmark Scheme 2, except that $\gamma_{RR}(i)$ is set to zero, i.e, to $|h_{RR}(i)|^2 = -\infty$ dB.

C. Buffer-Aided Relaying Schemes for Delay-Constrained Transmission

The proposed scheme in (7) gives the maximum achievable rate and the maximum throughput, however, it cannot fix the delay to a desired level. In the following, similar to [37], we propose a scheme for the state selection variables $q_k(i)$, $\forall k$, which holds the delay at a desired level.

The average delay of the considered network is given by Little's Law, as

$$E\{T(i)\} = \lim_{N\to\infty} \frac{\sum_{i=1}^{N} Q(i)}{\sum_{i=1}^{N} R_{SR}(i)}, \tag{54}$$

where $R_{SR}(i)$ and $Q(i)$ are the transmission rate of the source and the queue length in time slot i, respectively. The rate $R_{SR}(i)$ is defined in (8) for continuous-rate transmission and in (40) for discrete-rate transmission. Moreover, $Q(i)$ is defined in (12) for continuous-rate transmission and in (42) for discrete-rate transmission.

For the proposed delay-constrained scheme, we continue to use the general state selection scheme in (7), where $\Lambda_1(i)$, $\Lambda_2(i)$, and $\Lambda_3(i)$, are calculated using (17)-(19) for continuous-rate transmission with adaptive-power allocation, using (24)-(26) for continuous-rate transmission with fixed-power allocation, and using (48)-(50) for discrete-rate transmission. Note that $\Lambda_1(i)$, $\Lambda_2(i)$, and $\Lambda_3(i)$ in (17)-(19), (24)-(26), and (48)-(50) are all function of the parameter μ. In contrary to the proposed buffer-aided schemes in Theorems 1-3, where μ is found to satisfy the constant C1 in (16) and (47), in the buffer-aided relaying scheme for delay-constrained transmission, we use μ to ensure that the system achieves a desired average delay. To this end, μ is calculated as follows. Let us define T_0 as the desired average delay constraint of the considered relay network. Then, in time slot i, we can recursively compute an estimate of the constant μ, denoted by $\mu_e(i)$, as

$$\mu_e(i) = \mu_e(i-1) + \delta(i)\left[T_0 - \frac{Q(i)}{\bar{R}^e_{SR}(i)}\right], \tag{55}$$

where $Q(i)$ is the queue length, defined in (12) and (42) for continuous-rate transmission with fixed- and adaptive-power allocation schemes and discrete-rate transmission scheme, respectively. Furthermore, $\bar{R}^e_{SR}(i)$ is a real time estimate of $\bar{R}_{SR}$, calculated using (28), and initialized to zero for $i = 0$, i.e., $\bar{R}^e_{SR}(0) = 0$. Moreover, $\delta(i)$ is an adaptive step function, which can be chosen to be a properly monotonically decaying function of i with $\delta(1) < 1$.

D. Numerical Results

All of the presented results in this section are generated for Rayleigh fading by numerical evaluation of the derived results and are confirmed by Monte Carlo simulations.

In Fig. 2, we illustrate the rates achieved using the proposed FD buffer-aided schemes for continuous-rate transmission with adaptive-power allocation, continuous-rate transmission with fixed-power allocation, and discrete-rate transmissions as a function of the average consumed power P. Moreover, these rates are compared with the rate obtained by the proposed schemes in [10] and [29], as well as with the benchmark schemes outlined in Section VI-B. The average gain of the SI channel in this numerical example is set to $E\{|h_{RR}(i)|^2\} = -133$ dB. Also, in this example, the distances of the source-relay and relay-destination links are set to 500m for the symmetric (left) figure and to 700m and 300m for the asymmetric (right) figure, respectively. For the proposed scheme with continuous-rate transmission with fixed-power allocation and discrete-rate transmission, we set $P_S^{(1)}(i) = P$, $P_R^{(2)}(i) = P$, $P_S^{(3)}(i) = tP$ and $P_R^{(3)}(i) = (1-t)P$, where $t = 0.5$, $\forall i$. Moreover, for the proposed scheme with discrete-rate transmission with $M = 1$ and $M = 2$, the value of R is optimized numerically, for a given average power P, such that the throughput is maximized. For the adaptive-power allocation scheme proposed for a fixed SI channel in [10], we set the SI

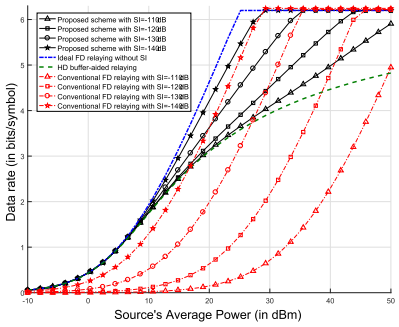

Fig. 3. Data rate vs. the average consumed power at the source node of the proposed buffer-aided scheme for continuous-rate transmission with fixed-power allocation and the benchmark schemes when the average power at the relay is set to 25 dBm.

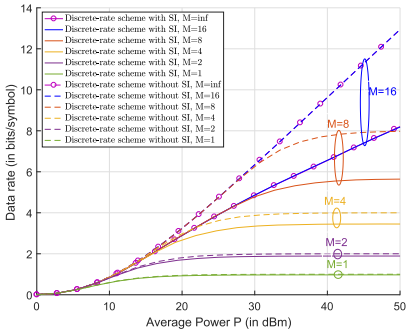

Fig. 4. Data rate/throughput vs. the average consumed power of proposed scheme with discrete-rate transmission.

channel gain to the mean of the SI channel. As can be seen from Fig. 2, by increasing the power, the interference becomes dominant and therefore, our proposed schemes achieve significant performance gains compared to the scheme in [10], which is due to the fact that our schemes are developed for a fading SI channel. Reference [11], proposes a continuous-rate fixed-power allocation buffer-aided scheme. However, without the direct S-D link, the buffer-aided scheme in [11] transforms to the conventional FD relaying scheme, which we already use as benchmark. In Fig. 2, we also considered the fixed-rate scheme proposed in [29] and compared it with our proposed discrete-rate scheme for two case of $M = 1$ and $M = 2$. For the case when we have $M = 1$, our proposed discrete-rate scheme and the scheme in [29] achieve the same throughput since both schemes are optimal for a single fixed-rate. However, for the case when we have $M = 2$, our scheme leads to substantial gains compared to the scheme in [29]. Finally, it is clear from Fig. 2, that the proposed buffer-aided schemes with and without power allocation achieve substantial gains compared to the Benchmark Schemes 1 and 2 in both symmetric and asymmetric geometries. Moreover, as can be seen from Fig. 2, the performance of the conventional FD relaying scheme, i.e, Benchmark Scheme 2, is very poor. In fact, even the proposed discrete-rate transmission scheme with $M = 2$ outperforms the conventional FD scheme for $P > 30$ dBm, and $P > 40$ dBm for symmetric and asymmetric geometries, respectively. This numerical result clearly shows the substantial gains that can be achieved with the proposed buffer-aided schemes compared conventional schemes and to all previous buffer-aided schemes available in the literature.

In Fig. 3, we compare the achievable rates of the proposed buffer-aided scheme for continuous-rate transmission with fixed-power allocation, with the capacity of the ideal two-hop FD relay channel without SI, conventional FD relaying, and the rate achieved by buffer-aided HD relaying as a function of the average transmit power at the source node, where $P_S^{(1)} = P_S^{(3)} = P_S$ is adopted, for different values of the SI. In this example, the power of the relay, $P_R^{(2)} = P_R^{(3)} = P_R$, is set to 25 dBm. This example models an HD base-station which can vary its average power P_S, that is helped by an FD relay with fixed average power of $P_R = 25$ dBm to transmit information to a destination. Since the transmitted power at the relay node is fixed, the maximum possible data rate on the R-D channel is around 6.2 bits per symbol. As can be observed from Fig. 3, the performance of the proposed FD buffer-aided scheme is considerably larger than the performance of buffer-aided HD relaying when the transmit power at the source (i.e., HD base-station) is larger than 25 dBm. For example, for 5 bits/symbol, the power gains are approximately 30 dB, 25 dB, 20 dB, and 15 dB compared to HD relaying for SI values of -140 dB, -130 dB, -120 dB, and -110 dB, respectively. Moreover, from Fig. 3 we can conclude that the conventional FD relaying scheme achieves a poor performance compared to proposed FD buffer-aided relaying scheme. Overall, this example clearly shows that indeed it is beneficial for FD buffer-aided relays to be employed around HD base stations in order to increase their performance significantly.

In Fig. 4, we illustrate the throughputs achieved with the proposed scheme for discrete-rate transmission with and without SI, as a function of the average consumed power, P, for $M = 1, 2, 4, 8, 16, \infty$, where R is set to $R = 1$ bits/symb. Moreover, we set $P_S^{(1)} = P$, $P_R^{(2)} = P$, $P_S^{(3)} = tP$ and $P_R^{(3)} = (1-t)P$, where $t = 0.5$. As can be seen from Fig. 4, the SI does not have a large influence on the throughput for low M, i.e., $M = 1$ and $M = 2$. As a result, the throughputs achieved with and without SI are almost identical. By increasing M, e.g. to $M \geq 4$, we can see from Fig. 4 that the achieved throughput is highly influenced by the SI. The reason for this behavior is because for $M = 1$ and large transmit powers, almost all of source's codewords with rate $R = M$ bits/symb can always be transmitted via the relay when the relay is in the full-duplex mode, despite the generated SI. However, when $M \geq 4$, at large transmit powers, source's codewords with rates close to $R = M$ bits/symb can be transmitted via the relay, in large percentage of the time,

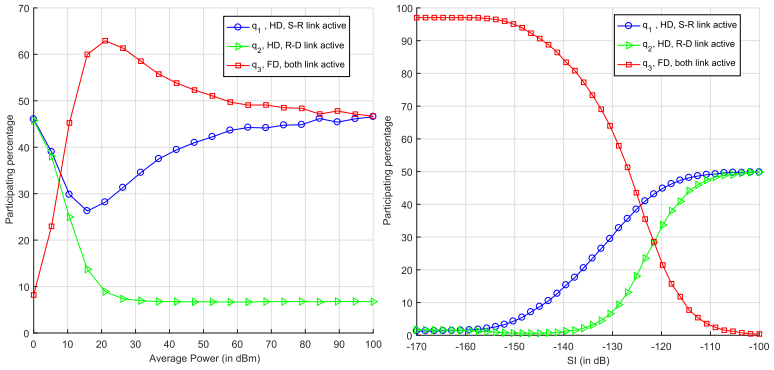

Fig. 5. Participating percentage of all three states. Left: As a function of average power. Right: As a function of SI.

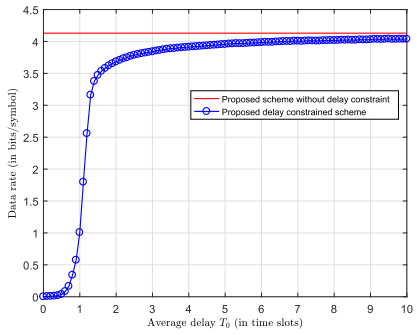

Fig. 6. Average delay until time slot i vs. time slot i, for proposed scheme with delay-constrained transmission compared to fixed desired value, T_0.

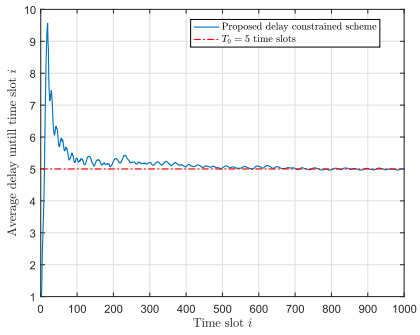

Fig. 7. Average delay until time slot i vs. time slot i, for proposed scheme with delay-constrained transmission compared to fixed desired value, T_0.

only when the relay is in the half-duplex mode, i.e., due to the generated SI, transmitting these codeword in the full-duplex mode is not reliable.

In Fig. 5, in the left and right figures we show the percentage of use of the three states, as a function of the average transmit power and SI, respectively. For the left figure, the average power of the SI channel is set to -133 dB. Whereas, for the right figure, the transmit power of the nodes is set to 25 dBm. We can see from the left figure that there are two different regions; noise dominant region and interference dominant region. In the noise dominant region, the usage of the FD mode is dominant. By increasing the power of the relay, the system falls in the interference dominant region, where the FD mode is selected less as opposed to the HD mode which is selected more frequently. On the other hand, we can see from the right figure that when the SI is high, the system works in the HD mode, with equal percentage for modes q_1 and q_2. As the SI decreases, the FD mode becomes more dominant. Finally, in the low SI region, the proposed scheme works in the FD mode, almost exclusively.

In Fig. 6, we demonstrate the achievable rate of the proposed delay-constrained buffer-aided scheme as a function of the average desired delay, T_0, and compare it with the maximum achievable rate obtained with the scheme in Theorem 2, which does not fix the delay. For this numerical example, we set $P_S^{(1)}(i) = 24$ dBm, $P_R^{(2)}(i) = 24$ dBm, $P_S^{(3)}(i) = 21$ dBm and $P_R^{(3)}(i) = 21$ dBm, $\forall i$. We can see from Fig. 6 that by increasing the average delay, T_0, both data rates converge fast. In fact, for a delay of 3 time slots, there is only 7% loss compared to the maximum rate. This shows that the proposed delay-constrained buffer-aided scheme achieves rate close to the maximum possible rate for a very small delay.

In Fig. 7, we plot the average delay of the proposed delay-constrained scheme until time slot i, for the case when $T_0 = 5$ time slots, as a function of time slot i. Fig. 7 reveals that the average delay until time slot i converges very fast to T_0 by increasing i. Moreover, when the average delay converges to

its desired level, it has relatively small fluctuations around it. This shows that the proposed delay-constrained scheme is very effective in reaching the desired level of delay fast.

VII. Conclusion

In this paper, we proposed three buffer-aided relaying schemes with adaptive reception-transmission at the FD relay for the two-hop FD relay channel with SI for the cases of continuous-rate transmission with adaptive-power allocation, continuous-rate transmission with fixed-power allocation, and discrete-rate transmission, respectively. The proposed schemes significantly improve the over-all performance by optimally selecting the FD relay to either receive, transmit, or simultaneously receive and transmit in a given time slot based on the qualities of the receiving, transmitting, and SI channels. Also, we proposed a relatively fast and practical buffer-aided scheme that holds the delay around a desirable value. Our numerical results have shown that significant performance gains are achieved using the proposed buffer-aided relaying schemes compared to conventional FD relaying, where the FD relay is forced to always simultaneously receive and transmit, to buffer-aided HD relaying, where the HD relay cannot simultaneously receive and transmit, and to all previous buffer-aided schemes available in the literature. This means that buffer-aided relaying should become an integral part of future FD relaying systems, i.e., that FD relaying systems without buffer-aided relaying miss-out on significant performance gains.

Appendix

A. Proof of Theorem 1

We relax constraints C2 and C3 such that $0 \leq q_k(i) \leq 1$, $\forall k$, and $0 \leq q_1(i)+q_2(i)+q_3(i) \leq 1$, and ignore constraint C5. Then, we use the Lagrangian method for solving this optimization problem. Thereby, with some simplification, we can obtain the Lagrangian function, $\mathcal{L}$, as

$$\begin{aligned}\mathcal{L} = &-q_2(i)\log_2\left(1+P_R^{(2)}(i)\gamma_{RD}(i)\right)\\ &-q_3(i)\log_2\left(1+P_R^{(3)}(i)\gamma_{RD}(i)\right)\\ &-\mu\Big[-q_2(i)\log_2\left(1+P_R^{(2)}(i)\gamma_{RD}(i)\right)\\ &-q_3(i)\log_2\left(1+P_R^{(3)}(i)\gamma_{RD}(i)\right)\\ &+q_1(i)\log_2\left(1+P_S^{(1)}(i)\gamma_{SR}(i)\right)\\ &+q_3(i)\log_2\left(1+\frac{P_S^{(3)}(i)\gamma_{SR}(i)}{P_R^{(3)}(i)\gamma_{RR}(i)+1}\right)\Big]\\ &+\zeta\Big(q_1(i)P_S^{(1)}(i)+q_3(i)P_S^{(3)}(i)\\ &+q_2(i)P_R^{(2)}(i)+q_3(i)P_R^{(3)}(i)\Big)\\ &-\lambda_1(i)q_1(i)-\lambda_2(i)(1-q_1(i))-\lambda_3(i)q_2(i)\\ &-\lambda_4(i)(1-q_2(i))-\lambda_5(i)q_3(i)-\lambda_6(i)(1-q_3(i))\\ &-\lambda_7(i)(q_1(i)+q_2(i)+q_3(i))\\ &-\lambda_8(i)(1-(q_1(i)+q_2(i)+q_3(i))),\end{aligned} \tag{56}$$

where $\mu, \zeta \geq 0$, and $\lambda_k(i) \geq 0$ are the Lagrangian multipliers. By differentiating $\mathcal{L}$ with respect to $P_S^{(k)}(i)$ and $P_R^{(k)}(i)$, $\forall k$, and then setting the result to zero, we obtain

$$\frac{d\mathcal{L}}{dP_S^{(1)}(i)} = \frac{\mu q_1(i)\gamma_{SR}(i)}{\ln(2)(1+P_S^{(1)}(i)\gamma_{SR}(i))} - \zeta q_1(i) = 0, \tag{57}$$

$$\frac{d\mathcal{L}}{dP_R^{(2)}(i)} = \frac{(1-\mu)q_2(i)\gamma_{RD}(i)}{\ln(2)(1+P_R^{(2)}(i)\gamma_{RD}(i))} - \zeta q_2(i) = 0, \tag{58}$$

$$\begin{aligned}\frac{d\mathcal{L}}{dP_S^{(3)}(i)} = &\frac{\mu q_3(i)\gamma_{SR}(i)}{\ln(2)(1+P_R^{(3)}(i)\gamma_{RR}(i)+P_S^{(3)}(i)\gamma_{SR}(i))}\\ &-\zeta q_3(i) = 0,\end{aligned} \tag{59}$$

and (60), as shown at the top of the next page.

Now, we calculate $P_S^{(k)}(i)$ and $P_R^{(k)}(i)$, $\forall k$, based on equations (57)-(60) and the following three different available states.

$q_1(i) = 1$: Since $q_1(i) = 1$, we set $q_2(i) = 0$ and $q_3(i) = 0$. As a result (57) becomes

$$\frac{d\mathcal{L}}{dP_S^{(1)}(i)} = \frac{\mu\gamma_{SR}(i)}{\ln(2)(1+P_S^{(1)}(i)\gamma_{SR}(i))} - \zeta = 0. \tag{61}$$

Solving (61), we can obtain $P_S^{(1)}(i)$ as in (20).

$q_2(i) = 1$: Since $q_2(i) = 1$, we set $q_1(i) = 0$ and $q_3(i) = 0$. As a result, (58) becomes

$$\frac{d\mathcal{L}}{dP_R^{(2)}(i)} = \frac{(1-\mu)\gamma_{RD}(i)}{\ln(2)(1+P_R^{(2)}(i)\gamma_{RD}(i))} - \zeta = 0. \tag{62}$$

Solving (62), we can obtain $P_R^{(2)}(i)$ as in (21).

$q_3(i) = 1$: Since $q_3(i) = 1$, we set $q_1(i) = 0$ and $q_2(i) = 0$. As a result, (59) and (60), simplify to (22) and (23), respectively. By solving (22) and (23), we can obtain $P_S^{(3)}(i)$ and $P_R^{(3)}(i)$. We note that, although in this case there is a closed form solution for $P_S^{(3)}(i)$ and $P_R^{(3)}(i)$, since the solution is very long, we have decided not to show it in this paper.

The Lagrangian function, $\mathcal{L}$, given by (VII-A) is bounded below if and only if

$$\begin{aligned}&-\mu\log_2\left(1+P_S^{(1)}(i)\gamma_{SR}(i)\right)+\zeta P_S^{(1)}(i)\\ &\quad-\lambda_1(i)+\lambda_2(i)-\lambda_7(i)+\lambda_8(i) = 0,\end{aligned} \tag{63}$$

$$\begin{aligned}&-(1-\mu)\log_2\left(1+P_R^{(2)}(i)\gamma_{RD}(i)\right)+\zeta P_R^{(2)}(i)\\ &\quad-\lambda_3(i)+\lambda_4(i)-\lambda_7(i)+\lambda_8(i) = 0,\end{aligned} \tag{64}$$

$$\begin{aligned}&-(1-\mu)\log_2\left(1+P_R^{(3)}(i)\gamma_{RD}(i)\right)\\ &\quad-\mu\log_2\left(1+\frac{P_S^{(3)}(i)\gamma_{SR}(i)}{P_R^{(3)}(i)\gamma_{RR}(i)+1}\right)\\ &\quad+\zeta P_S^{(3)}(i)+\zeta P_R^{(3)}(i)\\ &\quad-\lambda_5(i)+\lambda_6(i)-\lambda_7(i)+\lambda_8(i) = 0.\end{aligned} \tag{65}$$

We define $-\lambda_7(i)+\lambda_8(i) \triangleq \beta(i)$, and find the system selection schemes for the three different available cases as follows.

$q_1(i) = 1$: Since $q_1(i) = 1$, we set $q_2(i) = 0$ and $q_3(i) = 0$. As a result, we have $\lambda_1(i) = 0$, $\lambda_4(i) = 0$, and $\lambda_6(i) = 0$ (by complementary slackness in KKT condition). Thereby, we can

$$\frac{d\mathcal{L}}{dP_R^{(3)}(i)} = \frac{(1-\mu)q_3(i)\gamma_{RD}(i)}{\ln(2)(1+P_R^{(3)}(i)\gamma_{RD}(i))} - \zeta q_3(i) - \frac{\mu q_3(i)\gamma_{RR}(i)\gamma_{SR}(i)P_S^{(3)}(i)}{\ln(2)(1+P_R^{(3)}(i)\gamma_{RR}(i))(1+P_R^{(3)}(i)\gamma_{RR}(i)+P_S^{(3)}(i)\gamma_{SR}(i))} = 0. \quad (60)$$

rewrite (63), (64), and (65) as

$$\mu\log_2\left(1+P_S^{(1)}(i)\gamma_{SR}(i)\right) - \zeta P_S^{(1)}(i) - \beta(i) > 0,$$
$$(1-\mu)\log_2\left(1+P_R^{(2)}(i)\gamma_{RD}(i)\right) - \zeta P_R^{(2)}(i) - \beta(i) < 0,$$

And

$$(1-\mu)\log_2\left(1+P_R^{(3)}(i)\gamma_{RD}(i)\right) + \mu\log_2\left(1+\frac{P_S^{(3)}(i)\gamma_{SR}(i)}{P_R^{(3)}(i)\gamma_{RR}(i)+1}\right) - \zeta P_S^{(3)}(i) - \zeta P_R^{(3)}(i) - \beta(i) < 0, \quad (66)$$

respectively.

$q_2(i) = 1$: Since $q_2(i) = 1$, we set $q_1(i) = 0$ and $q_3(i) = 0$. As a result, we have $\lambda_2(i) = 0$, $\lambda_3(i) = 0$, and $\lambda_6(i) = 0$. Thereby, we can rewrite (63), (64), and (65) as

$$\mu\log_2\left(1+P_S^{(1)}(i)\gamma_{SR}(i)\right) - \zeta P_S^{(1)}(i) - \beta(i) < 0,$$
$$(1-\mu)\log_2\left(1+P_R^{(2)}(i)\gamma_{RD}(i)\right) - \zeta P_R^{(2)}(i) - \beta(i) > 0,$$

And

$$(1-\mu)\log_2\left(1+P_R^{(3)}(i)\gamma_{RD}(i)\right) + \mu\log_2\left(1+\frac{P_S^{(3)}(i)\gamma_{SR}(i)}{P_R^{(3)}(i)\gamma_{RR}(i)+1}\right) - \zeta P_S^{(3)}(i) - \zeta P_R^{(3)}(i) - \beta(i) < 0, \quad (67)$$

respectively.

$q_3(i) = 1$: Since $q_3(i) = 1$, we set $q_1(i) = 0$ and $q_2(i) = 0$. As a result, we have $\lambda_2(i) = 0$, $\lambda_4(i) = 0$, and $\lambda_5(i) = 0$. Thereby, we can rewrite (63), (64), and (65) as

$$\mu\log_2\left(1+P_S^{(1)}(i)\gamma_{SR}(i)\right) - \zeta P_S^{(1)}(i) - \beta(i) < 0,$$
$$(1-\mu)\log_2\left(1+P_R^{(2)}(i)\gamma_{RD}(i)\right) - \zeta P_R^{(2)}(i) - \beta(i) < 0,$$

And

$$(1-\mu)\log_2\left(1+P_R^{(3)}(i)\gamma_{RD}(i)\right) + \mu\log_2\left(1+\frac{P_S^{(3)}(i)\gamma_{SR}(i)}{P_R^{(3)}(i)\gamma_{RR}(i)+1}\right) - \zeta P_S^{(3)}(i) - \zeta P_R^{(3)}(i) - \beta(i) > 0, \quad (68)$$

respectively.

By substituting the corresponding terms in (VII-A), (VII-A), and (VII-A) by (17), (18), and (19) we can derive the optimal state selection scheme in Theorem 1. This completes the proof.

B. Proof of Theorem 3

We use the Lagrangian method for solving (47). With some simplification, we can obtain the Lagrangian function as

$$\begin{aligned}\mathcal{L} = &-\lim_{N\to\infty}\frac{1}{N}\sum_{i=1}^{N}\mu\Big[\sum_{m=1}^{M}R_S^m q_1^m(i)O_{SR,1}^m(i) + \sum_{m=1}^{M}\sum_{l=1}^{L}R_S^m q_3^{m,l}(i)O_{SR,3}^m(i)\Big]\\ &-\lim_{N\to\infty}\frac{1}{N}\sum_{i=1}^{N}(1-\mu)\Big[\sum_{l=1}^{L}R_R^l q_2^l(i)O_{RD,2}^l(i) + \sum_{l=1}^{L}\sum_{m=1}^{M}R_R^l q_3^{m,l}(i)O_{RD,3}^l(i)\Big]\\ &-\sum_{m=1}^{M}\lambda_1^m(i)q_1^m(i) - \left(1-\sum_{m=1}^{M}\lambda_2^m(i)q_1^m(i)\right)\\ &-\sum_{l=1}^{L}\lambda_3^l(i)q_2^l(i) - \left(1-\sum_{l=1}^{L}\lambda_4^l(i)q_2^l(i)\right)\\ &-\sum_{l=1}^{L}\sum_{m=1}^{M}\lambda_5^{m,l}(i)q_3^{m,l}(i) - \left(1-\sum_{l=1}^{L}\sum_{m=1}^{M}\lambda_6^{m,l}(i)q_3^{m,l}(i)\right)\\ &-\lambda_7(i)\left(\sum_{m=1}^{M}q_1^m(i)+\sum_{l=1}^{L}q_2^l(i)+\sum_{l=1}^{L}\sum_{m=1}^{M}q_3^{m,l}(i)\right)\\ &-\lambda_8(i)\left(1-\sum_{m=1}^{M}q_1^m(i)-\sum_{l=1}^{L}q_2^l(i)-\sum_{l=1}^{L}\sum_{m=1}^{M}q_3^{m,l}(i)\right),\end{aligned} \quad (69)$$

where $\lambda_1^m(i) \geq 0$, $\lambda_2^m(i) \geq 0$, $\lambda_3^l(i) \geq 0$, $\lambda_4^l(i) \geq 0$, $\lambda_5^{m,l}(i) \geq 0$, $\lambda_6^{m,l}(i) \geq 0$, $\lambda_7(i) \geq 0$, and $\lambda_8(i) \geq 0$, $\forall m, l, i$, are the Lagrangian multipliers. We can rewrite (VII-B) equivalently as

$$\begin{aligned}\mathcal{L} = &-\lim_{N\to\infty}\frac{1}{N}\sum_{i=1}^{N}\mu\Big[q_1(i)\max_m\{R_S^m O_{SR,1}^m(i)\} + q_3(i)\max_m\{R_S^m O_{SR,3}^m(i)\}\Big]\\ &-\lim_{N\to\infty}\frac{1}{N}\sum_{i=1}^{N}(1-\mu)\Big[q_2(i)\max_l\{R_R^l O_{RD,2}^l(i)\} + q_3(i)\max_l\{R_R^l O_{RD,3}^l(i)\}\Big]\end{aligned}$$

$$
\begin{aligned}
&- \sum_{m=1}^{M} \lambda_1^m(i) q_1^m(i) - \left(1 - \sum_{m=1}^{M} \lambda_2^m(i) q_1^m(i)\right) \\
&- \sum_{l=1}^{L} \lambda_3^l(i) q_2^l(i) - \left(1 - \sum_{l=1}^{L} \lambda_4^l(i) q_2^l(i)\right) \\
&- \sum_{l=1}^{L} \sum_{m=1}^{M} \lambda_5^{m,l}(i) q_3^{m,l}(i) \\
&- \left(1 - \sum_{l=1}^{L} \sum_{m=1}^{M} \lambda_6^{m,l}(i) q_3^{m,l}(i)\right) \\
&- \lambda_7(i)\left(q_1(i) + q_2(i) + q_3(i)\right) \\
&- \lambda_8(i)\left(1 - q_1(i) - q_2(i) - q_3(i)\right). \qquad (70)
\end{aligned}
$$

To find $q_k(i)$, $\forall k$, which maximize (70), first, we define $-\lambda_7(i) + \lambda_8(i) \triangleq \beta(i)$. Then, we find the optimal $q_k(i)$, $\forall k$, as follows.

$q_1(i) = 1$: Since $q_1(i) = 1$, we set $q_2(i) = 0$ and $q_3(i) = 0$. As a result, the conditions which maximize (70) in this case are

$$
\begin{aligned}
&\mu \max_m \{R_S^m O_{SR,1}^m(i)\} - \beta(i) > 0, \\
&\quad \text{And, } (1-\mu) \max_l \{R_R^l O_{RD,2}^l(i)\} - \beta(i) < 0, \\
&\quad \text{And, } \mu \max_m \{R_S^m O_{SR,3}^m(i)\} \\
&\quad + (1-\mu) \max_l \{R_R^l O_{RD,3}^l(i)\} - \beta(i) < 0. \qquad (71)
\end{aligned}
$$

$q_2(i) = 1$: Since $q_2(i) = 1$, we set $q_1(i) = 0$ and $q_3(i) = 0$. For maximizing (70), the following conditions must be held

$$
\begin{aligned}
&\mu \max_m \{R_S^m O_{SR,1}^m(i)\} - \beta(i) < 0, \\
&\quad \text{And, } (1-\mu) \max_l \{R_R^l O_{RD,2}^l(i)\} - \beta(i) > 0, \\
&\quad \text{And, } \mu \max_m \{R_S^m O_{SR,3}^m(i)\} \\
&\quad + (1-\mu) \max_l \{R_R^l O_{RD,3}^l(i)\} - \beta(i) < 0. \qquad (72)
\end{aligned}
$$

$q_3(i) = 1$: Since $q_3(i) = 1$, we set $q_1(i) = 0$ and $q_2(i) = 0$. Thereby, the conditions which maximize (70), in this case are

$$
\begin{aligned}
&\mu \max_m \{R_S^m O_{SR,1}^m(i)\} - \beta(i) < 0, \\
&\quad \text{And, } (1-\mu) \max_l \{R_R^l O_{RD,2}^l(i)\} - \beta(i) < 0, \\
&\quad \text{And, } \mu \max_m \{R_S^m O_{SR,3}^m(i)\} \\
&\quad + (1-\mu) \max_l \{R_R^l O_{RD,3}^l(i)\} - \beta(i) > 0. \qquad (73)
\end{aligned}
$$

By substituting the corresponding terms in (71), (72), and (73) by (48), (49), and (50), we obtain the optimal state selection scheme in Theorem 3. This completes the proof.

REFERENCES

[1] T. M. Cover and A. A. El Gamal, "Capacity theorems for the relay channel," *IEEE Trans. Inf. Theory*, vol. IT-25, no. 5, pp. 572–584, Sep. 1979.

[2] G. Liu, F. R. Yu, H. Ji, V. C. M. Leung, and X. Li, "In-band full-duplex relaying: A survey, research issues and challenges," *IEEE Commun. Surveys Tuts.*, vol. 17, no. 2, pp. 500–524, 2nd Quart., 2015.

[3] E. Ahmed and A. M. Eltawil, "All-digital self-interference cancellation technique for full-duplex systems," *IEEE Trans. Wireless Commun.*, vol. 14, no. 7, pp. 3519–3532, Jul. 2015.

[4] N. Zlatanov, V. Jamali, and R. Schober, "On the capacity of the two-hop half-duplex relay channel," in *Proc. IEEE Global Telecomm. Conf. (GLOBECOM)*, San Diego, CA, USA, Dec. 2015, pp. 1–7.

[5] A. Host-Madsen and J. Zhang, "Capacity bounds and power allocation for wireless relay channels," *IEEE Trans. Inf. Theory*, vol. 51, no. 6, pp. 2020–2040, Jun. 2005.

[6] N. Zlatanov, R. Schober, and P. Popovski, "Buffer-aided relaying with adaptive link selection," *IEEE J. Sel. Areas Commun.*, vol. 31, no. 8, pp. 1530–1542, Aug. 2013.

[7] N. Zlatanov, E. Sippel, V. Jamali, and R. Schober, "Capacity of the Gaussian two-hop full-duplex relay channel with residual self-interference," *IEEE Trans. Commun.*, vol. 65, no. 3, pp. 1005–1021, Mar. 2017.

[8] S. M. Kim and M. Bengtsson, "Virtual full-duplex buffer-aided relaying in the presence of inter-relay interference," *IEEE Trans. Wireless Commun.*, vol. 15, no. 4, pp. 2966–2980, Apr. 2016.

[9] N. Zlatanov, D. Hranilovic, and J. S. Evans, "Buffer-aided relaying improves throughput of full-duplex relay networks with fixed-rate transmissions," *IEEE Commun. Lett.*, vol. 20, no. 12, pp. 2446–2449, Dec. 2016.

[10] K. T. Phan and T. Le-Ngoc, "Power allocation for buffer-aided full-duplex relaying with imperfect self-interference cancelation and statistical delay constraint," *IEEE Access*, vol. 4, pp. 3961–3974, 2016.

[11] D. Qiao, "Effective capacity of buffer-aided full-duplex relay systems with selection relaying," *IEEE Trans. Commun.*, vol. 64, no. 1, pp. 117–129, Jan. 2016.

[12] M. Khafagy, A. Ismail, M.-S. Alouini, and S. Aissa, "On the outage performance of full-duplex selective decode-and-forward relaying," *IEEE Commun. Lett.*, vol. 17, no. 6, pp. 1180–1183, Jun. 2013.

[13] N. Nomikos, T. Charalambous, I. Krikidis, D. N. Skoutas, D. Vouyioukas, and M. Johansson, "A buffer-aided successive opportunistic relay selection scheme with power adaptation and inter-relay interference cancellation for cooperative diversity systems," *IEEE Trans. Commun.*, vol. 63, no. 5, pp. 1623–1634, May 2015.

[14] M. Shaqfeh, A. Zafar, H. Alnuweiri, and M.-S. Alouini, "Maximizing expected achievable rates for block-fading buffer-aided relay channels," *IEEE Trans. Wireless Commun.*, vol. 15, no. 9, pp. 5919–5931, Sep. 2016.

[15] O. Taghizadeh, J. Zhang, and M. Haardt, "Transmit beamforming aided amplify-and-forward MIMO full-duplex relaying with limited dynamic range," *Signal Proces.*, vol. 127, pp. 266–281, Oct. 2016.

[16] P. Xu, Z. Ding, I. Krikidis, and X. Dai, "Achieving optimal diversity gain in buffer-aided relay networks with small buffer size," *IEEE Trans. Veh. Technol.*, vol. 65, no. 10, pp. 8788–8794, Oct. 2016.

[17] Z. Tian, Y. Gong, G. Chen, and J. A. Chambers, "Buffer-aided relay selection with reduced packet delay in cooperative networks," *IEEE Trans. Veh. Technol.*, vol. 66, no. 3, pp. 2567–2575, Mar. 2017.

[18] V. Jamali, N. Zlatanov, H. Shoukry, and R. Schober, "Achievable rate of the half-duplex multi-hop buffer-aided relay channel with block fading," *IEEE Trans. Wireless Commun.*, vol. 14, no. 11, pp. 6240–6256, Nov. 2015.

[19] J. Hajipour, A. Mohamed, and V. C. M. Leung, "Efficient and fair throughput-optimal scheduling in buffer-aided relay-based cellular networks," *IEEE Commun. Lett.*, vol. 19, no. 8, pp. 1390–1393, Aug. 2015.

[20] T. Charalambous, N. Nomikos, I. Krikidis, D. Vouyioukas, and M. Johansson, "Modeling buffer-aided relay selection in networks with direct transmission capability," *IEEE Commun. Lett.*, vol. 19, no. 4, pp. 649–652, Apr. 2015.

[21] M. Darabi, V. Jamali, B. Maham, and R. Schober, "Adaptive link selection for cognitive buffer-aided relay networks," *IEEE Commun. Lett.*, vol. 19, no. 4, pp. 693–696, Apr. 2015.

[22] I. Krikidis, T. Charalambous, and J. S. Thompson, "Buffer-aided relay selection for cooperative diversity systems without delay constraints," *IEEE Trans. Wireless Commun.*, vol. 11, no. 5, pp. 1957–1967, May 2012.

[23] W. Wicke, N. Zlatanov, V. Jamali, and R. Schober, "Buffer-aided relaying with discrete transmission rates for the two-hop half-duplex relay network," *IEEE Trans. Wireless Commun.*, vol. 16, no. 2, pp. 967–981, Feb. 2017.

[24] K. T. Phan, T. Le-Ngoc, and L. B. Le, "Optimal resource allocation for buffer-aided relaying with statistical QoS constraint," *IEEE Trans. Commun.*, vol. 64, no. 3, pp. 959–972, Mar. 2016.

[25] T. Islam, D. S. Michalopoulos, R. Schober, and V. K. Bhargava, "Buffer-aided relaying with outdated CSI," *IEEE Trans. Wireless Commun.*, vol. 15, no. 3, pp. 1979–1997, Mar. 2016.

[26] S. Luo and K. C. Teh, "Buffer state based relay selection for buffer-aided cooperative relaying systems," *IEEE Trans. Wireless Commun.*, vol. 14, no. 10, pp. 5430–5439, Oct. 2015.
[27] C. Dong, L.-L. Yang, J. Zuo, S. X. Ng, and L. Hanzo, "Energy, delay, and outage analysis of a buffer-aided three-node network relying on opportunistic routing," *IEEE Trans. Commun.*, vol. 63, no. 3, pp. 667–682, Mar. 2015.
[28] D. Qiao and M. C. Gursoy, "Statistical delay tradeoffs in buffer-aided two-hop wireless communication systems," *IEEE Trans. Commun.*, vol. 64, no. 11, pp. 4563–4577, Nov. 2016.
[29] M. G. Khafagy, A. El Shafie, A. Sultan, and M.-S. Alouini, "Throughput maximization for buffer-aided hybrid half-/full-duplex relaying with self-interference," in *Proc. IEEE Int. Conf. Commun. (ICC)*, Jun. 2015, pp. 1926–1931.
[30] T. Riihonen, S. Werner, and R. Wichman, "Mitigation of loopback self-interference in full-duplex MIMO relays," *IEEE Trans. Signal Process.*, vol. 59, no. 12, pp. 5983–5993, Dec. 2011.
[31] B. P. Day, A. R. Margetts, D. W. Bliss, and P. Schniter, "Full-duplex MIMO relaying: Achievable rates under limited dynamic range," *IEEE J. Sel. Areas Commun.*, vol. 30, no. 8, pp. 1541–1553, Sep. 2012.
[32] M. Duarte, C. Dick, and A. Sabharwal, "Experiment-driven characterization of full-duplex wireless systems," *IEEE Trans. Wireless Commun.*, vol. 11, no. 12, pp. 4296–4307, Dec. 2012.
[33] D. Bharadia, E. McMilin, and S. Katti, "Full duplex radios," *SIGCOMM Comput. Commun. Rev.*, vol. 43, no. 4, pp. 375–386, Oct. 2013.
[34] I. Shomorony and A. S. Avestimehr, "Is Gaussian noise the worst-case additive noise in wireless networks?" in *Proc. IEEE Int. Sym. Inf. Theory (ISIT)*, Jul. 2012, pp. 214–218.
[35] S. Boyd and L. Vandenberghe, *Convex Optimization*. Cambridge, U.K.: Cambridge Univ. Press, 2004.
[36] N. Zlatanov and R. Schober, "Buffer-aided relaying with adaptive link selection—Fixed and mixed rate transmission," *IEEE Trans. Inf. Theory*, vol. 59, no. 5, pp. 2816–2840, May 2013.
[37] N. Zlatanov, V. Jamali, and R. Schober, "Achievable rates for the fading half-duplex single relay selection network using buffer-aided relaying," *IEEE Trans. Wireless Commun.*, vol. 14, no. 8, pp. 4494–4507, Aug. 2015.

Mohsen Mohammadkhani Razlighi (S'17) was born in Tehran, Iran, in 1987. He received the B.S. degree in electrical engineering from University of Zanjan in 2010, and the M.S. degree in telecommunication engineering from Sharif University of Technology in 2012. He is currently pursuing the Ph.D. degree with Monash University, Melbourne, Australia. His research interests include information theory, wireless communications, cooperative networks, and UEP codes.

Nikola Zlatanov (S'06–M'15) was born in Strumica, Macedonia. He received the Dipl.Ing. and master's degrees in electrical engineering from Ss. Cyril and Methodius University, Skopje, Macedonia, in 2007 and 2010, respectively, and the Ph.D. degree from the University of British Columbia (UBC), Vancouver, Canada, in 2015. He is currently a Lecturer (Assistant Professor) with the Department of Electrical and Computer Systems Engineering, Monash University, Melbourne, Australia. His current research interests include wireless communications and information theory. He received several scholarships/awards for his research including UBC's Four Year Doctoral Fellowship in 2010, UBC's Killam Doctoral Scholarship and Macedonia's Young Scientist of the Year in 2011, the Vanier Canada Graduate Scholarship in 2012, Best Journal Paper Award from the German Information Technology Society in 2014, and Best Conference Paper Award at ICNC in 2016. He serves as an Editor of the IEEE COMMUNICATIONS LETTERS. He has been a TPC member of various conferences, including Globecom, ICC, VTC, and ISWCS.

Chapter 3

Dynamic Time-Frequency Division Duplex

The preliminary results have been published in the IEEE ICC Workshops, Kansas City, MO, 2018

- M. M. Razlighi, N. Zlatanov and P. Popovski, ”On Distributed Dynamic-TDD Schemes for Base Stations with Decoupled Uplink-Downlink Transmissions,” IEEE ICC Workshops, Kansas City, MO, 2018.

The complete research, which includes detailed theorems and their proofs have been published in the IEEE Transactions on Wireless Communications, vol. 19, no. 5, pp. 3118-3132, May 2020, which included in this chapter.

- M. M. Razlighi, N. Zlatanov and P. Popovski, ”Dynamic Time-Frequency Division Duplex,” in IEEE Transactions on Wireless Communications, vol. 19, no. 5, pp. 3118-3132, May 2020.

Dynamic Time-Frequency Division Duplex

Mohsen Mohammadkhani Razlighi, *Student Member, IEEE*, Nikola Zlatanov, *Member, IEEE*, and Petar Popovski, *Fellow, IEEE*

***Abstract*— In this paper, we introduce dynamic time-frequency-division duplex (D-TFDD), which is a novel duplexing scheme that combines time-division duplex (TDD) and frequency-division duplex (FDD). In D-TFDD, a user receives from the base station (BS) on the downlink in one frequency band and transmits to the BS on the uplink in another frequency band, as in FDD. Next, the user shares its uplink transmission (downlink reception) on the corresponding frequency band with the uplink transmission or the downlink reception of another user in a D-TDD fashion. Hence, in a given frequency band, the BS communicates with user 1 (U1) and user 2 (U2) in a D-TDD fashion. The proposed D-TFDD scheme does not require inter-cell interference (ICI) knowledge and only requires channel state information (CSI) of the local BS-U1 and BS-U2 channels. Thereby, it is practical for implementation. The proposed D-TFDD scheme increases the throughput region between the BS and the two users in a given frequency band, and significantly decreases the outage probabilities on the corresponding BS-U1 and BS-U2 channels. Most importantly, the proposed D-TFDD scheme doubles the diversity gain on both the corresponding BS-U1 and the BS-U2 channels compared to the diversity gain of existing duplexing schemes, which results in very large performance gains.**

***Index Terms*— Interference, resource management, dynamic scheduling, throughput, base stations (BSs), dynamic time-division duplex (D-TDD), signal to noise ratio, fifth generation (5G) mobile communication, downlink, uplink.**

I. Introduction

TRADITIONALLY, a half-duplex (HD) base station (BS) operates in either the time-division duplex (TDD) mode or the frequency-division duplex (FDD) mode in order to receive and transmit information from/to its users. In the TDD mode, a user uses the same frequency band for uplink and downlink, while uplink and downlink transmissions occur in different time slots [2], see Fig. 1. On the other hand, in the FDD mode, a user is allocated two frequency bands, one dedicated for uplink and the other one for downlink, where the uplink and downlink transmissions occur simultaneously [2], see Fig. 1. In this paper, we introduce time-frequency-division duplex (TFDD), which is a novel duplexing scheme that combines TDD and FDD, and yields significant performance gains compared to TDD and FDD.

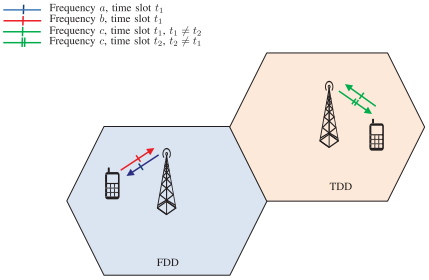

Fig. 1. System model of networks with FDD and TDD communication.

A. Background on the Different Types of Duplexing Schemes

1) Static vs. Dynamic Duplexing: In general, the duplexing method between a BS and its users can be static or dynamic. In static duplexing, the time-frequency resources in which the BS performs uplink receptions and downlink transmissions from/to the user are prefixed and unchangeable over time [3]. On the other hand, in dynamic duplexing schemes, each time-frequency resource unit can be dynamically allocated for communications based on the instantaneous channel state information (CSI). As a result, dynamic duplexing schemes achieve a much better performance compared to static duplexing schemes [4], [5], and thereby have attracted significant research interest [4]–[8].

2) Centralized Dynamic Duplexing vs. Distributed Dynamic Duplexing: A dynamic duplexing scheme can be implemented in either centralized or distributed fashion [6]. In centralized dynamic duplexing schemes, the decision for allocating the time-frequency resources for communication is performed at a central node, which then informs all BSs about the decision. In this way, the communication between neighbouring cells can be synchronized in order to minimize inter-cell interference[1] (ICI) [7]–[17]. However, centralized dynamic duplexing schemes require at the central node full CSI from all links in all cells in order for the central node to make an optimal decision for allocating the time-frequency resources for each BS. In addition, the central node also needs to

Manuscript received April 4, 2019; revised October 31, 2019; accepted January 19, 2020. Date of publication February 6, 2020; date of current version May 8, 2020. This work was supported by the Australian Research Council Discovery Project under Grant DP180101205. This article was presented in part at the IEEE ICC 2018. The associate editor coordinating the review of this article and approving it for publication was D. Guo. *(Corresponding author: Mohsen Mohammadkhani Razlighi.)*

Mohsen Mohammadkhani Razlighi and Nikola Zlatanov are with the Department of Electrical and Computer Systems Engineering, Monash University, Melbourne, VIC 3800, Australia (e-mail: mohsen.mohammadkhanirazlighi@monash.edu; nikola.zlatanov@monash.edu).

Petar Popovski is with the Department of Electronic Systems, Aalborg University, 9220 Aalborg, Denmark (e-mail: petarp@es.aau.dk).

Color versions of one or more of the figures in this article are available online at http://ieeexplore.ieee.org.

Digital Object Identifier 10.1109/TWC.2020.2970701

[1] ICI emerges when BSs and users in neighbouring cells transmit and receive on the same frequency band.

inform all other network nodes about the scheduling decisions. This requires a large amount of signalling information to be exchanged between the central node and all other network nodes. As a result, implementation of centralized dynamic duplexing schemes, in most cases, is infeasible in practice.

On the other hand, in distributed dynamic duplexing schemes, each BS allocates the time-frequency resources for its users without any synchronization with other BSs [13], [18], [19]. To this end, only local CSI is needed at each BS. As a result, distributed dynamic duplexing schemes are much more appropriate for practical implementation compared to the centralized dynamic duplexing scheme. However, distributed dynamic duplexing schemes have to cope with higher ICI than centralized dynamic duplexing schemes.

The proposed TFDD scheme can be characterized as a distributed dynamic duplexing scheme, which means it is suitable for practical implementation.

B. Contribution

In this paper, we introduce dynamic time-frequency-division duplex (D-TFDD), which is a novel duplexing scheme that combines D-TDD and FDD. In D-TFDD, a user receives from the BS on the downlink in one frequency band and transmits to the BS on the uplink in another frequency band, as in FDD. Next, the user shares its uplink transmission (downlink reception) on the corresponding frequency band with the uplink transmission or the downlink reception of another user in a D-TDD fashion. Hence, in a given frequency band, the BS communicates with user 1 (U1) and user 2 (U2) in a D-TDD fashion. The proposed D-TFDD scheme does not require ICI knowledge and only requires CSI of the local BS-U1 and BS-U2 channels. Thereby, it is practical for implementation. The proposed D-TFDD scheme increases the throughput region between the BS and the two users in a given frequency band, and significantly decreases the outage probabilities on the corresponding BS-U1 and BS-U2 channels. Most importantly, the proposed D-TFDD scheme doubles the diversity gain on both the corresponding BS-U1 and the BS-U2 channels compared to the diversity gain of existing duplexing schemes, which results in very large performance gains.

C. Relevance of D-TFDD to 5G and Beyond

One of the prominent aspects of fifth generation (5G) mobile networks is having a flexible physical layer design. In one hand, this capability facilitates implementing challenging physical layer protocols, and on the other hand opens the door for unconventional schemes to be implemented on the physical layer. Such a flexible hardware-software design can easily accommodate our D-TFDD scheme and thereby improve the performance of 5G networks [20]. In addition, distributed resource allocation for dense heterogeneous wireless networks is in one of the main scopes of 5G [20], which also fits well with our D-TFDD scheme. Moreover, proposed scheme is applicable to multi-tier multi-cell systems, which is another feature of 5G networks.

D. Related Works on D-TDD and D-FDD

Distributed D-TDD schemes for BSs have been investigated in [18], [19], [21]–[25] and references therein. In particular, [18] proposed cooperation among cells that resembles a centralized D-TDD scheme. The authors in [19] proposed a D-TDD scheme which alleviates the ICI impairment by splitting the uplink and downlink frequency. Authors in [21] and [22] investigate a distributed D-TDD scheme designed for multiple-antennas. The work in [23] proposes a distributed multi-user D-TDD scheduling scheme, where the ICI is not taken into account, which may lead to poor performance in practice. The authors in [24] investigated an identical network as in [23], but with ICI taken into account. However, the solution in [24] is based on a brute-force search algorithm for allocating the time slots. Authors in [25] proposed a D-TDD scheme that performs optimal power, rate, and user allocation. However, the ICI level in [25] is assumed to be fixed during all time slots, which may not be an accurate model of ICI in practice, since due to the fading and the power-allocations at neighbouring BSs, the ICI varies with time.

On the other hand, D-FDD has been introduced in [13], where the authors proposed a scheme for adapting the downlink to uplink bandwidth ratio.

We note that [13], [18], [19], [21]–[25] require full knowledge of the ICI, which may not be practical, as discussed in Sec. II-D. We also note that the schemes in [13], [18], [19], [21]–[25] transform to the static-TDD and/or static-FDD scheme when ICI is not known. Hence, the static-TDD and/or static-FDD are much more practical for implementation than the D-FDD duplexing scheme since they do not require ICI knowledge.

The rest of this paper is organized as follows. In Section II, we present the system and channel model. In Sections III and IV, we present the D-TFDD schemes for the cases when the ICI is known and unknown, respectively. Simulation and numerical results are provided in Section V, and the conclusions are drawn in Section VI.

II. System and Channel Model

In the following, we consider a cellular network consisting of cells, where each cell has a single BS and users that the BS serves.

A. Frequency and Time Allocation in D-TFDD

In the proposed D-TFDD scheme, we have two possible frequency allocation schemes at each BS, Frequency Allocation Scheme 1 shown in Fig. 2 and Frequency Allocation Scheme 2 shown in Fig. 3. In both frequency allocation schemes, each user is allocated two distinct frequency bands whithin the cell, one for uplink transmission and the other for downlink reception, identical as in FDD, see Figs. 2 and 3. In Frequency Allocation Scheme 1, the frequency band of a user allocated for uplink transmission (downlink reception) is shared in a D-TDD fashion with the uplink transmission (downlink reception) of another user, as shown in Figs. 2. Whereas, in Frequency Allocation Scheme 2, the frequency

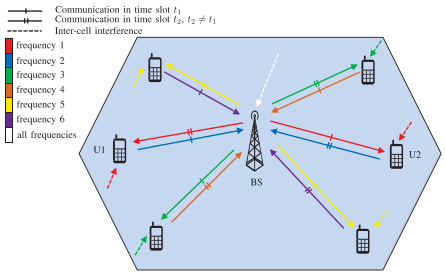

Fig. 2. Frequency allocation Scheme 1.

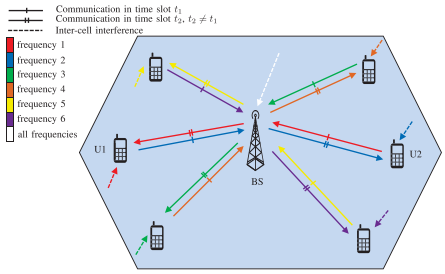

Fig. 3. Frequency allocation Scheme 2.

band of a user allocated for uplink transmission (downlink reception) is shared in a D-TDD fashion with the downlink reception (uplink transmission) of another user, as shown in Figs. 3. Hence, for N users, the BS needs to allocate N frequency bands in D-TFDD, same as in TDD.

Frequency Allocation Scheme 1 is more appropriate for cellular communication networks, where the transmit powers of BSs are much higher than the transmit powers of the users. Specifically, when Frequency Allocation Scheme 1 is applied to every BS in the cellular network such that the uplink frequency bands are used only for uplink and the downlink frequency bands are used only for downlink at all BSs, then all uplink links receive inter-cell interference only from other uplink transmissions and all downlink links receive inter-cell interference only from other downlink transmissions. As a result, the problem in existing D-TDD schemes of strong downlink transmission from one BS interfering with the weak uplink reception at another BS is avoided in D-TFDD with Frequency Allocation Scheme 1. On the other hand, Frequency Allocation Scheme 2 might be more suitable for networks where the uplink and downlink transmissions have equal powers.

B. The Three-Node Subnetwork

We assume that there is no interference between different frequency bands. The only interference at a user/BS in a given frequency band is a result of the transmission in the same frequency band from the users and the BSs in other cells. As a result, for a given frequency band, the considered cellular network employing the D-TFDD scheme can be divided into three-node subnetworks, where each subnetwork consists of a BS and two users working in the same frequency band that are impaired by ICI coming from the rest of the subnetworks working in the same frequency band, as shown in Fig. 4. Depending on whether the downlink reception (uplink transmission) in a given frequency band is shared with the downlink reception or the uplink transmission of another user, there can be three types of three-node subnetworks, as shown in Fig. 4. Type 1 is when both users perform downlink receptions in the given frequency band. Type 2 is when both users perform uplink transmissions in the given frequency band. And Type 3 is when one of the users performs uplink transmission and the other user performs downlink reception in the given frequency band. Note that the three types of three-node subnetworks differ only in the direction of the transmission on the BS-U1 and BS-U2 channels.

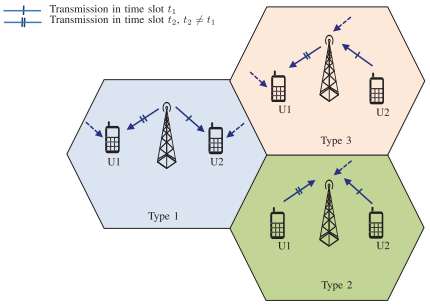

Fig. 4. System model of a BS and two users employing D-TFDD on a specific frequency band for Type 1, 2 and 3.

Now, in order for the D-TFDD to be a distributed duplexing scheme, each of the three-node subnetworks must perform D-TFDD independently from the rest of the subnetworks in the cellular network. As a result, without loss of generality, the equivalent system model that needs to be investigated is comprised of a BS communicating with U1 and U2 in different time slots but in the same frequency band, where receivers are impaired by ICI, as shown in Fig. 4.

Remark 1: The considered three-node subnetworks shown in Fig. 4 can also represent the decoupled access [26], [27] by BS and users switching places, where a user is connected to two BSs and performs uplink-transmission or downlink-reception to/from BS1 and uplink-transmission or downlink-reception to/from BS2 in the same frequency band. Since the decoupled system can be obtained by the proposed system where BS and users switch places, the proposed D-TFDD scheme is also applicable to the decoupled access.

C. Inter-Cell Interference

The receiving nodes of a given three-node subnetwork are impaired by interference from all other nodes in the network

that transmit on the frequency band used for reception at the BS, and/or U1, and/or U2, also referred to as ICI, see Fig. 4. Let the power of the ICI at the receiving nodes on the BS-U1 and BS-U2 channels in time slot[2] t be denoted[3] by $\gamma_{I1}(t)$ and $\gamma_{I2}(t)$, respectively. Then, we can obtain $\gamma_{I1}(t)$ and $\gamma_{I2}(t)$ as[4]

$$\gamma_{I1}(t) = \sum_{k\in\mathcal{K}} P_k\gamma_{k1}(t), \tag{1}$$

$$\gamma_{I2}(t) = \sum_{k\in\mathcal{K}} P_k\gamma_{k2}(t), \tag{2}$$

where $\mathcal{K}$ is the set of interfering nodes, P_k is the power of interfering node k, and $\gamma_{k1}(t)$ and $\gamma_{k2}(t)$ are the square of the channel gains between interfering node k and the receiver on the BS-U1 channel, and interfering node k and the receiver one the BS-U2 channel, in time slot t, respectively.

D. Inter-Cell Interference Estimation Overhead

A network comprised of K HD nodes, all operating in the same frequency band, requires at least K estimation periods in order for the ICI to be estimated at all K nodes. To see this, note that a HD node can either receive or transmit in a given frequency band. As a result, in order for a HD node to estimate the interference from the remaining $K-1$ HD nodes, an estimation period must be dedicated for this purpose in which the considered HD node receives and the rest of the $K-1$ HD transmit. Since this process has to be repeated for each of the K HD nodes, it follows that a network comprised of K HD nodes, all operating in the same frequency band, must dedicate K time periods for ICI estimation at the K HD nodes. Hence, ICI estimation at K HD nodes entails an overhead of K estimation periods. In addition, since the transmission schedule of the different HD nodes is not known in advance, the estimated ICI may differ significantly than the real one, which means that the overhead of K time periods is a lower bound of the actual number of time periods needed for estimation of the actual ICI. In fact, this is a key point. The only realistic way to have the transmission schedule of the HD nodes known in advance is to have a central controller that gathers all the channels, makes a scheduling decision for each link in each time slot and forwards that decision to the nodes. This is not feasible in current systems and will likely not be feasible in future systems as long as the coherence time equals a time slot during which the CSI acquisition, the transmission of the scheduling decisions, and the actual transmission of data need to take place.

The overhead needed for ICI estimation requires resources that may prohibit ICI estimation in practice. As a result, in this paper, we investigate the practical case without ICI knowledge, and propose a distributed D-TFDD scheme for this practical scenario. In addition, in order to obtain an upper bound on the performance of the D-TFDD in terms of outage probability and throughput rate for unknown ICI, we will also investigate the case where the ICI is known at the nodes. Consequently, we will propose distributed D-TFDD schemes for the cases with and without ICI knowledge, and show that the proposed distributed D-TFDD scheme without ICI knowledge has performance which is close to its upper bound achieved when the ICI is known.

Remark 2: The above method for estimating the interference works only if K is known. In practice, K is unknown and, in that case, estimating the interference requires even more resources.

E. Channel Model

In a given subnetwork, we assume that the BS-U1 and BS-U2 channels are complex-valued additive white Gaussian noise (AWGN) channels impaired by slow fading and ICI. Next, we assume that the transmission time is divided into $T \to \infty$ time slots. Furthermore, we assume that the fading is constant during one time slot and changes from one time slot to the next. In time slot t, let the complex-valued fading gains of the BS-U1 and BS-U2 channels be denoted by $h_1(t)$ and $h_2(t)$, respectively. Moreover, let the variances of the complex-valued AWGNs at receiving nodes of the the BS-U1 and BS-U2 channels be denoted by σ_1^2 and σ_2^2, respectively.[5] For convenience, we define normalized magnitude-squared fading gains of the BS-U1 and BS-U2 channels as $\gamma_1(t) = |h_1(t)|^2/\sigma_1^2$ and $\gamma_2(t) = |h_2(t)|^2/\sigma_2^2$, respectively. Furthermore, let the transmit powers of the transmit nodes on the BS-U1 and BS-U2 channels in time slot t be denoted by P_1 and P_2, $\forall t$, respectively.

Using the above notation and taking into account the AWGNs and the ICIs given by (1) and (2), and treating the ICI as noise, the capacities of the BS-U1 and BS-U2 channels in time slot t, denoted by $C_1(t)$ and $C_2(t)$, respectively, are obtained as

$$C_1(t) = \log_2\left(1 + \frac{P_1\gamma_1(t)}{1+\gamma_{I1}(t)}\right), \tag{3}$$

$$C_2(t) = \log_2\left(1 + \frac{P_2\gamma_2(t)}{1+\gamma_{I2}(t)}\right). \tag{4}$$

F. Discrete-Rate Transmission

We assume that the transmit nodes on the BS-U1 or the BS-U2 channels transmit their codewords with rates which are selected from discrete finite sets of data rates, denoted by $\mathcal{R}_1 = \{R_1^1, R_1^2, \ldots, R_1^M\}$ and $\mathcal{R}_2 = \{R_2^1, R_2^2, \ldots, R_2^L\}$, respectively, where M and L denote the total number of non-zero data rates available for transmission at the transmit nodes on the BS-U1 and BS-U2 channels, respectively. This allows us to have a transmission model used in practice which also converges to continuous transmission rates model when $M \to \infty$ and $L \to \infty$, and to the single fixed-rate transmission model when $M = 1$ and $L = 1$.

[2]Time slot is a time interval that is equal or smaller than the duration of the coherence interval. Moreover, we assume that a time slot is long enough such that a capacity achieving codeword can be transmitted during one time slot.

[3]The subscripts 1 and 2 are used to symbolize the BS-U1 and the BS-U2 channels, respectively.

[4]For D-TFDD Type 3, $\gamma_{I1}(t) = \gamma_{I2}(t)$.

[5]For D-TFDD Type 2, $\sigma_1^2 = \sigma_2^2$.

III. D-TFDD for Known ICI

In this section, we assume that the ICI is known at the nodes at the start of each time slot. Although this assumption is not practical as discussed in Sec. II-D, it will enable us to obtain an upper bound on the practical D-TFDD without ICI knowledge at the nodes.

A. BS-U1 and BS-U2 Throughput Region

In a given time slot, depending on whether we are communicating on the BS-U1 and BS-U2 channels, the considered three-node subnetwork, shown in Fig. 4, can be in one of the following three states

State 0: No transmission occurs on both BS-U1 and BS-U2 channels.

State 1: Channel BS-U1 is selected for transmission and channel BS-U2 is inactive/silent.

State 2: Channel BS-U2 is selected for transmission and channel BS-U1 is inactive/silent.

In State 1, the transmitting node on the BS-U1 channel can choose to transmit with any rate in the set $\mathcal{R}_1$. Similarly, in State 2, the transmitting node on the BS-U2 channel can choose to transmit with any rate in the set $\mathcal{R}_2$. In order to model these states for time slot t, we introduce the binary variables $q_1^m(t)$, $m = 1, 2 \ldots, M$ and $q_2^l(t)$, for $l = 1, \ldots, L$, defined as

$$q_1^m(t) = \begin{cases} 1 & \text{if channel BS-U1 is selected for the} \\ & \text{transmission of a codeword} \\ & \text{with rate } R_1^m \\ & \text{and power } P_1 \text{ in time slot } t \\ 0 & \text{otherwise,} \end{cases} \tag{5}$$

$$q_2^l(t) = \begin{cases} 1 & \text{if channel BS-U2 is selected for the} \\ & \text{transmission of a codeword} \\ & \text{with rate } R_2^m \\ & \text{and power } P_2 \text{ in time slot } t \\ 0 & \text{otherwise,} \end{cases} \tag{6}$$

respectively. In addition, since the considered network can be in one and only one state in time slot t, the following has to hold

$$\sum_{m=1}^{M} q_1^m(t) + \sum_{l=1}^{L} q_2^l(t) \in \{0, 1\}, \tag{7}$$

where if $\sum_{m=1}^{M} q_1^m(t) + \sum_{l=1}^{L} q_2^l(t) = 0$ holds, then both the BS-U1 and the BS-U2 channels are inactive in time slot t. Condition (7) results from the HD constraint of the BS, i.e., the BS can either receive or transmit in a given time slot on the same frequency band.

Since the available transmission rates are discrete, outages can occur. An outage is defined as the event when data rate of the transmitted codeword is larger than the capacity of the underlying channel. To model the outages on the BS-U1 and the BS-U2 channels, we introduce the following auxiliary binary variables, $O_1^m(t)$, for $m = 1, \ldots, M$, and $O_2^l(t)$, for $l = 1, \ldots, L$, respectively, defined as

$$O_1^m(t) = \begin{cases} 1 & \text{if } C_1(t) \geq R_1^m \\ 0 & \text{if } C_1(t) < R_1^m, \end{cases} \tag{8}$$

$$O_2^l(t) = \begin{cases} 1 & \text{if } C_2(t) \geq R_2^l \\ 0 & \text{if } C_2(t) < R_2^l. \end{cases} \tag{9}$$

Using $O_1^m(t)$, we can obtain that in time slot t a codeword transmitted on the BS-U1 channel with rate R_1^m can be decoded correctly at the receiver if and only if (iff) $q_1^m(t)O_1^m(t) > 0$ holds. Similarly, using $O_2^l(t)$, we can obtain that in time slot t a codeword ctransmitted on the BS-U2 channel with rate R_2^l can be decoded correctly at receiver iff $q_2^l(t)O_2^l(t) > 0$ holds. Thereby, the average achieved throughputs during $T \to \infty$ time slots on the BS-U1 and BS-U2 channels, denoted by $\bar{R}_1$ and $\bar{R}_2$, respectively, are given by

$$\bar{R}_1 = \lim_{T\to\infty} \frac{1}{T} \sum_{t=1}^{T} \sum_{m=1}^{M} R_1^m q_1^m(t) O_1^m(t), \tag{10}$$

$$\bar{R}_2 = \lim_{T\to\infty} \frac{1}{T} \sum_{t=1}^{T} \sum_{l=1}^{L} R_2^l q_2^l(t) O_2^l(t). \tag{11}$$

The throughput pair $(\bar{R}_1, \bar{R}_2)$, defined by (10) and (11), for some fixed vectors $[q_1^m(1), q_1^m(2), \ldots, q_1^m(T)]$ and $[q_2^l(1), q_2^l(2), \ldots, q_2^l(T)]$ gives one point on the graph where $\bar{R}_1$ and $\bar{R}_2$ are axis. All possible combinations of $[q_1^m(1), q_1^m(2), \ldots, q_1^m(T)]$ and $[q_2^l(1), q_2^l(2), \ldots, q_2^l(T)]$ give a region of points that is bounded by a maximum boundary line of the BS-U1 and BS-U2 throughput region. Our task now is to find the maximum boundary line of this BS-U1 and BS-U2 throughput region, $(\bar{R}_1, \bar{R}_2)$, by selecting the optimal values of $q_1^m(t)$, $q_2^l(t)$, $\forall m, l, t$, respectively.

The maximum boundary line of the BS-U1 and BS-U2 throughput region $(\bar{R}_1, \bar{R}_2)$, given by (10) and (11), can be found from the following maximization problem

$$\begin{aligned} &\underset{q_1^m(t), q_2^l(t),\, \forall l,m,t.}{\text{Maximize:}} \quad \mu\bar{R}_1 + \big(1-\mu\big)\bar{R}_2 \\ &\text{Subject to :} \\ &\qquad \text{C1}: \ q_1^m(t) \in \{0,1\}, \quad \forall m \\ &\qquad \text{C2}: \ q_2^l(t) \in \{0,1\}, \quad \forall l \\ &\qquad \text{C3}: \ \sum_{m=1}^{M} q_1^m(t) + \sum_{l=1}^{L} q_2^l(t) \in \{0,1\}, \end{aligned} \tag{12}$$

where μ is a priori given constant which satisfies $0 \leq \mu \leq 1$. A specific value of μ provides one point on the boundary line of the BS-U1 and BS-U2 throughput region[6] $(\bar{R}_1, \bar{R}_2)$. By varying μ from zero to one, the entire boundary line of the BS-U1 and BS-U2 throughput region $(\bar{R}_1, \bar{R}_2)$ can be obtained. The solution of (12) is given in the following theorem.

Theorem 1: The optimal state and rate selection variables, $q_1^m(t)$ and $q_2^l(t)$, of the D-TFDD scheme for known ICI that maximize the BS-U1 and BS-U2 throughput region of

[6]Note that the defined throughput region is not the capacity region.

the considered subnetwork, which are found as the solution of (12), are given as

$$\begin{aligned}
\text{BS-U1 transmission} \blacktriangleright\ & q_1^{m^*}(t)=1, q_1^m(t)=0,\ \forall m\neq m^* \\
& \text{and } q_2^l(t)=0,\ \forall l \\
& \text{if } \Big[\Lambda_1^{m^*}(t)\geq \Lambda_2^{l^*}(t) \text{ and } \Lambda_1^{m^*}(t)>0\Big], \\
\text{BS-U2 transmission} \blacktriangleright\ & q_2^{l^*}(t)=1, q_2^l(t)=0,\ \forall l\neq l^* \\
& \text{and } q_1^m(t)=0,\ \forall m \\
& \text{if } \Big[\Lambda_2^{l^*}(t)>\Lambda_1^{m^*}(t) \text{ and } \Lambda_2^{l^*}(t)>0\Big], \\
\text{Silence} \blacktriangleright\ & q_1^m(t)=0,\ \forall m \text{ and } q_2^l(t)=0,\ \forall l \\
& \text{if } \Big[\Lambda_1^{m^*}(t)=0 \text{ and } \Lambda_2^{l^*}(t)=0\Big], \qquad (13)
\end{aligned}$$

where $\Lambda_1^m(t)$, $\Lambda_2^l(t)$, m^* and l^* are defined as

$$\Lambda_1^m(t) = \mu R_1^m O_1^m(t), \qquad (14)$$

$$\Lambda_2^l(t) = (1-\mu) R_2^l O_2^l(t)\ , \qquad (15)$$

$$m^* = \arg\max_m \{\Lambda_1^m(t)\}, \qquad (16)$$

$$l^* = \arg\max_l \{\Lambda_2^l(t)\}. \qquad (17)$$

Proof: Please refer to Appendix A for the proof. ■

Note that for the proposed D-TFDD scheme in Theorem 1 to operate, the receivers of the BS-U1 and BS-U2 channels need to know $O_1^m(t)$ and $O_2^l(t)$, respectively, $\forall m,l$, at the start of time slot t, which requires knowledge of the ICI.

B. Diversity Gain of the Proposed D-TFDD for Known ICI

It is quite interesting to investigate the diversity gain achieved with the D-TFDD scheme for known ICI proposed in Theorem 1. In the literature, the asymptotic outage probability, from which the diversity gain is obtained, is derived assuming only a single available transmission rate at the transmitter, see [28]. Following this convention, in the following, we derive the asymptotic outage probabilities of the BS-U1 and the BS-U2 channels, denoted by P_{out}, achieved with the D-TFDD scheme for known ICI proposed in Theorem 1 for $\mu=\frac{1}{2}$, $M=L=1$, $P_1=P_2$, and $R_1^1=R_2^1=R_0$. For simplicity, we only investigate the case of Rayleigh fading, and also assume that the BS-U1 and BS-U2 channels are affected by independent and identically distributed (i.i.d) fading.

Theorem 2: The asymptotic outage probability of the D-TFDD scheme for known ICI proposed in Theorem 1 for the case of Rayleigh fading and when $\mu=\frac{1}{2}$, $M=L=1$, $P_1=P_2=P$, and $R_1^1=R_2^1=R_0$ hold, is given by

$$P_{\text{out}} \to \frac{\gamma_{\text{th}}^2 \hat{\Omega}_I}{\Omega_0^2}, \quad \text{as } P\to\infty, \qquad (18)$$

where $\gamma_{\text{th}}=\frac{2^{R_0}-1}{P}$, $\Omega_0 = E\left\{\frac{|h_1(t)|^2}{\sigma_1^2}\right\} = E\left\{\frac{|h_2(t)|^2}{\sigma_2^2}\right\}$, and $\hat{\Omega}_I = E\Big\{(1+\gamma_{I1}(t))(1+\gamma_{I2}(t))\Big\}$.

As can be seen from (18), the outage probability P_{out} has a diversity gain of two.

Proof: Please refer to Appendix B for the proof. ■

Note that existing D-TDD and D-FDD schemes achieve a diversity gain of one, which leads to the conclusion that the proposed D-TFDD scheme doubles the diversity gain compared to existing duplexing schemes, which in turn leads to very large performance gains, cf. Sec. V.

IV. D-TFDD for Unknown ICI

The D-TFDD scheme proposed in Section III requires the receivers of the BS-U1 and BS-U2 channels to know $O_1^m(t)$ and $O_2^l(t)$, respectively, $\forall m,l$, at the start of time slot t, for $t=1,2,\dots T$, which requires ICI knowledge. However, as discussed in Sec. II-D, the estimation of the ICI entails huge cost for a cellular network comprised of K HD nodes which may not be practical. Motivated by this problem, in the following, we propose a D-TFDD scheme where the nodes do not have knowledge of the ICI, and as a result, the network nodes do not have to waste huge resources for estimating the ICI. We only assume that the CSI of the BS-U1 and BS-U2 channels are known at the BS, i.e., we assume local CSI knowledge at the BS. Specifically, the BS knows $\gamma_1(t)$ and $\gamma_2(t)$ at the start of time slot t, which can be acquired by allocating two estimation periods; one for the BS-U1 channel and the other for the BS-U2 channel, which is a huge improvement compared to the K estimation periods that need to be allocated when the ICI needs to be estimated, see Sec. II-D.

A. Proposed D-TFDD for Unknown ICI

The throughput region of the BS-U1 and BS-U2 channels employing the D-TFDD scheme for unknown ICI is also given by (10) and (11), where $O_1^m(t)$ and $O_2^l(t)$ are defined in (8) and (9), respectively. The only difference now is that $q_1^m(t)$ and $q_2^l(t)$ in (10) and (11) are different when the D-TFDD for unknown ICI is applied. The optimal $q_1^m(t)$ and $q_2^l(t)$, which maximize the throughput region, defined by (10) and (11), of the D-TFDD scheme for unknown ICI are given in the following.

For the case when the ICI is unknown at the nodes, first we define

$$m^* \triangleq \arg\max_m \{R_1^m O_{1,e}^m(t)\}, \qquad (19)$$

$$l^* \triangleq \arg\max_l \{R_2^l O_{2,e}^l(t)\}, \qquad (20)$$

where $O_{1,e}^m(t)$ and $O_{2,e}^l(t)$ are defined as

$$O_{1,e}^m(t) = \begin{cases} 1 & \text{if } C_1^e(t)\geq R_1^m \\ 0 & \text{if } C_1^e(t)< R_1^m, \end{cases} \qquad (21)$$

$$O_{2,e}^l(t) = \begin{cases} 1 & \text{if } C_2^e(t)\geq R_2^l \\ 0 & \text{if } C_2^e(t)< R_2^l. \end{cases} \qquad (22)$$

The variables, $C_1^e(t)$ and $C_2^e(t)$, used in (21) and (22), are defined as

$$C_1^e(t) = \log_2\left(1+\frac{P_1\gamma_1(t)}{1+\gamma_{I1}^e(t)}\right), \qquad (23)$$

$$C_2^e(t) = \log_2\left(1+\frac{P_2\gamma_2(t)}{1+\gamma_{I2}^e(t)}\right), \qquad (24)$$

where $\gamma_{I1}^e(t)$ and $\gamma_{I2}^e(t)$ are given in Proposition 1 in the following, and they can be thought of as estimates of the ICI in time slot t.

The optimal $q_1^m(t)$ and $q_2^l(t)$, which maximize the throughput region, defined by (10) and (11), of the D-TFDD for unknown ICI are as follows

$$\begin{aligned}
&\text{BS-U1 transmission} \ \blacktriangleright \ q_1^{m^*}(t)=1, q_1^m(t)=0,\ \forall m\neq m^* \\
&\qquad \text{and } q_2^l(t)=0,\ \forall l, \\
&\qquad \text{if } [\Lambda_1(t)\geq\Lambda_2(t) \text{ and } \Lambda_1(t)>0], \\
&\text{BS-U2 transmission} \ \blacktriangleright \ q_2^{l^*}(t)=1, q_2^l(t)=0,;\forall l\neq l^*, \\
&\qquad \text{and } q_1^m(t)=0,\ \forall m, \\
&\qquad \text{if } [\Lambda_2(t)\geq\Lambda_1(t) \text{ and } \Lambda_2(t)>0], \\
&\text{Silence} \ \blacktriangleright \ q_1^m(t)=0, \forall m \text{ and } q_2^l(t)=0,\ \forall l, \\
&\qquad \text{if } [\Lambda_1(t)=0 \text{ and } \Lambda_2(t)=0], \quad (25)
\end{aligned}$$

where $\Lambda_1(t)$ and $\Lambda_2(t)$ are given by

$$\Lambda_1(t)=\mu C_1^e(t), \quad (26)$$

$$\Lambda_2(t)=(1-\mu)C_2^e(t), \quad (27)$$

and m^* and l^* are given by (19) and (20), respectively. In (26) and (27), μ is a priori given constant which satisfies $0\leq\mu\leq 1$. By varying μ from zero to one, the entire boundary line of the BS-U1 and BS-U2 throughput region can be obtained.

Proposition 1: The variables $\gamma_{I1}^e(t)$ and $\gamma_{I2}^e(t)$, found in the expressions in (23) and (24), which maximize the BS-U1 and BS-U2 throughput region of the D-TFDD scheme for unknown ICI proposed in (25) are found as follow

$$\gamma_{I1}^e(t+1)=\gamma_{I1}^e(t)-\delta_1(t)\,\Phi_1(t), \quad (28)$$

$$\gamma_{I2}^e(t+1)=\gamma_{I2}^e(t)-\delta_2(t)\,\Phi_2(t), \quad (29)$$

where $\delta_k(t)$, for $k\in\{1,2\}$, can be some properly chosen monotonically decaying function of t with $\delta_k(1)<1$, such as $\frac{1}{2t}$. Furthermore, $\Phi_1(t)$ and $\Phi_2(t)$ in (28) and (29) are obtained as respectively, where $\delta_1^{m^*}(t)$ and $\delta_2^{l^*}(t)$, are defined as

$$\delta_1^{m^*}(t)=\begin{cases}1 & \text{if } \left(R_1^{m^*}-C_1^e(t-1)\right)\left(R_1^{m^*}-C_1^e(t)\right)\leq 0\\ 0 & \text{if } \left(R_1^{m^*}-C_1^e(t-1)\right)\left(R_1^{m^*}-C_1^e(t)\right)>0,\end{cases} \quad (32)$$

and

$$\delta_2^{l^*}(t)=\begin{cases}1 & \text{if } \left(R_2^{l^*}-C_2^e(t-1)\right)\left(R_2^{l^*}-C_2^e(t)\right)\leq 0\\ 0 & \text{if } \left(R_2^{l^*}-C_2^e(t-1)\right)\left(R_2^{l^*}-C_2^e(t)\right)>0,\end{cases} \quad (33)$$

respectively. On the other hand, the variables $\chi_1^e(t)$ and $\chi_2^e(t)$ in (30) and (31), shown at the bottom of this page, are calculated as

$$\chi_k^e(t+1)=\chi_k^e(t)+\delta_k^\chi(t)\left[\bar{\epsilon}_k(t)-\epsilon\right]^+, \quad k\in\{1,2\}, \quad (34)$$

where $\delta_k^\chi(t)$ for $k\in\{1,2\}$ can be some properly chosen monotonically decaying function of t with $\delta_k^\chi(1)<1$, such as $\frac{1}{2t}$, ϵ is a small constant which can be configured at the system level, and $[.]^+$ denotes only positive values. Moreover, in (34), $\bar{\epsilon}_k(t)$, for $k\in\{1,2\}$, are obtained as

$$\bar{\epsilon}_1(t)=\frac{t-1}{t}\bar{\epsilon}_U(t-1)+\frac{1}{t}q_1^{m^*}(t)\left(O_1^{m^*}(t)-O_{1,e}^{m^*}(t)\right)^2, \quad (35)$$

$$\bar{\epsilon}_2(t)=\frac{t-1}{t}\bar{\epsilon}_D(t-1)+\frac{1}{t}q_2^{l^*}(t)\left(O_2^{l^*}(t)-O_{2,e}^{l^*}(t)\right)^2. \quad (36)$$

Finally, we note that, $\bar{\epsilon}_k(0)$, $\Phi_k(0)$, $\chi_k^e(0)$, and $\gamma_{Ik}^e(0)$, $k\in\{1,2\}$, found in (28)-(36), are initialized to zero. The variables $\Phi_1(t)$, $\Phi_2(t)$, $\chi_1^e(t+1)$, $\chi_2^e(t+1)$, $\delta_1^{m^*}(t)$, $\delta_2^{l^*}(t)$, $\bar{\epsilon}_1(t)$ and $\bar{\epsilon}_2(t)$ are auxiliary variables used for real-time estimation of the ICIs $\gamma_{I1}^e(t)$ and $\gamma_{I2}^e(t)$.

The D-TFDD scheme for unknown ICI is provided in an algorithmic form in Algorithm 1.

Proof: Please refer to Appendix C for the proof. ■

Remark 3: All equations from (19) to (36) are straightforward calculations that do not depend on any hidden function or loop routines. As a result, the complexity of Algorithm 1 grows linearly with M or L.

Remark 4: Note that for the D-TFDD scheme for unknown ICI proposed above, the functions $\Phi_1(t)$ and $\Phi_2(t)$ need to be calculated at the end of time slot t. To this end, note that all the variables in (30) and (31) are known at the end of time time slot t. In particular, the outage variables $O_1^{m^*}(t)$ and $O_2^{l^*}(t)$ either are already available at the BS if the BS is the receiver node at the end of time slot t, or are computed at the BS by a 1-bit feedback from the transmitting node. Moreover, $O_1^{m^*}(t)=1$ if the message received by the receiving node of the BS-U1 channel is decoded successfully in time slot t, otherwise $O_1^{m^*}(t)=0$. Similarly, $O_2^{l^*}(t)=1$ if the message received by the receiving node of the BS-U2 channel is decoded successfully in time slot t, otherwise $O_2^{l^*}(t)=0$. Hence, the BS is able to calculate (30) and (31) at the end of time slot t, compute $\gamma_{I1}^e(t+1)$ and $\gamma_{I2}^e(t+1)$ by using (28) and (29) at the end of time slot t, and use it at the start of

$$\begin{aligned}
\Phi_1(t)=&\frac{t-1}{t}\,\Phi_1(t-1)\\
&-\frac{1}{t}\frac{P_1\gamma_1(t)\delta_1^{m^*}(t)\ q_1^{m^*}(t)\left(2\chi_1^e(t)\left[O_{1,e}^{m^*}(t)-O_1^{m^*}(t)\right]-\mu R_1^{m^*}\right)}{\ln(2)\left(1+\gamma_{I1}^e(t)+P_1\gamma_1(t)\right)\left(1+\gamma_{I1}^e(t)\right)}
\end{aligned} \quad (30)$$

$$\begin{aligned}
\Phi_2(t)=&\frac{t-1}{t}\,\Phi_2(t-1)\\
&-\frac{1}{t}\frac{P_2\gamma_2(t)\delta_2^{l^*}(t)q_2^{l^*}(t)\left(-1mm2\chi_2^e(t)\left[O_{2,e}^{l^*}(t)-O_2^{l^*}(t)\right]-(1--1mm\mu)R_2^{l^*}\right)}{\ln(2)\left(1+\gamma_{I2}^e(t)+P_2\gamma_2(t)\right)\left(1+\gamma_{I2}^e(t)\right)}
\end{aligned} \quad (31)$$

Algorithm 1 Finding the Optimal Decision Variables, $q_1^m, \forall m$, and $q_2^l(t), \forall l$, for a Given Value of μ

Initiate $\bar{\epsilon}_k(0)$, $\Phi_k(0)$, $\chi_k^e(1)$, and $\gamma_{Ik}^e(1)$, $k \in \{1,2\}$ to zero
procedure $\forall\, t \in \{1,2,\ldots,T\}$
  ****** Start of time slot t*****
  compute $C_1^e(t)$ and $C_2^e(t)$ with (23) and (24);
  compute $O_{1,e}^m(t)$ and $O_{2,e}^l(t)$ with (21) and (22);
  compute m^* and l^* with (19) and (20);
  compute $\Lambda_1(t)$ and $\Lambda_2(t)$ with (26) and (27);
  compute $q_1^m, \forall m$ and $q_2^l(t), \forall l$ with (25);
  ******Scheduling Decisions Sent for Execution*****
  ******Transmission of data begins*****
  ******Transmission of data ends*****
  ******Feedback, $O_1^{m^*}(t)/O_2^{l^*}(t)$, Received*****
  update $\bar{\epsilon}_1(t)$ and $\bar{\epsilon}_2(t)$ with (35) and (36);
  compute $\delta_1^{m^*}(t)$ and $\delta_2^{l^*}(t)$ with (32) and (33);
  update $\Phi_1(t)$ and $\Phi_2(t)$ with (30) and (31);
  ******Estimation for Next Time Slot, $t+1$*****
  update $\chi_1^e(t+1)$ and $\chi_2^e(t+1)$ with (34);
  update $\gamma_{I1}^e(t+1)$ and $\gamma_{I2}^e(t+1)$ with (28) and (29);
  ****** End of time slot t*****

time slot $t+1$ by plugging in (23) and (24), then plug (23) and (24) into (26) and (27), respectively, and thereby be able to compute the selection variables in (25).

Remark 5: If the statistical characteristics of the ICI remain constant over time, $\gamma_{I1}^e(t)$ and $\gamma_{I2}^e(t)$ in (28) and (29) converge to constants such as $\lim_{t\to\infty} \gamma_{I1}^e(t) = \gamma_{I1}$ and $\lim_{t\to\infty} \gamma_{I2}^e(t) = \gamma_{I2}$. On the other hand, if the statistical characteristics of the ICI is slowly changing over time, the proposed D-TFDD still works.

B. Diversity Gain of the Proposed D-TFDD for Unknown ICI

It is quite interesting to investigate the diversity gain that the D-TFDD scheme for unknown ICI, proposed in Section IV-A, achieves. In the following, we derive the asymptotic outage probabilities of the BS-U1 and the BS-U2 channels, achieved with the D-TFDD scheme for unknown ICI proposed in Sec. IV-A for the case when $\mu = \frac{1}{2}$, $M = L = 1$, and $R_1^1 = R_2^1 = R_0$.

Theorem 3: The asymptotic outage probability of the D-TFDD scheme for unknown ICI, proposed in Section IV-A, for the case of Rayleigh fading and when $\mu = \frac{1}{2}$, $M = L = 1$, $P_1 = P_2 = P$, and $R_1^1 = R_2^1 = R_0$ hold, is given by

$$P_{\text{out}} \to \frac{\gamma_{\text{th}}^2}{\Omega_0^2}\left[\hat{\Omega}_{I1} + \hat{\Omega}_{I2} + \hat{\Omega}_{IS}\right], \quad \text{as } P \to \infty, \tag{37}$$

where $\gamma_{\text{th}} = \frac{2^{R_0}-1}{P}$, $\Omega_0 = E\left\{\frac{|h_1(t)|^2}{\sigma_1^2(1+\gamma_{I1})}\right\} = E\left\{\frac{|h_2(t)|^2}{\sigma_2^2(1+\gamma_{I2})}\right\}$,

$$\hat{\Omega}_{I1} = \Omega_I\left(\frac{1+\gamma_{I2}}{1+\gamma_{I1}}\right) \times \left(\sum_{n=0}^{K-1}[1+(n+1)\Omega_I]e^{-\frac{\gamma_{I1}}{\Omega_I}}\sum_{t=0}^{n}\frac{\left(\frac{\gamma_{I1}}{\Omega_I}\right)^i}{t!}\right), \tag{38}$$

$$\hat{\Omega}_{I2} = \Omega_I\left(\frac{1+\gamma_{I1}}{1+\gamma_{I2}}\right) \times \left(\sum_{n=0}^{K-1}[1+(n+1)\Omega_I]e^{-\frac{\gamma_{I2}}{\Omega_I}}\sum_{t=0}^{n}\frac{\left(\frac{\gamma_{I2}}{\Omega_I}\right)^i}{t!}\right), \tag{39}$$

$$\hat{\Omega}_{IS} = (1+\gamma_{I1})(1+\gamma_{I2}), \tag{40}$$

$$\Omega_I = E\{\gamma_{I1}(t)\} = E\{\gamma_{I2}(t)\}. \tag{41}$$

In the above expression, γ_{I1} and γ_{I2} are constant values obtained as $\lim_{t\to\infty} \gamma_{I1}^e(t) = \gamma_{I1}$ and $\lim_{t\to\infty} \gamma_{I2}^e(t) = \gamma_{I2}$. It is clear from (37) that P_{out} has a diversity gain of two.

Proof: Please refer to Appendix D for the proof. ■

The result in Theorem 3 shows that the D-TFDD scheme for unknown ICI proposed in Sec. IV-A achieves double the diversity gain compared to existing duplexing schemes, which leads to very large performance gains. Moreover, Theorem 3 shows that doubling of the diversity gain on both the BS-U1 and BS-U2 channels is achievable even when there is no ICI knowledge at the nodes, which is a very interesting result that shows the superior performance of the D-TFDD scheme for unknown ICI proposed in Sec. III-A compared to existing duplexing schemes.

V. Simulation and Numerical Results

In this section, we evaluate the performance of the proposed D-TFDD scheme for unknown ICI and its upper bound, the proposed D-TFDD scheme for known ICI. Then, we compare its performance to the performance achieved with a static-TDD scheme and to the state-of-the-art D-TDD and D-FDD schemes. To this end, we first introduce the benchmark schemes and then present the numerical results.

A. Benchmark Schemes

1) Static-TDD: In the static-TDD scheme, see [2], the BS receives and transmits in prefixed time slots. Assuming single transmission rates at the transmitting nodes of the BS-U1 and BS-U2 channels, and assuming that that the fractions of the total number of time slots, T, allocated on the BS-U1 and BS-U2 channels are μ and $1-\mu$, respectively, e.g., channel BS-U1 is active in the first μT and channel BS-U2 is active in following $(1-\mu)T$ time slots, the BS-U1 and BS-U2 throughput during $T \to \infty$ time slots, is given by

$$\bar{R}_k = \lim_{T\to\infty} \frac{\mu_k}{T}\sum_{t=1}^{T} O_k^1(t)R_k^1, \quad k \in \{1,2\}, \tag{42}$$

and the outage probability is given by

$$P_{\text{out}} = 1 - \lim_{T\to\infty}\left(\frac{1}{T}\sum_{t=1}^{\mu T} O_1^1(t) + \sum_{t=\mu T+1}^{T} O_2^1(t)\right), \tag{43}$$

where $O_k^1(t)$, $k \in \{1,2\}$, is defined as

$$O_k^1(t) = \begin{cases} 1 & \text{if } \log_2\left(1+\frac{P_k}{\mu_k}\gamma_k(t)\right) \geq R_k^1 \\ 0 & \text{if } \log_2\left(1+\frac{P_k}{\mu_k}\gamma_k(t)\right) < R_k^1. \end{cases} \tag{44}$$

2) D-TDD Scheme: The distributed D-TDD scheme proposed in [25] is considered as a benchmark for comparison. We note that this scheme requires full knowledge of the ICI, which, as argued in Section II-D, is not practical. In addition, we note that this scheme without ICI knowledge transforms to the static-TDD. Hence, the practical distributed TDD scheme

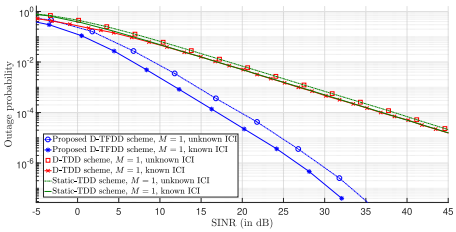

Fig. 5. Outage probability of the proposed D-TFDD schemes. Local-CSI and Full-CSI labels highlight that the corresponding schemes are without and with ICI knowledge, respectively.

is the static-TDD since it does not need ICI knowledge. The distributed D-TDD scheme in [25] can serve only as an upper bound to the practical static-TDD.

Note that D-TDD and D-FDD schemes only different in how they share the time and frequency resources, but achieve the same performance. Therefore, for comparison purposes, we can use either of them. In the following, we choose the D-TDD scheme.

B. Numerical Results

All of the results presented in this section have been performed by numerical evaluation of the derived results and are confirmed by Monte Carlo simulations. Moreover, Rayleigh fading for the BS-U1 and BS-U2 channels, and Chi-square distribution for the ICI at the receiving nodes of the BS-U1 and BS-U2 channels are assumed. In all the numerical examples in Figs. 5-7, we assume $M = L$ and $R_1^k = R_2^k = kR$, for $k = 1, 2, \ldots, M$, where R is defined differently depending on the corresponding example. The signal to interference plus noise ratio (SINR) is defined as the ratio of the average received signal power to interference power plus the noise power.

1) Constraint on the Average Transmit Power: In the numerical examples, we select the fixed powers P_1 and P_2 such that the following long-term power constraints hold

$$\lim_{T\to\infty} \frac{1}{T} \sum_{t=1}^{T} \sum_{m=1}^{M} q_1^m(t) P_1 \leq \bar{P}_1$$
$$\text{and} \quad \lim_{T\to\infty} \frac{1}{T} \sum_{t=1}^{T} \sum_{l=1}^{L} q_2^l(t) P_2 \leq \bar{P}_2. \tag{45}$$

This enables all duplexing schemes to use identical average transmit powers, and thereby enable fair comparison between the different schemes.

2) Outage Probability: In Fig. 5, we illustrate the outage probabilities of the proposed D-TFDD schemes for unknown ICI and its upper bound, the D-TFDD for known ICI, as well as the benchmark schemes as a function of the SINR for $M = 1$, $\mu = \frac{1}{2}$, where R is set to $R = 1$ bits/symb. As predicted by Theorems 2 and 3, Fig. 5 shows that the proposed D-TFDD schemes for unknown and known ICI achieve double the diversity gain compared to the benchmark schemes. Intuitively, the doubling of the diversity gain occurs since the proposed D-TFDD schemes can select for transmission between two independent channels, in each time slot, compared to the existing D-TDD and D-FDD system, which can select between two dependent channels, in each time slot. The doubling of the diversity gain leads to very large performance gains in terms of SINR. For example, SINR gains of 10 dB and 15 dB can be achieved for outage probabilities of 10^{-2} and 10^{-3}, respectively. On the other hand, the proposed D-TFDD schemes for unknown ICI has around 3 dB penalty loss compared its upper bound, the proposed D-TFDD schemes for known ICI. This example shows the large performance gains of the proposed D-TFDD scheme with unknown ICI compared to existing D-TDD and/or static-TDD schemes.

3) Throughput Region: For the example in Fig. 6 users have ominidirectional antenna with unity gain and the BS has a directional antenna with gain of 16 dBi. The power at the users is set to 24 dBm and the power at BS is set to 46 dBm, and we use the proposed scheme with Type 1 and Type 2 for this example. The distances between U1 and BS, as well as BS and U2, are assumed to be fixed and set to 700m. The noise figure of BS and U2 are set to 2 dB and 7 dB, respectively. The above parameters reflect the parameters used in practice. In addition, the mean power of the channel gains of the BS-U1 and BS-U2 channels are calculated using the standard path-loss model as [29]–[31]

$$E\{|h_k(t)|^2\} = \left(\frac{c}{4\pi f_c}\right)^2 d_k^{-\beta} \quad \text{for } k \in \{1, 2\}, \tag{46}$$

where c is the speed of light, f_c is the carrier frequency, d_k is the distance between the transmitter and the receiver of link k, and β is the path loss exponent. Moreover, the carrier frequency is set to $f_c = 1.9$ GHz, and we assume $\beta = 3.6$ for the BS-U1 and BS-U2 channels.

In Fig. 6, we show the throughput region achieved with the proposed D-TFDD schemes for unknown and known ICI with $M = 1$, for two different scenarios, one with high interference, SINR=10 dB, and the other one with low interference, SINR=20 dB. Furthermore, we show the throughput regions achieved with the benchmark schemes. For the proposed and the benchmark schemes the value of R is optimized numerically for a given μ such that the throughput is maximized. As can be seen from Fig. 6, the proposed D-TDD scheme without ICI knowledge achieves almost the exact throughput region as its upper bound achieved with D-TFDD with full ICI knowledge for SINR=20 dB. Also, in the relatively high interference region, i.e., SINR=10 dB, the proposed D-TFDD scheme without ICI knowledge achieves a throughput region which is very close to its upper bound achieved with the D-TFDD scheme with ICI knowledge. On the other hand, the throughput that the proposed D-TFDD scheme for unknown ICI achieves is close or higher than the throughput achieved with the benchmark D-TDD scheme with ICI knowledge, which is an interesting result since the proposed scheme without ICI knowledge wastes only two time slots compared to the K time slots that the D-TDD and D-FDD schemes with ICI knowledge waste. More importantly, the gains that the proposed D-TFDD scheme for unknown ICI achieves compared to the benchmark schemes without ICI knowledge are considerable. For example, the proposed D-TFDD scheme

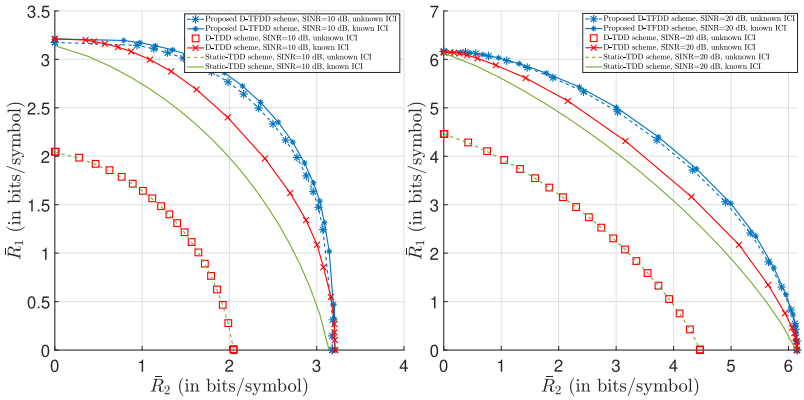

Fig. 6. Throughput regions of the proposed D-TFDD schemes: left for SINR=10 dB, and right for SINR=20 dB.

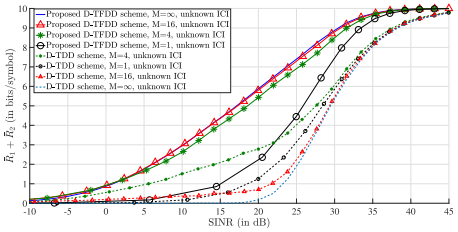

Fig. 7. Throughputs vs. SINR of the proposed D-TFDD schemes with and without ICI knowledge with different discrete-rates quantization level.

for unknown ICI has a BS-U1 throughput gain of about 66%, 80% and 100%, for SINR=10 dB, and about 17%, 18% and 38%, for SINR=20 dB, compared to the existing D-TDD and to the static-TDD schemes without ICI knowledge for a BS-U2 throughput of 2, 3, and 4 bits/symb, respectively.

4) Sum Throughput: In Fig. 7, we illustrate the sum of the BS-U1 and BS-U2 throughputs achieved with the proposed D-TFDD scheme for unknown ICI and the static-TDD as a function of the SINR for $M = 1, 4, 16, \infty$, where R is set to $R = 10/M$ bits/symb. From Fig. 7 we can see that by increasing M from 1 to 4 in the proposed D-TFDD scheme for unknown ICI, we can gain more than 10 dBs in SINR for around 4 bits/symb sum throughput. Whereas, by increasing M from 4 to 16 we can gain an additional 1 dB in SINR for around 4 bits/symb of the sum throughput. Moreover, the proposed D-TFDD scheme for unknown ICI achieves substantial gains compared to the static-TDD. For example, about 3 dB and 10 dB SINR gain is achieved for $M = 1$ and $M = 4$, respectively, for around 4 bits/symb sum throughput. Finally, Fig. 7 shows that the proposed scheme for $M = 4$ performs very close to the case when $M = \infty$. Note that in Fig. 7, the throughputs saturate since as a function of M, the transmission rates are $10/M$ bits/symb. Hence, the maximum possible transmission rate is 10 bits/symb, even if the channels are error-free, which is the case in the high SINR.

The above numerical examples show that the proposed D-TFDD scheme provides double the diversity gain compared to existing TDD/FDD schemes, which improves that reliability of the communication. Moreover, since the proposed D-TFDD scheme works in a distributed fashion, it does not need any coordination of the BSs. Another strength is that is does not require ICI estimation, which makes it practical for implementation. Finally, the proposed D-TFDD scheme fits well into the scope of 5G. On the other hand, a weakness of the proposed D-TFDD scheme is the requirement of local CSI of the U1-BS and U2-BS channels at the BS, which entails signalling overhead.

VI. Conclusion

In this paper, we proposed a distributed D-TFDD scheme for unknown ICI. Using the proposed D-TFDD scheme, in a given frequency band, the BS adaptively selects to either communicate with U1 or with U2 in a given time slot based on the qualities of the BS-U1 and BS-U2 channels without ICI knowledge such that the BS-U1 and BS-U2 throughput region is maximized. We have shown that the proposed D-TFDD scheme provides significant throughput and outage probability gains compared to the conventional static-TDD scheme, as well as to the D-TDD and D-FDD schemes. Moreover, we observed the the proposed D-TFDD scheme doubles the diversity gain on both the BS-U1 and BS-U2 channels compared to existing duplexing schemes, even when the ICI is unknown, which leads to very large performance gains.

Appendix

A. Proof of Theorem 1

Constraints C1, C2 and C3 in (12) make the problem non-convex. To solve (12), we first we relax these constraints to $0 \leq q_1^m(t) \leq 1$, $0 \leq q_2^l(t) \leq 1$, and $0 \leq \sum_{m=1}^{M} q_1^m(t) + \sum_{l=1}^{L} q_2^l(t) \leq 1$, thereby making the relaxed problem convex. The solutions of the relaxed convex

problem is then shown to be such that $q_1^m(t)$ and $q_2^l(t)$ take the limiting values 0 or 1, and not the values between 0 and 1. As a result, the relaxed convex problem is equivalent to the original problem. To solve the relaxed problem, we use the Lagrangian. Thereby, we obtain

$$\begin{aligned}\mathcal{L} = &- \lim_{T\to\infty}\frac{1}{T}\sum\nolimits_{t=1}^{T}\sum\nolimits_{m=1}^{M}\mu R_1^m q_1^m(t)O_1^m(t)\\ &- \lim_{T\to\infty}\frac{1}{T}\sum\nolimits_{t=1}^{T}\sum\nolimits_{l=1}^{L}(1-\mu)R_2^l q_2^l(t)O_2^l\\ &-\sum\nolimits_{m=1}^{M}\lambda_1^m(t)q_1^m(t) - \left(1-\sum\nolimits_{m=1}^{M}\lambda_2^m(t)q_1^m(t)\right)\\ &-\sum\nolimits_{l=1}^{L}\lambda_3^l(t)q_2^l(t) - \left(1-\sum\nolimits_{l=1}^{L}\lambda_4^l(t)q_2^l(t)\right)\\ &-\lambda_5(t)\left(\sum\nolimits_{m=1}^{M}q_1^m(t)+\sum\nolimits_{l=1}^{L}q_2^l(t)\right)\\ &-\lambda_6(t)\Big(1-\sum_{m=1}^{M}q_1^m(t)-\sum_{l=1}^{L}q_2^l(t)\Big),\end{aligned} \tag{47}$$

where $\lambda_1^m(t) \geq 0$, $\lambda_2^m(t) \geq 0$, $\lambda_3^l(t) \geq 0$, $\lambda_4^l(t) \geq 0$, $\lambda_5(t) \geq 0$, and $\lambda_6(t) \geq 0$, $\forall m, l, i$, are the Lagrangian multipliers. Next, we rewrite (47) as

$$\begin{aligned}\mathcal{L} = &- \lim_{T\to\infty}\frac{1}{T}\sum_{t=1}^{T}\mu q_1(t)\max_m\{R_1^m O_1^m(t)\}\\ &- \lim_{T\to\infty}\frac{1}{T}\sum\nolimits_{t=1}^{T}(1-\mu)q_2(t)\max_l\{R_2^l O_2^l(t)\}\\ &-\sum\nolimits_{m=1}^{M}\lambda_1^m(t)q_1^m(t) - \left(1-\sum\nolimits_{m=1}^{M}\lambda_2^m(t)q_1^m(t)\right)\\ &-\sum\nolimits_{l=1}^{L}\lambda_3^l(t)q_2^l(t) - \left(1-\sum\nolimits_{l=1}^{L}\lambda_4^l(t)q_2^l(t)\right)\\ &-\lambda_5(t)\left(q_1(t)+q_2(t)\right) - \lambda_6(t)\left(1-q_1(t)-q_2(t)\right).\end{aligned} \tag{48}$$

Now, using (48) and defining $-\lambda_5(t)+\lambda_6(t) \triangleq \beta(t)$, we can find the optimal state-selection variables $q_1^m(t)$ and $q_2^l(t)$ as follows. The conditions which maximize (47), in the cases when the transmit node on the BS-U1 channel transmits with R_1^m and the transmit node on the BS-U2 channel is silent, are

$$\begin{aligned}&[\mu\max_m\{R_1^m O_1^m(t)\} - \beta(t) > 0]\\ \text{and}\quad &[(1-\mu)\max_l\{R_2^l O_2^l(t)\} - \beta(t) < 0].\end{aligned} \tag{49}$$

On the other hand, the conditions for maximizing (48) in the case when the transmit node on the BS-U2 channel transmits with R_2^l and the transmit node on the BS-U1 channel is silent, are

$$\begin{aligned}&[\mu\max_m\{R_1^m O_1^m(t)\} - \beta(t) < 0]\\ \text{and}\quad &[(1-\mu)\max_l\{R_2^l O_2^l(t)\} - \beta(t) > 0].\end{aligned} \tag{50}$$

In (49) and (50), we can substitute $\mu R_1^m O_1^m(t)$ with $\Lambda_1^m(t)$ and $(1-\mu)R_2^l O_2^l(t)$ with $\Lambda_2^l(t)$, and thereby obtain $q_1^m(t)$ and $q_2^l(t)$ as in (13). This completes the proof.

B. Proof of Theorem 2

In time slot t, an outage occurs if the BS-U1 channel is selected for transmission and the BS-U1 channel is too weak to support the rate R_0, i.e., $q_1^1(t) = 1$ and $O_1^1(t) = 0$, or if the BS-U2 channel is selected to transmit and the BS-U2 channel is too weak to support the rate R_0, i.e., $q_2^1(t) = 1$ and $O_2^1(t) = 0$, or if both the BS-U1 the BS-U2 channels are not selected for transmission in time slot t, i.e., if $q_1^1(t) = q_2^1(t) = 0$, since in that case the time slot t is wasted. Hence, the outage probability P_{out} can be obtained as

$$\begin{aligned}P_{\text{out}} &= \Pr\Big\{[q_1^1(t)=1 \text{ AND } O_1^1(t)=0]\\ &\qquad \text{OR } [q_2^1(t)=1 \text{ AND } O_2^1(t)=0]\\ &\qquad \text{OR } [q_1^1(t)=q_2^1(t)=0]\Big\}\\ &\overset{(a)}{=} \Pr\big\{q_1^1(t)=1 \text{ AND } O_1^1(t)=0\big\}\\ &\quad + \Pr\big\{q_2^1(t)=1 \text{ AND } O_2^1(t)=0\big\}\\ &\quad + \Pr\big\{q_1^1(t)=q_2^1(t)=0\big\},\end{aligned} \tag{51}$$

where (a) follows since the events $q_1^1(t) = 1$ and $q_1^1(t) = 0$, and also the events $q_2^1(t) = 1$ and $q_2^1(t) = 0$ are mutually exclusive. Since $\mu = \frac{1}{2}$, $\Lambda_1^1(t)$ and $\Lambda_2^1(t)$ in (14) and (15) simplify to

$$\Lambda_k^1(t) = \frac{1}{2}R_0 O_k^1(t), \quad k \in \{1,2\}. \tag{52}$$

Now, inserting $\Lambda_1^1(t)$ and $\Lambda_2^1(t)$ from (52) into (13), we obtain that $q_1^1(t) = 1$ if $O_1^1(t) \geq O_2^1(t)$ and $O_1^1(t) > 0$, which means that $q_1^1(t) = 1$ occurs if $O_1^1(t) = 1$. Hence, the event $q_1^1(t) = 1$ and $O_1^1(t) = 0$ is an impossible event, thereby leading to $\Pr\{q_2^1(t) = 1 \text{ AND } O_2^1(t) = 0\} = 0$ in (51). Similarly, we can conclude that $\Pr\{q_1^1(t) = 1 \text{ AND } O_1^1(t) = 0\} = 0$ in (51). Next, we obtain that $q_1^1(t) = q_2^1(t) = 0$ occurs iff $O_1^1(t) = O_2^1(t) = 0$ holds, thereby leading to $\Pr\{q_1^1(t) = q_2^1(t) = 0\} = \Pr\{O_1^1(t) = 0 \text{ AND } O_2^1(t) = 0\}$ in (51). Inserting this into (51), we obtain

$$\begin{aligned}P_{\text{out}} &= \Pr\{O_1^1(t)=0 \text{ AND } O_2^1(t)=0\}\\ &= \Pr\Bigg\{\log_2\left(1+P\frac{|\gamma_1(t)|^2}{1+\gamma_{I1}(t)}\right) < R_0\\ &\qquad \text{AND } \log_2\left(1+P\frac{|\gamma_2(t)|^2}{1+\gamma_{I2}(t)}\right) < R_0\Bigg\}\\ &= \Pr\Big\{\frac{|\gamma_1(t)|^2}{1+\gamma_{I1}(t)} < \gamma_{\text{th}} \text{ AND } \frac{|\gamma_2(t)|^2}{1+\gamma_{I2}(t)} < \gamma_{\text{th}}\Big\},\end{aligned} \tag{53}$$

where $\gamma_{\text{th}} = \frac{2^{R_0}-1}{P}$. The variables $\gamma_1(t)$ and $\gamma_2(t)$ have identical and independent exponential distributions with PDFs denoted by $f_{\gamma_1}(\gamma_1)$ and $f_{\gamma_2}(\gamma_2)$, respectively, both with mean $\Omega_0 = E\{\frac{|h_1(t)|^2}{\sigma_1^2}\} = E\{\frac{|h_2(t)|^2}{\sigma_2^2}\}$. On the other hand, the variables $\gamma_{I1}(t)$ and $\gamma_{I2}(t)$ have identical yet dependent exponential distributions with joint PDF denoted by $f_{\gamma_{I1},\gamma_{I2}}(Z_1, Z_2)$. As a result, (53) can be obtained as

$$\begin{aligned}P_{\text{out}} = \int_0^\infty\int_0^\infty \int_0^{\gamma_{\text{th}}(1+Z_1)}\int_0^{\gamma_{\text{th}}(1+Z_2)} &f_{\gamma_1,\gamma_2,\gamma_{I1},\gamma_{I2}}(\gamma_1,\gamma_2,Z_1,Z_2)\\ &\times d\gamma_1 d\gamma_2 dZ_1 dZ_2.\end{aligned} \tag{54}$$

We can rewrite $f_{\gamma_1,\gamma_2,\gamma_{I1},\gamma_{I2}}(\gamma_1,\gamma_2,Z_1,Z_2)$ in (54) as

$$\begin{aligned}f_{\gamma_1,\gamma_2,\gamma_{I1},\gamma_{I2}}(\gamma_1,\gamma_2,Z_1,Z_2) &= f_{\gamma_1|\gamma_{I1},\gamma_{I2}}(\gamma_1)\\ &\quad\times f_{\gamma_2|\gamma_{I1},\gamma_{I2}}(\gamma_2) f_{\gamma_{I1},\gamma_{I2}}(Z_1,Z_2),\end{aligned} \tag{55}$$

since γ_1 and γ_2 have independent distributions. By substituting the PDFs of γ_1 and γ_2 into (55), then inserting (55) into (54), we can obtain (54) as

$$P_{\text{out}}=\int_0^{\infty}\int_0^{\infty}\frac{1}{\Omega_0}\int_0^{\gamma_{\text{th}}(1+Z_2)} e^{-(\frac{\gamma_2}{\Omega_0})}d\gamma_2\times\frac{1}{\Omega_0}\int_0^{\gamma_{\text{th}}(1+Z_1)} e^{-(\frac{\gamma_1}{\Omega_0})}d\gamma_1 \times f_{\gamma_{I1},\gamma_{I2}}(Z_1,Z_2)dZ_1dZ_2. \quad (56)$$

In (56), by integrating over γ_1 and γ_2, and letting $P\to\infty$ (consequently $\gamma_{\text{th}}\to 0$), we obtain

$$P_{\text{out}}\to\int_0^{\infty}\int_0^{\infty}\frac{\gamma_{\text{th}}(1+Z_2)}{\Omega_0}\times\frac{\gamma_{\text{th}}(1+Z_1)}{\Omega_0} \times f_{\gamma_{I1},\gamma_{I2}}(Z_1,Z_2)dZ_1dZ_2 \text{ as } P\to\infty. \quad (57)$$

Finally, by replacing

$$E\Big\{(1+\gamma_{I1}(t))(1+\gamma_{I2}(t))\Big\} =\int_0^{\infty}\int_0^{\infty}(1+Z_2)\times(1+Z_1)\times f_{\gamma_{I1},\gamma_{I2}}(Z_1,Z_2)dZ_1dZ_2, \quad (58)$$

into (57), the outage is obtained as in (18). This completes the proof.

C. Proof of Proposition 1

The BS-U1 and BS-U2 throughputs are given in (10) and (11), respectively. However, since we can not compute $O_1^m(t)$ and $O_2^l(t)$, instead of (10) and (11), we use estimates for (10) and (11), given by

$$\bar{R}_{1,e}=\lim_{T\to\infty}\frac{1}{T}\sum_{t=1}^{T}\sum_{m=1}^{M}R_1^m q_1^m(t)O_{1,e}^m(t), \quad (59)$$

$$\bar{R}_{2,e}=\lim_{T\to\infty}\frac{1}{T}\sum_{t=1}^{T}\sum_{l=1}^{L}R_2^l q_2^l(t)O_{2,e}^l(t). \quad (60)$$

The accuracy of the estimates $\bar{R}_{1,e}$ and $\bar{R}_{2,e}$, depends on the following expressions

$$\delta_1=\lim_{T\to\infty}\frac{1}{T}\sum_{t=1}^{T}q_1^m(t)\Big(O_1^m(t)-O_{1,e}^m(t)\Big)^2. \quad (61)$$

$$\delta_2=\lim_{T\to\infty}\frac{1}{T}\sum_{t=1}^{T}q_2^l(t)\Big(O_2^l(t)-O_{2,e}^l(t)\Big)^2. \quad (62)$$

Hence, (61) and (62) express the average of the difference squared between the outages when the ICI is known and the estimation of the outages when the ICI is unknown. The smaller (61) and (62) are, the more accurate the estimates $\bar{R}_{1,e}$ and $\bar{R}_{2,e}$ become. In fact, when $\delta_1\to 0$, and $\delta_2\to 0$, $\bar{R}_{1,e}\to\bar{R}_1$ and $\bar{R}_{2,e}\to\bar{R}_2$.

Now, if $\delta_1<\epsilon$ and $\delta_2<\epsilon$ hold, the constants γ_{I1} and γ_{I2} that maximize the estimated BS-U1 and BS-U2 throughput region, defined in (59) and (60), can be found from the following maximization problem

$$\underset{\gamma_{I1},\gamma_{I2}.}{\text{Maximize:}}\ \lim_{T\to\infty}\frac{1}{T}\sum_{t=1}^{T}\mu R_1^{m^*}q_1^{m^*}(t)O_{1,e}^{m^*}(t) + \lim_{T\to\infty}\frac{1}{T}\sum_{t=1}^{T}(1-\mu)R_2^{l^*}q_2^{l^*}(t)O_{2,e}^{l^*}(t)$$

$$\text{Subject to :}$$

$$\text{C1}:\lim_{T\to\infty}\frac{1}{T}\sum_{t=1}^{T}q_1^{m^*}(t)\Big(O_1^{m^*}(t)-O_{1,e}^{m^*}(t)\Big)^2\le\epsilon,$$

$$\text{C2}:\lim_{T\to\infty}\frac{1}{T}\sum_{t=1}^{T}q_2^{l^*}(t)\Big(O_2^{l^*}(t)-O_{2,e}^{l^*}(t)\Big)^2\le\epsilon, \quad (63)$$

where $m^*=\arg\max_m\{R_1^mO_{1,e}^m(t)\}$ and $l^*=\arg\max_l\{R_2^lO_{2,e}^l(t)\}$.

By applying the Lagrangian function on (63), we obtain

$$\begin{aligned}\mathcal{L}=&-\lim_{T\to\infty}\frac{1}{T}\sum\nolimits_{t=1}^{T}\mu R_1^{m^*}q_1^{m^*}(t)O_{1,e}^{m^*}(t)\\&-\lim_{T\to\infty}\frac{1}{T}\sum\nolimits_{t=1}^{T}(1-\mu)R_2^{l^*}q_2^{l^*}(t)O_{2,e}^{l^*}(t)\\&+\lim_{T\to\infty}\frac{1}{T}\sum\nolimits_{t=1}^{T}\chi_1q_1^{m^*}(t)\Big(O_1^{m^*}(t)-O_{1,e}^{m^*}(t)\Big)^2\\&+\lim_{T\to\infty}\frac{1}{T}\sum\nolimits_{t=1}^{T}\chi_2q_2^{l^*}(t)\Big(O_2^{l^*}(t)-O_{2,e}^{l^*}(t)\Big)^2, \quad (64)\end{aligned}$$

where $\chi_1\ge 0$ and $\chi_2\ge 0$ are the Lagrangian multipliers, found such that C1 and C2 in (63) hold. By differentiating $\mathcal{L}$ in (64) with respect to γ_{I1} and γ_{I2}, and equivalenting the results to zero, we obtain

$$\lim_{T\to\infty}\frac{1}{T}\sum_{t=1}^{T}\left[\frac{-P_1\gamma_1(t)\delta_1^{m^*}(t)q_1^{m^*}(t)}{\ln(2)\Big(1+\gamma_{I1}+P_1\gamma_1(t)\Big)\Big(1+\gamma_{I1}\Big)}\times\Big(-\mu R_1^{m^*}+2\chi_1\big[O_{1,e}^{m^*}(t)-O_1^{m^*}(t)\big]\Big)\right]=0, \quad (65)$$

$$\lim_{T\to\infty}\frac{1}{T}\sum_{t=1}^{T}\left[\frac{-P_2\gamma_2(t)\delta_2^{l^*}(t)q_2^{l^*}(t)}{\ln(2)\Big(1+\gamma_{I2}+P_2\gamma_2(t)\Big)\Big(1+\gamma_{I2}\Big)}\times\Big(-(1-\mu)R_2^{l^*}+2\chi_2\big[O_{2,e}^{l^*}(t)-O_2^{l^*}(t)\big]\Big)\right]=0. \quad (66)$$

Due to the law of large numbers, (65) and (66) can be written as

$$E\left[\frac{-P_1\gamma_1(t)\delta_1^{m^*}(t)q_1^{m^*}(t)}{\ln(2)\Big(1+\gamma_{I1}+P_1\gamma_1(t)\Big)\Big(1+\gamma_{I1}\Big)}\times\Big(-\mu R_1^{m^*}+2\chi_1\big[O_{1,e}^{m^*}(t)-O_1^{m^*}(t)\big]\Big)\right]=0, \quad (67)$$

$$E\left[\frac{-P_2\gamma_2(t)\delta_2^{l^*}(t)q_2^{l^*}(t)}{\ln(2)\Big(1+\gamma_{I2}+P_2\gamma_2(t)\Big)\Big(1+\gamma_{I2}\Big)}\times\Big(-(1-\mu)R_2^{l^*}+2\chi_2\big[O_{2,e}^{l^*}(t)-O_2^{l^*}(t)\big]\Big)\right]=0. \quad (68)$$

Calculating the constants γ_{I1} and γ_{I2} from (67) and (68) requires the derivation of the above expectations. Instead, we use a more practical approach, where the constants γ_{I1} and γ_{I2} are estimated as $\gamma_{I1}^e(t)$ and $\gamma_{I2}^e(t)$ in time slot t. To this end, we apply the gradient descent method [32] on (65) and (66) to obtain $\gamma_{I1}^e(t)$ and $\gamma_{I2}^e(t)$ as in (28) and (29), where $\delta_k(t)$ for $k\in\{1,2\}$ is an adaptive step size which controls the speed of convergence of $\gamma_{Ik}^e(t)$ to γ_{Ik}, for $k\in\{1,2\}$, which can be some properly chosen monotonically decaying

function of t with $\delta_k(1) < 1$. Note that $\lim_{t\to\infty} \gamma^e_{I1}(t) = \gamma_{I1}$ and $\lim_{t\to\infty} \gamma^e_{I2}(t) = \gamma_{I2}$. This completes the proof.

D. Proof of Theorem 3

In time slot t, an outage occurs if the BS-U1 channel is selected for transmission and the BS-U1 channel is too weak to support the rate R_0, i.e., $q^1_1(t) = 1$ and $O^1_1(t) = 0$, or if the BS-U2 channel is selected to transmission and the BS-U2 channel is too weak to support the rate R_0, i.e., $q^1_2(t) = 1$ and $O^1_2(t) = 0$, or if both the BS-U1 and BS-U2 channels are not selected for transmission in time slot t, i.e., if $q^1_1(t) = q^1_2(t) = 0$, since in that case the time slot t is wasted. Assuming that $\gamma^e_{I1}(t)$ and $\gamma^e_{I2}(t)$ have converged to their steady states given by $\lim_{t\to\infty} \gamma^e_{I1}(t) = \gamma_{I1}$ and $\lim_{t\to\infty} \gamma^e_{I2}(t) = \gamma_{I2}$, the outage probability, P_{out}, can be found as

$$\begin{aligned} P_{\text{out}} \;=\; & \Pr\Big\{[q^1_1(t) = 1 \text{ AND } O^1_1(t) = 0] \\ & \quad \text{OR } [q^1_2(t) = 1 \text{ AND } O^1_2(t) = 0] \\ & \quad \text{OR } [q^1_1(t) = q^1_2(t) = 0]\Big\} \\ \overset{(a)}{=} \; & \Pr\big\{q^1_1(t) = 1 \text{ AND } O^1_1(t) = 0\big\} \\ & + \Pr\big\{q^1_2(t) = 1 \text{ AND } O^1_2(t) = 0\big\} \\ & + \Pr\big\{q^1_1(t) = q^1_2(t) = 0\big\}, \end{aligned} \tag{69}$$

where (a) follows since the events $q^1_1(t) = 1$ and $q^1_1(t) = 0$, and also the events $q^1_2(t) = 1$ and $q^1_2(t) = 0$ are mutually exclusive.

We divide (69) into three events; BS-U1 communication event, $[q^1_1(t) = 1 \text{ AND } O^1_1(t) = 0]$, BS-U2 communication event $[q^1_2(t) = 1 \text{ AND } O^1_2(t) = 0]$, and the silent event $[q^1_1(t) = q^1_2(t) = 0]$. In the following, we calculate the probability of these three events.

For the BS-U1 communication event, we have $q^1_1(t) = 1$ when either of the two following events occur

- $O^1_{1,e}(t) = 1$ and $O^1_{2,e}(t) = 0$. This event occurs when $\frac{\gamma_1(t)}{1+\gamma_{I1}} \geq \gamma_{\text{th}}$ and $\frac{\gamma_2(t)}{1+\gamma_{I2}} < \gamma_{\text{th}}$, where $\gamma_{\text{th}} = \frac{2^{R_0}-1}{P}$.
- $O^1_{1,e}(t) = O^1_{2,e}(t) = 1$ and $\gamma^e_U(t) \geq \gamma^e_D(t)$. This event occurs when $\frac{\gamma_1(t)}{1+\gamma_{I1}} > \gamma_{\text{th}}$, $\frac{\gamma_2(t)}{1+\gamma_{I2}} > \gamma_{\text{th}}$, and $\frac{\gamma_1(t)}{1+\gamma_{I1}} \geq \frac{\gamma_2(t)}{1+\gamma_{I2}}$.

On the other hand, the event $O^1_1(t) = 0$ occurs with the following probability

$$\Pr\Big\{O^1_1(t) = 0\Big\} = \Pr\left(\frac{\gamma_1(t)}{1+\gamma_{I1}(t)} < \gamma_{\text{th}}\right), \tag{70}$$

where $\gamma_{I1}(t)$ is the sum of K identical and independent random variables with mean (identical mean is assumed for simplicity) Ω_I, which has the following PDF

$$f_{\gamma_{I1}}(z) = \frac{z^{K-1}e^{-\frac{z}{\Omega_I}}}{\Omega^K_I(K-1)!} \tag{71}$$

and the following cumulative distribution function (CDF)

$$F_{\gamma_{I1}}(z) = 1 - \sum_{n=0}^{K-1} \frac{1}{n!} e^{-\frac{z}{\Omega_I}} \left(\frac{z}{\Omega_I}\right)^n. \tag{72}$$

In addition, the variables $\gamma_1(t)$ and $\gamma_2(t)$ have i.i.d. exponential distributions with PDFs, $f_{\gamma_1}(\gamma_1)$ and $f_{\gamma_2}(\gamma_2)$, respectively, that have mean $\Omega_0 = E\{\frac{|h_1(t)|^2}{\sigma^2_1}\} = E\{\frac{|h_2(t)|^2}{\sigma^2_2}\}$.

Using the above, we can rewrite $\Pr\Big\{q^1_1(t) = 1 \text{ AND } O^1_1(t) = 0\Big\}$ in an integral form as

$$\begin{aligned} & \Pr\Big\{q^1_1(t) = 1 \text{ AND } O^1_1(t) = 0\Big\} \\ & = \int_{\gamma_{\text{th}}(1+\gamma_{I2})}^{\infty} \int_{0}^{\gamma_{\text{th}}(1+\gamma_{I1})} \Pr\left(Z > \frac{\gamma_1}{\gamma_{\text{th}}} - 1\right) f_{\gamma_1}(\gamma_1) f_{\gamma_2}(\gamma_2) d\gamma_2 d\gamma_1 \\ & \quad + \int_{\gamma_{\text{th}}(1+\gamma_{I2})}^{\infty} \int_{\gamma_2\left(\frac{1+\gamma_{I1}}{1+\gamma_{I2}}\right)}^{\infty} \Pr\left(Z > \frac{\gamma_1}{\gamma_{\text{th}}} - 1\right) f_{\gamma_1}(\gamma_1) f_{\gamma_2}(\gamma_2) d\gamma_1 d\gamma_2 \\ & \overset{(a)}{=} \int_{\gamma_{\text{th}}(1+\gamma_{I1})}^{\infty} \int_{0}^{\gamma_1\left(\frac{1+\gamma_{I2}}{1+\gamma_{I1}}\right)} \sum_{n=0}^{K-1} \frac{1}{n!} e^{-\left(\frac{[\frac{\gamma_1}{\gamma_{\text{th}}} - 1]}{\Omega_I}\right)} \left(\frac{[\frac{\gamma_1}{\gamma_{\text{th}}} - 1]}{\Omega_I}\right)^n \\ & \quad \times f_{\gamma_1}(\gamma_1) f_{\gamma_2}(\gamma_2) d\gamma_2 d\gamma_1, \end{aligned} \tag{73}$$

where (a) follows from (72). Now, performing the integration with respect to γ_2, we obtain

$$\begin{aligned} & \Pr\Big\{q^1_1(t) = 1 \text{ AND } O^1_1(t) = 0\Big\} \\ & = \frac{\gamma_{\text{th}}\Omega_I e^{-\left(\frac{\gamma_{\text{th}}}{\Omega_0}\right)}}{\Omega_0} \int_{\frac{\gamma_{I1}}{\Omega_I}}^{\infty} \sum_{n=0}^{K-1} \frac{1}{n!} e^{-U'} (U')^n e^{-\left(\frac{\gamma_{\text{th}}\Omega_I U'}{\Omega_0}\right)} \\ & \quad \times \left(1 - e^{-\left[\left(\frac{\gamma_{\text{th}}}{\Omega_0}\right)(1+\Omega_I U')\left(\frac{1+\gamma_{I2}}{1+\gamma_{I1}}\right)\right]}\right) dU', \end{aligned} \tag{74}$$

where $U' = \frac{\left(\frac{\gamma_1}{\gamma_{\text{th}}} - 1\right)}{\Omega_I}$. In (74), when $P \to \infty$, and consequently $\gamma_{\text{th}} \to 0$, we can approximate $(1 - e^{-[(\frac{\gamma_{\text{th}}}{\Omega_0})(1+\Omega_I U')(\frac{1+\gamma_{I2}}{1+\gamma_{I1}})]})$ by $([(\frac{\gamma_{\text{th}}}{\Omega_0})(1 + \Omega_I U')(\frac{1+\gamma_{I2}}{1+\gamma_{I1}})])$, $e^{-(\frac{\gamma_{\text{th}}}{\Omega_0})}$ by 1, and $e^{-(\frac{\gamma_{\text{th}}\Omega_I U'}{\Omega_0})}$ by 1. As a result, (74) can be rewritten as

$$\begin{aligned} & \Pr\Big\{q^1_1(t) = 1 \text{ AND } O^1_1(t) = 0\Big\} \\ & \to \frac{\gamma^2_{\text{th}}\Omega_I}{\Omega^2_0} \times \frac{1+\gamma_{I2}}{1+\gamma_{I1}} \left[\sum_{n=0}^{K-1} \frac{1}{n!} \int_{\frac{\gamma_{I1}}{\Omega_I}}^{\infty} e^{-U'} (U')^n dU' \right. \\ & \quad \left. + \Omega_I \sum_{n=0}^{K-1} \frac{1}{n!} \int_{\frac{\gamma_{I1}}{\Omega_I}}^{\infty} e^{-U'} (U')^{n+1} dU'\right] \text{ as } P \to \infty. \end{aligned} \tag{75}$$

By calculating the integrals and the summations in (75), we obtain

$$\Pr\Big\{q^1_1(t) = 1 \text{ AND } O^1_1(t) = 0\Big\} \to \frac{\gamma^2_{\text{th}}\hat{\Omega}_{I1}}{\Omega^2_0} \quad \text{as } P \to \infty, \tag{76}$$

where $\hat{\Omega}_{I1}$ is given in (38).

For the BS-U2 communication event, we obtain that $q^1_2(t) = 1$ if $O^1_{2,e}(t) = 1$ and $O^1_{1,e}(t) = 0$, or $O^1_{2,e}(t) = O^1_{1,e}(t) = 1$ and $\frac{\gamma_1(t)}{1+\gamma_{I1}} < \frac{\gamma_2(t)}{1+\gamma_{I2}}$. The

event $O^1_{2,e}(t)=1$ and $O^1_{1,e}(t)=0$ occurs when $\frac{\gamma_2(t)}{1+\gamma_{I2}} > \gamma_{\rm th}$ and $\frac{\gamma_1(t)}{1+\gamma_{I1}} < \gamma_{\rm th}$. The event $O^1_{2,e}(t)=O^1_{1,e}(t)=1$ and $\frac{\gamma_1(t)}{1+\gamma_{I1}} < \frac{\gamma_2(t)}{1+\gamma_{I2}}$ occurs when $\frac{\gamma_2(t)}{1+\gamma_{I2}} > \gamma_{\rm th}$, $\frac{\gamma_1(t)}{1+\gamma_{I1}} > \gamma_{\rm th}$, and $\frac{\gamma_1(t)}{1+\gamma_{I1}} < \frac{\gamma_2(t)}{1+\gamma_{I2}}$. Using this, we can derive $\Pr\Big\{q^1_2(t)=1 \text{ AND } O^1_2(t)=0\Big\}$ with a similar approach as the calculation of $\Pr\Big\{q^1_1(t)=1 \text{ AND } O^1_1(t)=0\Big\}$, which results in

$$\Pr\Big\{q^1_2(t)=1 \text{ AND } O^1_2(t)=0\Big\} \to \frac{\gamma^2_{\rm th}\hat{\Omega}_{I2}}{\Omega^2_0} \quad \text{as } P\to\infty, \quad (77)$$

where $\hat{\Omega}_{I2}$ is given in (39).

Finally, for the silent event, we obtain that $q^1_1(t)=q^1_2(t)=0$ occurs iff $O^1_{1,e}(t)=O^1_{2,e}(t)=0$ holds, which occurs when $\frac{\gamma_2(t)}{1+\gamma_{I2}} < \gamma_{\rm th}$, and $\frac{\gamma_1(t)}{1+\gamma_{I1}} < \gamma_{\rm th}$. The probability of the silent event can be calculated by

$$\Pr\big\{q^1_1(t)=q^1_2(t)=0\big\} = \frac{1}{\Omega^2_0}\int_0^{\gamma_{\rm th}(1+\gamma_{I2})}\int_0^{\gamma_{\rm th}(1+\gamma_{I1})} e^{-(\frac{\gamma_1}{\Omega_0})}e^{-(\frac{\gamma_2}{\Omega_0})}d\gamma_1 d\gamma_2. \quad (78)$$

The expression in (78) for $P\to\infty$, and consequently $\gamma_{\rm th}\to 0$, converges to

$$\Pr\big\{q^1_1(t)=q^1_2(t)=0\big\} \to \frac{\gamma^2_{\rm th}}{\Omega^2_0}\hat{\Omega}_{IS} \quad \text{as } P\to\infty, \quad (79)$$

where $\hat{\Omega}_{IS}$ is given in (40).

Now, by adding (76), (77), and (79), we obtain the asymptotic outage probability as in (37). This completes the proof.

REFERENCES

[1] M. M. Razlighi, N. Zlatanov, and P. Popovski, "On distributed dynamic-TDD schemes for base stations with decoupled uplink-downlink transmissions," in *Proc. IEEE Int. Conf. Commun. Workshops (ICC Workshops)*, May 2018, pp. 1–6.

[2] H. Holma and A. Toskala, *LTE for UMTS: Evolution to LTE-Advanced*. Hoboken, NJ, USA: Wiley, 2011.

[3] *Further Advancements for E-UTRA Physical Layer Aspects*, document TR 36.814, Release 9, v9.0.0, 3GPP, Mar. 2010.

[4] A. K. Gupta *et al.*, "Rate analysis and feasibility of dynamic TDD in 5G cellular systems," in *Proc. IEEE Int. Conf. Commun. (ICC)*, May 2016, pp. 1–6.

[5] Z. Shen, A. Khoryaev, E. Eriksson, and X. Pan, "Dynamic uplink-downlink configuration and interference management in TD-LTE," *IEEE Commun. Mag.*, vol. 50, no. 11, pp. 51–59, Nov. 2012.

[6] S. Adireddy and L. Tong, "Exploiting decentralized channel state information for random access," *IEEE Trans. Inf. Theory*, vol. 51, no. 2, pp. 537–561, Feb. 2005.

[7] S. Lagen, A. Agustin, and J. Vidal, "Joint user scheduling, precoder design, and transmit direction selection in MIMO TDD small cell networks," *IEEE Trans. Wireless Commun.*, vol. 16, no. 4, pp. 2434–2449, Apr. 2017.

[8] K. Lee, Y. Park, M. Na, H. Wang, and D. Hong, "Aligned reverse frame structure for interference mitigation in dynamic TDD systems," *IEEE Trans. Wireless Commun.*, vol. 16, no. 10, pp. 6967–6978, Oct. 2017.

[9] H. Haas and S. Mclaughlin, "A dynamic channel assignment algorithm for a hybrid TDMA/CDMA-TDD interface using the novel TS-opposing technique," *IEEE J. Sel. Areas Commun.*, vol. 19, no. 10, pp. 1831–1846, Oct. 2001.

[10] C. Yoon and D.-H. Cho, "Energy efficient beamforming and power allocation in dynamic TDD based C-RAN system," *IEEE Commun. Lett.*, vol. 19, no. 10, pp. 1806–1809, Oct. 2015.

[11] P. Popovski, O. Simeone, J. J. Nielsen, and C. Stefanovic, "Interference spins: Scheduling of multiple interfering two-way wireless links," *IEEE Commun. Lett.*, vol. 19, no. 3, pp. 387–390, Mar. 2015.

[12] K. Sivarajah and H. Al-Raweshidy, "Dynamic channel allocation for ongoing calls in UTRA TDD system," *Electron. Lett.*, vol. 40, no. 19, pp. 1197–1198, 2004.

[13] C.-H. Chiang, W. Liao, T. Liu, I. Chan, and H.-L. Chao, "Adaptive downlink and uplink channel split ratio determination for TCP-based best effort traffic in TDD-based WiMAX networks," *IEEE J. Sel. Areas Commun.*, vol. 27, no. 2, pp. 182–190, Feb. 2009.

[14] J. Huang, K. Qi, Z. Xu, and C. Yang, "Hybrid full and half duplex networking," in *Proc. IEEE/CIC Int. Conf. Commun. China (ICCC)*, Jul. 2016, pp. 1–6.

[15] J. Liu, S. Han, W. Liu, and C. Yang, "The value of full-duplex for cellular networks: A hybrid duplex-based study," *IEEE Trans. Commun.*, vol. 65, no. 12, pp. 5559–5573, Dec. 2017.

[16] S. Goyal, P. Liu, and S. S. Panwar, "User selection and power allocation in full-duplex multicell networks," *IEEE Trans. Veh. Technol.*, vol. 66, no. 3, pp. 2408–2422, Mar. 2017.

[17] K. Smiljkovikj, P. Popovski, and L. Gavrilovska, "Analysis of the decoupled access for downlink and uplink in wireless heterogeneous networks," *IEEE Wireless Commun. Lett.*, vol. 4, no. 2, pp. 173–176, Apr. 2015.

[18] A. A. Dowhuszko, O. Tirkkonen, J. Karjalainen, T. Henttonen, and J. Pirskanen, "A decentralized cooperative Uplink/Downlink adaptation scheme for TDD small cell networks," in *Proc. IEEE 24th Annu. Int. Symp. Pers., Indoor, Mobile Radio Commun. (PIMRC)*, Sep. 2013, pp. 1682–1687.

[19] B. Yu, L. Yang, H. Ishii, and S. Mukherjee, "Dynamic TDD support in macrocell-assisted small cell architecture," *IEEE J. Sel. Areas Commun.*, vol. 33, no. 6, pp. 1201–1213, Jun. 2015.

[20] *Key Technologies for 5G Wireless Systems*. Cambridge Univ. Press, Cambridge, U.K., 2017.

[21] R. Veronesi, V. Tralli, J. Zander, and M. Zorzi, "Distributed dynamic resource allocation for multicell SDMA packet access net," *IEEE Trans. Wireless Commun.*, vol. 5, no. 10, pp. 2772–2783, Oct. 2006.

[22] I. Spyropoulos and J. Zeidler, "Supporting asymmetric traffic in a TDD/CDMA cellular network via interference-aware dynamic channel allocation and space–time LMMSE joint detection," *IEEE Trans. Veh. Technol.*, vol. 58, no. 2, pp. 744–759, Feb. 2009.

[23] Y. Yu and G. Giannakis, "Opportunistic medium access for wireless networking adapted to decentralized CSI," *IEEE Trans. Wireless Commun.*, vol. 5, no. 6, pp. 1445–1455, Jun. 2006.

[24] V. Venkatasubramanian, M. Hesse, P. Marsch, and M. Maternia, "On the performance gain of flexible UL/DL TDD with centralized and decentralized resource allocation in dense 5G deployments," in *Proc. IEEE 25th Annu. Int. Symp. Pers., Indoor, Mobile Radio Commun. (PIMRC)*, Sep. 2014, pp. 1840–1845.

[25] R. Wang and V. N. Lau, "Robust optimal cross-layer designs for TDD-OFDMA systems with imperfect CSIT and unknown interference: State-space approach based on 1-bit ACK/NAK feedbacks," *IEEE Trans. Commun.*, vol. 56, no. 5, pp. 754–761, May 2008.

[26] S. Sekander, H. Tabassum, and E. Hossain, "Decoupled uplink-downlink user association in multi-tier full-duplex cellular networks: A two-sided matching game," *IEEE Trans. Mobile Comput.*, vol. 16, no. 10, pp. 2778–2791, Oct. 2017.

[27] F. Boccardi *et al.*, "Why to decouple the uplink and downlink in cellular networks and how to do it," *IEEE Commun. Mag.*, vol. 54, no. 3, pp. 110–117, Mar. 2016.

[28] J. Laneman, D. Tse, and G. Wornell, "Cooperative diversity in wireless networks: Efficient protocols and outage behavior," *IEEE Trans. Inf. Theory*, vol. 50, no. 12, pp. 3062–3080, Dec. 2004.

[29] D. Nguyen, L.-N. Tran, P. Pirinen, and M. Latva-aho, "On the spectral efficiency of full-duplex small cell wireless systems," *IEEE Trans. Wireless Commun.*, vol. 13, no. 9, pp. 4896–4910, Sep. 2014.

[30] S. Goyal, P. Liu, S. S. Panwar, R. A. Difazio, R. Yang, and E. Bala, "Full duplex cellular systems: Will doubling interference prevent doubling capacity?" *IEEE Commun. Mag.*, vol. 53, no. 5, pp. 121–127, May 2015.

[31] Y. Sun, D. W. K. Ng, J. Zhu, and R. Schober, "Multi-objective optimization for robust power efficient and secure full-duplex wireless communication systems," *IEEE Trans. Wireless Commun.*, vol. 15, no. 8, pp. 5511–5526, Aug. 2016.

[32] S. Boyd and L. Vandenberghe, *Convex Optimization*. Cambridge, U.K.: Cambridge Univ. Press, 2004.

Mohsen Mohammadkhani Razlighi (Student Member, IEEE) was born in Tehran, Iran, in 1987. He received the B.S. degree in electrical engineering from the University of Zanjan in 2010 and the M.S. degree in telecommunication engineering from the Sharif University of Technology in 2012. He is currently pursuing the Ph.D. degree with Monash University, Melbourne, Australia. His research interests include information theory, wireless communications, and machine learning.

Nikola Zlatanov (Member, IEEE) was born in Macedonia. He received the Dipl.Ing. and master's degrees in electrical engineering from Ss. Cyril and Methodius University, Skopje, Macedonia, in 2007 and 2010, respectively, and the Ph.D. degree from The University of British Columbia (UBC), Vancouver, Canada, in 2015. He is currently a Lecturer (U.S. equivalent to an Assistant Professor) with the Department of Electrical and Computer Systems Engineering (ECSE), Monash University, Melbourne, Australia. His current research interests include wireless communications, information theory, and machine learning. He received several scholarships/awards/grants for his work, including the UBC's Four Year Doctoral Fellowship in 2010, the UBC's Killam Doctoral Scholarship, the Macedonia's Young Scientist of the Year in 2011, the Vanier Canada Graduate Scholarship in 2012, the Best Journal Paper Award from the German Information Technology Society (ITG) in 2014, the Best Conference Paper Award at ICNC in 2016, the ARC Discovery Project, and the ARC Discovery Early Career Researcher Award in 2018.

Petar Popovski (Fellow, IEEE) received the Dipl.-Ing and M.Sc. degrees in communication engineering from the University of Sts. Cyril and Methodius, Skopje, and the Ph.D. degree from Aalborg University in 2005. He is currently a Professor of Aalborg University, where he heads the research section on Connectivity. His research interests are in the area of wireless communication and communication theory. He is also a Steering Committee Member of the IEEE SmartGridComm and the IEEE TRANSACTIONS ON GREEN COMMUNICATIONS AND NETWORKING. He previously served as a Steering Committee Member for the IEEE INTERNET OF THINGS JOURNAL. He received the ERC Consolidator Grant in 2015, the Danish Elite Researcher Award in 2016, the IEEE Fred W. Ellersick Prize in 2016, the IEEE Stephen O. Rice Prize in 2018, and the Technical Achievement Award from the IEEE Technical Committee on Smart Grid Communications in 2019. He was the General Chair of the IEEE SmartGridComm 2018 and the IEEE Communication Theory Workshop 2019. He is currently a Member at Large at the Board of Governors in the IEEE Communication Society. He is also an Area Editor of the IEEE TRANSACTIONS ON WIRELESS COMMUNICATIONS.

Chapter 4

Optimal Centralized Dynamic-Time-Division-Duplex

The preliminary results have been published in the IEEE WCNC, Marrakesh, Morocco, 2019.

- M. M. Razlighi, N. Zlatanov and P. Popovski, "Optimal Centralized Dynamic-TDD Scheduling Scheme for a General Network of Half-Duplex Nodes," IEEE WCNC, Marrakesh, Morocco, 2019.

The complete research, which includes detailed theorems and their proofs have been published in the IEEE Transactions on Wireless Communications as an early access article with doi: 10.1109/TWC.2020.3022990, which included in this chapter.

. M. Razlighi, N. Zlatanov, S. R. Pokhrel and P. Popovski, "Optimal Centralized Dynamic-Time-Division-Duplex," in IEEE Transactions on Wireless Communications, doi: 10.1109/TWC.2020.3022990.

This article has been accepted for publication in a future issue of this journal, but has not been fully edited. Content may change prior to final publication. Citation information: DOI 10.1109/TWC.2020.3022990, IEEE Transactions on Wireless Communications

Optimal Centralized Dynamic-Time-Division-Duplex

Mohsen Mohammadkhani Razlighi, *Student Member, IEEE*, Nikola Zlatanov, *Member, IEEE*, Shiva Raj Pokhrel, *Member, IEEE* , and Petar Popovski, *Fellow, IEEE*

***Abstract*—The study of optimal properties of centralized dynamic-time-division-duplex (D-TDD) employed at a wireless network consisting of multiple nodes is a highly challenging and partially understood problem in the literature. In this paper, we develop an optimal centralized D-TDD scheme for a wireless network comprised of K full-duplex nodes impaired by self-interference and additive white Gaussian noise. As a special case, we also propose the optimal centralized D-TDD scheme when part or all nodes in the wireless network are half-duplex. Thereby, we derive the optimal adaptive scheduling of the reception, transmission, simultaneous reception and transmission, and silence at every node in the network in each time slot such that the rate region of the network is maximized. The performance of the optimal centralized D-TDD can serve as an upper-bound to any other TDD scheme, which is useful in qualifying the relative performance of TDD schemes. The numerical results show that the proposed centralized D-TDD scheme achieves significant rate gains over existing centralized D-TDD schemes.**

***Index Terms*—Dynamic TDD, centralized network, self-interference, cross-interference, full-duplex, half-duplex, adaptive scheduling, rate region.**

I. Introduction

Time-division duplex (TDD) is a communication protocol where the receptions and transmissions to and from the network nodes are allocated to non-overlapping time slots in the same frequency band. TDD has wide use in 3G, 4G, and 5G and allows for an easy and scalable control over the flow of uplink and downlink traffic at the nodes. Typically, it is achieved by changing the portion of time slots allocated to reception and transmission at the nodes [2], [3].

In general, the TDD scheme can be static or dynamic. In static-TDD, each node pre-allocates a fraction of the total number of time slots for transmission and the rest of the time slots for reception regardless of the channel conditions and the interference in the network [2]. Due to the scheme being static, the time slots in which the nodes perform reception and the time slots in which the nodes perform transmission are prefixed and unchangeable over long periods [3]. On the other hand, in dynamic (D)-TDD, each time slot can be dynamically allocated either for reception or for transmission at the nodes based on the channel gains of the network links in order to maximize the overall network performance. Thereby, D-TDD schemes achieve higher performance gains compared to static-TDD schemes at the expense of overheads. As a result, D-TDD schemes have attracted significant research interest, see [4]–[11] and references therein. Motivated by this, in this paper we investigate D-TDD schemes.

D-TDD schemes can be implemented in either distributed or centralized fashion. In distributed D-TDD schemes, the individual nodes, or a group of nodes, make decisions for transmission, reception, or silence without synchronizing with the rest of the nodes in the network [12]–[15]. As a result, a distributed D-TDD scheme is practical for implementation, however, it does not maximize the overall network performance. On the other hand, in centralized D-TDD schemes, the decision of whether a node should receive, transmit or stay silent in a given time slot is performed at a central processor in the network, which then informs the node about its decision. To this end, centralized D-TDD schemes require full channel state information (CSI) of all network links at the central processor. In this way, the receptions, transmissions, and silences of the nodes are synchronized by the central processor in order to maximize the overall network performance. Since centralized D-TDD schemes require full CSI of all network links, they induce excessive overhead and thus are not practical for implementation. However, knowing the performance of the optimal centralized D-TDD scheme is highly valuable since it serves as an upper bound and thus serves as the ultimate benchmark for any practical TDD scheme. The optimal centralized D-TDD scheme for a wireless network is an open problem. Motivated by this, in this paper we derive the optimal centralized D-TDD scheme for a wireless network.

A network node can operate in two different modes, namely, full-duplex (FD) mode and half-duplex (HD) mode. In the FD mode, transmission and reception at the node can occur simultaneously and in the same frequency band. However, due to the in-band simultaneous reception and transmission, nodes are impaired by self-interference (SI), which occurs due to leakage of energy from the transmitter-end into the receiver-end of the nodes. Currently, there are advanced hardware designs which can suppress the SI by about 110 dB in certain scenarios, see [16]. On the other hand, in the HD mode, transmission and reception take place in the same frequency band but in different time slots, or in the same time slot but in different frequency bands, which avoids the creation of SI. However, since a FD node uses the resources twice as much as compared to a HD node, the achievable data rates of a network comprised of FD nodes may be significantly higher than that comprised of HD nodes. Motivated by this, in this paper we investigate a network comprised of FD nodes. In addition, we aim to show that D-TDD is applicable to the wireless networks comprised of FD nodes. This is because, contrary to main-stream belief, it is not always

This work has been published in part at IEEE WCNC 2019 [1].

This work was supported by the Australian Research Council Discovery Project under Grant DP180101205.

M. M. Razlighi N. Zlatanov are with the Department of Electrical and Computer Systems Engineering, Monash University, Melbourne, VIC 3800, Australia (e-mails: mohsen.mohammadkhanirazlighi@monash.edu and nikola.zlatanov@monash.edu.)

S. R. Pokhrel is with the School of IT, Deakin University, Geelong Australia (e-mail: shiva.pokhrel@deakin.edu.au)

P. Popovski is with the Department of Electronic Systems, Aalborg University, Denmark (e-mail: petarp@es.aau.dk).

This article has been accepted for publication in a future issue of this journal, but has not been fully edited. Content may change prior to final publication. Citation information: DOI 10.1109/TWC.2020.3022990, IEEE Transactions on Wireless Communications

optimal for a FD node to simultaneously receive and transmit in each time slot. In fact, whether a FD node should receive, transmit, or simultaneously receive and transmit in a given time slot, such that some objective function is maximized, depends on the network fading gains. As a result, the literature lacks a D-TDD scheme that, based on the network fading gains and the traffic model, selects optimally whether a given network node should receive, transmit, or simultaneously receive and transmit such that some performance function is maximized. This paper fills in this gap in the literature. In addition, we also provide the optimal centralized D-TDD scheme when all or part of the network nodes operate in the HD mode, which is motivated by the fact that in all current wireless networks, the nodes operate in the HD mode. Moreover, we show that the FD mode is a generalization of the HD node. As a result, once the optimal FD D-TDD scheme is obtained, the optimal HD D-TDD can be obtained as a special case from the FD D-TDD.

D-TDD schemes have been investigated in [14], [17]–[28], where [17]–[23] investigate distributed D-TDD schemes and centralized D-TDD schemes are investigated in [14], [24]–[28]. The authors in [24] propose a centralized D-TDD scheme named SPARK that provides more than 120% improvement compared to similar distributed D-TDD schemes. In [25] the authors proposed a centralized D-TDD scheme but do not provide a mathematical analysis of the proposed scheme. In [14], the authors minimize the total transmit sum-power by exploiting beamforming from multi-antenna transmitters. Specifically, an optimal beamforming scheme from the multi-antenna transmitters is proposed to guarantee a minimum signal-to-interference-plus-noise ratio at the users. The work in [26] proposes a centralized D-TDD scheme for a wireless network where the decisions for transmission and reception at the nodes are chosen from a finite and predefined set of configurations, which is not optimal in general and may limit the network performance. A network comprised of two-way links is investigated in [27], where each link can be used either for transmission or reception in a given time slot, with the aim of optimising the direction of the two-way links in each time slot. However, the solution in [27] is sub-optimal since not only nodes can not freely select to transmit or receive in each time slot but also the investigated problem is relaxed to obtain a solution. The work in [28] investigates a wireless network, where the nodes can select to transmit, receive, or be silent in a given time slot. However, the proposed solution in [28] is again sub-optimal since the investigated problem is non convex and some constraints are non-continuous, hence authors proposed an algorithm that yields a local optimum solution to the problem. On the other hand, [29], [30] investigate centralized D-TDD schemes for a wireless network comprised of FD nodes. Specifically, the authors in [29] used an approximation to develop a non-optimum game theoretic centralized D-TDD scheme, which uses round-robin scheduling, and they provide analysis for a cellular network comprised of two cells. In [30], the authors investigate a sub-optimal centralized D-TDD scheme that performs FD and HD mode selection at the nodes based on geometric programming.

To the best of our knowledge, the optimal centralized D-TDD scheme for a wireless network comprised of FD and/or HD nodes is an open problem in the literature. As a result, in this paper, we derive the optimal centralized D-TDD scheme for a wireless network comprised of FD nodes. In particular, we derive the optimal scheduling of the reception, transmission, simultaneous reception and transmission, or silence at every FD node in a given time slot such that the rate region of the network is maximized. In addition, as a special case, we also derive the optimal centralized D-TDD scheme for a network comprised of HD and/or FD nodes. Our numerical results show that the proposed optimal centralized D-TDD scheme achieves significant gains over existing centralized D-TDD schemes.

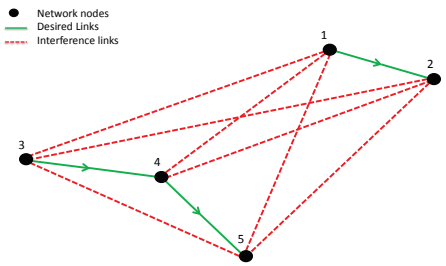

Fig. 1. A wireless network comprised of 5 nodes.

The rest of this paper is organized as follows. In Section II, we present the system and channel models. In Section III, we formulate the centralized D-TDD problem. In Section IV, we present the optimal centralized D-TFDD scheme for a wireless network comprised of FD and HD nodes. In Section V, we investigate a rate allocation scheme and propose a corresponding rate allocation scheme based on rate demands . Simulation and numerical results are provided in Section VI, and the conclusions are drawn in Section VII.

II. System Model

In this section, we present the system and channel models.

A. System Model

We consider a wireless network comprised of K FD nodes. Each network node is able to wirelessly communicate with the rest of the nodes in the network and in a given time slot operate as: 1) a receiver that receives information from other network nodes; 2) a transmitter that sends information to other network nodes; 3) simultaneously receive and transmit information from/to other network nodes; or 4) be silent. The nodes can change their state from one time slot to the next. Moreover, in the considered network, we assume that each node is able to receive information from multiple nodes simultaneously utilizing a multiple-access channel scheme, see [31, Ch. 15.1.2]. However, a node cannot transmit information to more than one node, i.e., we assume that information-theoretic broadcasting schemes, see [31, Ch. 15.1.3], are not employed. Hence, the considered network is a collection of many multiple-access channels all operating in the same frequency band.

In the considered wireless network, we assume that there is a link between any two nodes in the network, i.e., that the

This article has been accepted for publication in a future issue of this journal, but has not been fully edited. Content may change prior to final publication. Citation information: DOI 10.1109/TWC.2020.3022990, IEEE Transactions on Wireless Communications

network graph is a complete graph. Each link is assumed to be impaired by independent flat fading, which is modelled via the channel gain of the link. The channel gain between any two nodes can be set to zero during the entire transmission time, which in turn models the case when the wireless signal sent from one of the two nodes can not propagate and reach the other node. Otherwise, if the channel gain is non-zero in any time slot during the transmission, then the wireless signal sent from one of the two nodes can reach the other node. Obviously, not all of the links leading to a given node carry desired information and are thereby desired by the considered node. There are links which carry undesired information to a considered node, which are referred to as interference links. An interference link causes the signal transmitted from a given node to reach an unintended destination node and acts as interference to that node. For example, in Fig. 1, we have a wireless network comprised of 5 nodes where node 2 wants to receive information from node 1. However, since nodes 3 and 4 are also transmitting in the same time slot, node 2 would experience interference from nodes 3 and 4. Similarly, nodes 4 and 5 experience interference from node 1. It is easy to see that for node 2 it is beneficial if all other nodes, except node 1, are either receiving or silent. However, such a scenario would be harmful for the rest of the network nodes since they won't be able to receive and transmit any data. In the example shown in Fig. 1, as an special case we can consider that node 4 is a FD base station and nodes, 1,2,3, and 5, are HD mobile stations.

In order to model the desired and undesired links for each node, we introduce a binary matrix $\mathbf{Q}$ defined as follows. The (j,k) element of $\mathbf{Q}$ is equal to 1 if node k regards the signal transmitted from node j as a desired signal, and is equal to 0 if node k regards the signal transmitted from node j as an interference signal. Moreover, let $\bar{\mathbf{Q}}$ denote an identical matrix as $\mathbf{Q}$ but with flipped binary values. Hence, the (j,k) element of $\bar{\mathbf{Q}}$ assumes the value 1 if node k regards the signal transmitted from node j as interference, and the (j,k) element of $\bar{\mathbf{Q}}$ is 0 when node k regards the signal transmitted from node j as a desired signal.

The matrix $\mathbf{Q}$, and thereby also the matrix $\bar{\mathbf{Q}}$, are set before the start of the transmission in the network. How a receiving node decides from which nodes it receives desired signals, and thereby from which node it receives interference signals, is unconstrained for the analyses in this paper.

B. Channel Model

We assume that each node in the considered network is impaired by unit-variance additive white Gaussian noise (AWGN), and that the links between the nodes are impaired by block fading. In addition, due to the in-band simultaneous reception-transmission, each node is also impaired by SI, which occurs due to leakage of energy from the transmitter-end into the receiver-end of the node. The SI impairs the decoding of the received information signal significantly, since the SI signal has a relatively higher power compared to the power of the desired signal. Let the transmission on the network be carried-out over $T \to \infty$ time slots, where a time slot is small enough such that the fading on all network links, including the SI links, can be considered constant during a time slot. Hence, the instantaneous fading gain of the links are assumed to change only from one time slot to the next and not within a time slot. Let $g_{j,k}(i)$ denote the fading coefficient of the channel between nodes j and k in the considered network in time slot i. Then $\gamma_{j,k}(i) = P_j|g_{j,k}(i)|^2$ denotes the received signal power from nodes j to node k in time slot i, and P_j is the transmit power at node j. Since the wireless channel is impaired by large-scale fading, the mean of the received signal power can be obtained as

$$E\{\gamma_{j,k}(i)\} = P_j \left(\frac{c}{4\pi f_c}\right)^2 \chi_{jk}^{-\beta}, \tag{1}$$

where c is the speed of light, f_c is the carrier frequency, χ_{jk} is the distance between node j and k, and β is the path loss exponent. The case when $j = k$ models the received signal power through the SI channel of node k in time slot i, given by $\gamma_{k,k}(i) = P_k|g_{k,k}(i)|^2$. Note that since the links are impaired by fading, the values of $\gamma_{j,k}(i)$ change from one time slot to the next.

Finally, let $\mathbf{G}(i)$ denote the weighted connectivity matrix of the graph of the considered network in time slot i, where the (j,k) element in the matrix $\mathbf{G}(i)$ is equal to the received signal power through the link (j,k), $\gamma_{j,k}(i)$.

C. Rate Region

Let $SINR_k(i)$ denote the signal-to-interference-plus-noise-ratio (SINR) at node k in time slot i. Then, the average rate received at node k over $T \to \infty$ time slots is given by

$$\bar{R}_k = \lim_{T\to\infty} \frac{1}{T} \sum_{i=1}^{T} \log_2\left(1 + SINR_k(i)\right). \tag{2}$$

Using (2), $\forall k$, we define a weighted sum-rate as

$$\Lambda = \sum_{k=1}^{N} \mu_k \bar{R}_k, \tag{3}$$

where $\bar{R}_k$ is the average received rate at node k and μ_k is the weight associated with $\bar{R}_k$ for $k = 1, 2, ..., N$, where $0 \leq \mu_k \leq 1$ and $\sum_{k=1}^{N} \mu_k = 1$. The weights μ_k, $\forall k$, model the traffic model. In particular, the higher μ_k is, the more traffic node k requires and its rate is given higher priority to be increased compared to the other rates. The weighted sum rate is general enough such that it can provide all points of the rate region of the network, which means that it can model all possible traffic models. Only in the special case when $\mu_k = 1/N$, $\forall k$, our objective function, the weighted sum rate, transforms to the the sum-rate. Moreover, even if the traffic requirements are time dependent, meaning that μ_k, $\forall k$, are time dependent, our solution can be extended to a slow varying network traffic where μ_k captures the short term averages of the traffic rate, i.e., the probability that a new data arrives at k'th node is μ_k and all nodes are back-logged with data, but we decide to serve them according to average incoming rate using μ_k.The fast varying case requires further investigations in future works.

III. Problem Formulation

Each node in the network can be in one of the following four states: receive (r), transmit (t), simultaneously receive and

This article has been accepted for publication in a future issue of this journal, but has not been fully edited. Content may change prior to final publication. Citation information: DOI 10.1109/TWC.2020.3022990, IEEE Transactions on Wireless Communications

transmit (f), and silent (s). The main problem in the considered wireless network is to find the optimal state of each node in the network in each time slot, based on global knowledge of the channel fading gains, such that the weighted sum-rate of the network, given by (3), is maximized. To model the modes of each node in each time slot, we define the following binary variables for node k in time slot i

$$r_k(i) = \begin{cases} 1 & \text{if node } k \text{ receives in time slot } i \\ 0 & \text{otherwise,} \end{cases} \tag{4}$$

$$t_k(i) = \begin{cases} 1 & \text{if node } k \text{ transmits in time slot } i \\ 0 & \text{otherwise,} \end{cases} \tag{5}$$

$$f_k(i) = \begin{cases} 1 & \text{if node } k \text{ simultaneously receives} \\ & \text{and transmits in time slot } i \\ 0 & \text{otherwise,} \end{cases} \tag{6}$$

$$s_k(i) = \begin{cases} 1 & \text{if node } k \text{ is silent in time slot } i \\ 0 & \text{otherwise.} \end{cases} \tag{7}$$

Since node k can be in one and only one mode in each time slot, i.e., it can either receive, transmit, simultaneously receive and transmit, or be silent, the following has to hold

$$r_k(i) + t_k(i) + f_k(i) + s_k(i) = 1, \ \forall k. \tag{8}$$

For the purpose of simplifying the analytical derivations, it is more convenient to represent (8) as

$$r_k(i) + t_k(i) + f_k(i) \in \{0, 1\}, \ \forall k, \tag{9}$$

where if $r_k(i) + t_k(i) + f_k(i) = 0$ holds, then node k is silent in time slot i.

Now, using the binary variables defined in (4)-(7), we define vectors $\mathbf{r}(i)$, $\mathbf{t}(i)$, $\mathbf{f}(i)$, and $\mathbf{s}(i)$ as

$$\mathbf{r}(i) = [r_1(i), \ r_2(i), \ ..., \ r_K(i)], \tag{10}$$

$$\mathbf{t}(i) = [t_1(i), \ t_2(i), \ ..., \ t_K(i)], \tag{11}$$

$$\mathbf{f}(i) = [f_1(i), \ f_2(i), \ ..., \ f_K(i)], \tag{12}$$

$$\mathbf{s}(i) = [s_1(i), \ s_2(i), \ ..., \ s_K(i)]. \tag{13}$$

Hence, the k-th element of the vector $\mathbf{r}(i)$/$\mathbf{t}(i)$/$\mathbf{f}(i)$/$\mathbf{s}(i)$ is $r_k(i)$/$t_k(i)$/$f_k(i)$/$s_k(i)$ and this element shows whether the k-th node is receiving/transmitting/simultaneously receiving and transmitting/silent. Therefore, the four vectors $\mathbf{r}(i)$, $\mathbf{t}(i)$, $\mathbf{f}(i)$, and $\mathbf{s}(i)$, given by (10)-(13), show which nodes in the network are receiving, transmitting, simultaneously receiving and transmitting, and are silent in time slot i, respectively. Due to condition (8), the elements in the vectors $\mathbf{r}(i)$, $\mathbf{t}(i)$, $\mathbf{f}(i)$, and $\mathbf{s}(i)$ are mutually dependent and have to satisfy the following condition

$$\mathbf{r}(i) + \mathbf{t}(i) + \mathbf{f}(i) + \mathbf{s}(i) = \mathbf{e}, \tag{14}$$

where $\mathbf{e}$ is the all-ones vector, i.e., $\mathbf{e} = [1, 1, ..., 1]$.

The main problem in the considered wireless network is finding the optimum vectors $\mathbf{r}(i)$, $\mathbf{t}(i)$, $\mathbf{f}(i)$, and $\mathbf{s}(i)$ that maximize the boundary of the rate region of the network, i.e., the weighted sum-rate, which can be obtained by using the following optimization problem

$$\begin{aligned} &\underset{\mathbf{r}(i),\mathbf{t}(i),\mathbf{f}(i),\mathbf{s}(i),\forall i}{\text{Maximize:}} \quad \Lambda \\ &\text{Subject to :} \\ &\qquad \text{C1} : t_v(i) \in \{0, 1\}, \ \forall v \\ &\qquad \text{C2} : r_v(i) \in \{0, 1\}, \ \forall v \\ &\qquad \text{C3} : f_v(i) \in \{0, 1\}, \ \forall v \\ &\qquad \text{C4} : s_v(i) \in \{0, 1\}, \ \forall v \\ &\qquad \text{C5} : s_v(i) + r_v(i) + f_v(i) + s_v(i) = 1, \ \forall v, \end{aligned} \tag{15}$$

where Λ is given by (3) and μ_k are fixed. The solution of this problem is given in Theorem 2 in Section IV.

Before investigating the problem in (15), we define two auxiliary matrices that will help us derive the main result. Specifically, using matrices $\mathbf{G}(i)$, $\mathbf{Q}$, and $\bar{\mathbf{Q}}$ defined in Sec. II, we define two auxiliary matrices $\mathbf{D}(i)$ and $\mathbf{I}(i)$, as

$$\mathbf{D}(i) = \mathbf{G}(i) \circ \mathbf{Q}, \tag{16}$$

$$\mathbf{I}(i) = \mathbf{G}(i) \circ \bar{\mathbf{Q}}, \tag{17}$$

where $\circ$ denotes the Hadamard product of matrices, i.e., the element wise multiplication of two matrices. Hence, elements in the matrix $\mathbf{D}(i)$ are the received signal powers through the desired links which carry desired information. Conversely, the elements in the matrix $\mathbf{I}(i)$ are the received signal powers through the interference links which carry undesired information. Let $\mathbf{d}_k^\intercal(i)$ and $\mathbf{i}_k^\intercal(i)$ denote the k-th column vectors of the matrices $\mathbf{D}(i)$ and $\mathbf{I}(i)$, respectively. The vectors $\mathbf{d}_k^\intercal(i)$ and $\mathbf{i}_k^\intercal(i)$ show the received signal powers through the desired and the interference links for node k in time slot i, respectively. For example, if the third and fourth elements in $\mathbf{d}_k^\intercal(i)$ are non-zero and thereby equal to $\gamma_{3,k}(i)$ and $\gamma_{4,k}(i)$, respectively, then this means that the k-th node receives desired signals from the third and the fourth elements in the network via channels which have received signal powers $\gamma_{3,k}(i)$ and $\gamma_{4,k}(i)$, respectively. Similar, if the fifth, sixth, and k-th elements in $\mathbf{i}_k^\intercal(i)$ are non-zeros and thereby equal to $\gamma_{5,k}(i)$, $\gamma_{6,k}$ and $\gamma_{k,k}(i)$, respectively, it means that the k-th node receives interference signals from the fifth and the sixth nodes in the network via channels which have received signal powers $\gamma_{5,k}(i)$ and $\gamma_{6,k}(i)$, respectively, and that the k-th node suffers from SI with received signal power $\gamma_{k,k}(i)$.

Remark 1: A central processor is assumed to collect all received signal powers, $\gamma_{j,k}(i)$, and thereby construct $\mathbf{G}(i)$ at the start of time slot i. This central unit will then decide the optimal values of $\mathbf{r}(i)$, $\mathbf{t}(i)$, $\mathbf{f}(i)$ and $\mathbf{s}(i)$, defined in (10)-(13), based on the proposed centralized D-TDD scheme, and broadcast these values to the rest of the nodes. Once the optimal values of $\mathbf{r}(i)$, $\mathbf{t}(i)$, $\mathbf{f}(i)$, and $\mathbf{s}(i)$ are known at all nodes the transmissions, receptions, simultaneous transmission and reception, and silences of the nodes can start in time slot i. Obviously, acquiring global CSI at a central processor is impossible in practice as it incurs a huge overhead and, by the time it is used, the CSI will likely be outdated. However, this assumption will allow us to compute an upper bound on the network performance which will serve as an upper bound to the performance of other D-TDD schemes. The purpose for proposing this optimal TDD scheme is to show that there is a large gap between the performance of current TDD

This article has been accepted for publication in a future issue of this journal, but has not been fully edited. Content may change prior to final publication. Citation information: DOI 10.1109/TWC.2020.3022990, IEEE Transactions on Wireless Communications

schemes and the proposed optimal TDD scheme. As a result, we show that there is space for other more practical D-TDD scheme to be developed that would outperform existing D-TDD schemes. Also, although full CSI knowledge seems unrealistic with today's technology, it may be possible with some future technology on some specific networks.

Remark 2: Note that the optimal state of the nodes of the network (i.e., receive, transmit, simultaneously receive and transmit, or silent) in each time slot can also be obtained by brute-force search. However, this is only for small networks since the complexity grows as 3^k, where k is the number of nodes. Even if this is possible for a small network, an analytical solution of the problem provides depth insights into the corresponding problem.

Remark 3: In this paper, we only optimize the reception-transmission schedule of the nodes, and not the transmission coefficients of the nodes, which leads to interference alignment [32]. Combining adaptive reception-transmission with interference alignment is left for future work.

IV. The Optimal Centralized D-TDD Scheme

Using the notations in Sections II and III, we state a theorem that models the received rate at node k in time slot i.

Theorem 1: The received rate at node k in time slot i is given by

$$R_k(i) = \log_2\left(1+[r_k(i)+f_k(i)]\frac{[\mathbf{t}(i)+\mathbf{f}(i)]\,\mathbf{d}_k^{\intercal}(i)}{1+[\mathbf{t}(i)+\mathbf{f}(i)]\,\mathbf{i}_k^{\intercal}(i)}\right), \quad (18)$$

which is achieved by a multiple-access channels scheme between the desired nodes of node k acting as transmitter and node k acting as a receiver. To this end, node k employs successive interference cancellation to the codewords from the desired nodes whose rates are appropriately adjusted in order for (18) to hold.

Proof: Please refer to Appendix A for the proof. ■

In (18), we have obtained a very simple and compact expression for the received rate at each node of the network in each time slot. As can be seen from (18), the rate depends on the fading channel gains of the desired links via $\mathbf{d}_k^{\intercal}(i)$ and the interference links via $\mathbf{i}_k^{\intercal}(i)$, as well as the state selection vectors of the network via $\mathbf{t}(i)$, $\mathbf{r}(i)$, and $\mathbf{f}(i)$.

Using the received rate at each node of the network, defined by (18), we obtain the average received rate at node k as

$$\bar{R}_k = \lim_{T\to\infty}\frac{1}{T}\sum_{i=1}^{T} R_k(i), \forall k. \quad (19)$$

Inserting (18) into (19), and then (19) into (3), we obtain the weighted sum-rate of the network as

$$\Lambda = \lim_{T\to\infty}\frac{1}{T}\sum_{i=1}^{T}\sum_{k=1}^{N}\mu_k\log_2\Big(1 + [r_k(t)+f_k(t)]\,\frac{[\mathbf{t}(i)+\mathbf{f}(i)]\,\mathbf{d}_k^{\intercal}(i)}{1+[\mathbf{t}(i)+\mathbf{f}(i)]\,\mathbf{i}_k^{\intercal}(i)}\Big). \quad (20)$$

Now, note that the only variables that can be manipulated in (20) in each time slot are the values of the elements in the vectors $\mathbf{t}(i)$, $\mathbf{r}(i)$, and $\mathbf{f}(i)$, and the values of $\mu_k, \forall k$. We use $\mathbf{t}(i)$, $\mathbf{r}(i)$, and $\mathbf{f}(i)$ to maximize the boundary of the rate region for a given $\mu_k, \forall k$, in the following. In addition, later on in Section V, we use the constants $\mu_k, \forall k$, to establish a scheme that establishes rate allocation based on rate demands between the nodes of the network.

The optimum vectors $\mathbf{r}(i)$, $\mathbf{t}(i)$, $\mathbf{f}(i)$, and $\mathbf{s}(i)$ that maximize the boundary of the rate region of the network can be obtained by the following optimization problem

$$\underset{\mathbf{r}(i),\mathbf{t}(i),\mathbf{f}(i),\mathbf{s}(i),\forall i}{\text{Maximize:}} \lim_{T\to\infty}\frac{1}{T}\sum_{i=1}^{T}\sum_{k=1}^{N}\mu_k\log_2\Big(1 + [r_k(t)+f_k(t)]\,\frac{[\mathbf{t}(i)+\mathbf{f}(i)]\,\mathbf{d}_k^{\intercal}(i)}{1+[\mathbf{t}(i)+\mathbf{f}(i)]\,\mathbf{i}_k^{\intercal}(i)}\Big)$$

$$\begin{aligned}
&\text{Subject to :}\\
&\quad \text{C1}: t_v(i)\in\{0,1\},\ \forall v\\
&\quad \text{C2}: r_v(i)\in\{0,1\},\ \forall v\\
&\quad \text{C3}: f_v(i)\in\{0,1\},\ \forall v\\
&\quad \text{C4}: s_v(i)\in\{0,1\},\ \forall v\\
&\quad \text{C5}: s_v(i)+r_v(i)+f_v(i)+s_v(i)=1,\ \forall v, \quad (21)
\end{aligned}$$

where μ_k are fixed. The solution of this problem is given in the following theorem.

Theorem 2: The optimal values of the vectors $\mathbf{t}(i)$, $\mathbf{r}(i)$, $\mathbf{f}(i)$, and $\mathbf{s}(i)$, which maximize the boundary of the rate region of the network, found as the solution of (21), is given by Algorithm 1, which is explained in details in the following.

Algorithm 1 Finding the optimal vector, $\mathbf{t}(i)$

procedure $\forall\, i \in \{1,2,...,T\}$
  Initiate $n=0$, and $t_x(i)_0$, $w_x(i)_0$ and $l_x(i)_0$ randomly, $x\in\{1,2,..,K\}$, where $\mathcal{K}_d$ is the set of desired nodes.
  ****** Iterative-loop starts*****
  while exit-loop-flag == FALSE **do**
    if (27) holds **then**
      exit-loop-flag ← TRUE
    else
      n++
      compute $t_x(i)_n$ with (22)
      compute $w_x(i)_n$ with (23)
      compute $l_x(i)_n$ with (26)
  ****** Iterative-loop end*****
  if $t_x(i)=0$ and $t_k(i)=1, \forall k$, where (x,k) element of $\mathbf{Q}$ is one **then**
    $r_x(i)=1$
  if $t_x(i)=0$ and $t_k(i)=0, \forall k$, where (x,k) element of $\mathbf{Q}$ is one **then**
    $s_x(i)=1$
  if $t_x(i)=1$ and $t_k(i)=1, \forall k$, where (x,k) element of $\mathbf{Q}$ is one **then**
    $f_x(i)=1$ and $t_x(i)=0$
  if $t_x(i)=1$ and $t_k(i)=0, \forall k$, where (x,k) element of $\mathbf{Q}$ is one **then**
    $t_x(i)$ remains unchanged
  return $\mathbf{t}(i)$, $\mathbf{r}(i)$, $\mathbf{f}(i)$, $\mathbf{s}(i)$

Algorithm 1 is an iterative algorithm. Each iteration has its own index, denoted by n. In each iteration, we compute

This article has been accepted for publication in a future issue of this journal, but has not been fully edited. Content may change prior to final publication. Citation information: DOI 10.1109/TWC.2020.3022990, IEEE Transactions on Wireless Communications

the vector $\mathbf{t}(i)$ in addition to two auxiliary vectors $\mathbf{w}(i) = \{w_1(i), w_2(i), ... , w_N(i)\}$ and $\mathbf{l}(i) = \{l_1(i), l_2(i), ..., l_N(i)\}$. Since the computation process is iterative, we add the index n to denote the n'th iteration. Hence, the variables $t_x(i)$, $w_x(i)$, and $l_x(i)$ in iteration n are denoted by $t_x(i)_n$, $w_x(i)_n$, and $l_x(i)_n$, respectively. In each iteration, n, the variable $t_x(i)_n$, for $x \in \{1, 2, ..., N\}$, is calculated as

$$\bullet\ t_x(i)_n = 0 \ \text{ if } \ \sum_{k=1}^{N} \frac{\mu_k l_k(i)_{n-1}}{\ln 2}\Big[d_{x,k}(i)\Big(1 - \frac{w_k(i)_{n-1}}{\sqrt{\sum_{v=1, v\neq x}^{N} t_v(i)_{n-1} d_{v,k}(i)}}\Big) + i_{x,k}(i)\Big] \geq 0,$$

$$\bullet\ t_x(i)_n = 1 \ \text{ if otherwise.} \tag{22}$$

In (22), $d_{v,k}(i)$ and $i_{v,k}(i)$ are the (v, k) elements of the matrices $\mathbf{D}(i)$ and $\mathbf{I}(i)$, respectively. Whereas, $l_k(i)_n$ and $w_k(i)_n$ are the auxiliary variables, and they are treated as constants in this stage and will be given in the following.

In iteration n, the variable $w_x(i)_n$, for $x \in \{1, 2, ..., N\}$, is calculated as

$$w_x(i)_n = \frac{A_x(i) + B_x(i)}{\sqrt{A_x(i)}}, \tag{23}$$

where $A_x(i)$ and $B_x(i)$ are defined as

$$A_x(i) = \mathbf{t}(i)_n \mathbf{d}_x^{\intercal}(i), \tag{24}$$

$$B_x(i) = 1 + \mathbf{t}(i)_n \mathbf{i}_x^{\intercal}(i). \tag{25}$$

In iteration n, the variable $l_x(i)_n$, for $x \in \{1, 2, ..., N\}$, is calculated as

$$l_x(i)_n = \frac{1}{\Big(|\sqrt{A_x(i)} - w_x(i)_n|^2 + B_x(i)\Big)}, \tag{26}$$

where $w_x(i)_n$ is treated as constant in this stage. In addition, $A_x(i)$ and $B_x(i)$, are given by (24) and (25), respectively.

The process of updating the variables $t_x(i)_n$, $w_x(i)_n$, and $l_x(i)_n$ for each time slot i is repeated until convergence occurs, which can be checked by the following equation

$$|\Lambda_n - \Lambda_{n-1}| < \epsilon, \tag{27}$$

where $\Lambda_n = \sum_{k=1}^{N} \mu_k \log_2\Big(1 + \frac{\mathbf{t}(i)_n \mathbf{d}_k^{\intercal}(i)}{1 + \mathbf{t}(i)_n \mathbf{i}_k^{\intercal}(i)}\Big)$. Moreover, $\epsilon > 0$ is a relatively small constant, such as $\epsilon = 10^{-6}$.

Once $t_x(i), \forall x$, is decided, the other variables, $r_x(i)$, $f_x(i)$, and $s_x(i)$ can be calculated as follows. If $t_x(i) = 0$, $t_k(i) = 1$, and the (x, k) element of $\mathbf{Q}$ is equal to one, then $r_x(i) = 1$. If $t_x(i) = 0$, $t_k(i) = 0$, and (x, k) element of $\mathbf{Q}$ is equal to one, then $s_x(i) = 1$. If $t_x(i) = 1$, $t_k(i) = 1$, and (x, k) element of $\mathbf{Q}$ is equal to one, then $f_x(i) = 1$ and we set $t_x(i) = 0$. Finally, if $t_x(i) = 1$, $t_k(i) = 0$, and (x, k) element of $\mathbf{Q}$ is equal to one, then $t_x(i)$ remains unchanged.

Proof: Please refer to Appendix B for the proof. ■

A. Special Case of the Proposed Centralized D-TDD Scheme for HD nodes

As a special case of the proposed centralized D-TDD scheme for a network comprised of FD nodes proposed in Theorem 2, we investigate the optimal centralized D-TDD scheme for network comprised of HD nodes that maximizes the rate region.

For the case of a network comprised of HD nodes, we again use the vectors $\mathbf{r}(i)$, $\mathbf{t}(i)$, and $\mathbf{s}(i)$, and set the vector $\mathbf{f}(i)$ to all zeros due to the HD mode. The optimum vectors $\mathbf{r}(i)$, $\mathbf{t}(i)$, and $\mathbf{s}(i)$ that maximize the boundary of the rate region of a network comprised of HD nodes can be obtained by the following optimization problem

$$\underset{\mathbf{r}(i),\mathbf{t}(i),\mathbf{s}(i),\forall i}{\text{Maximize:}} \ \lim_{T\to\infty} \frac{1}{T} \sum_{i=1}^{T} \sum_{k=1}^{N} \mu_k \log_2\Big(1 + r_k(t) \frac{\mathbf{t}(i)\mathbf{d}_k^{\intercal}(i)}{1 + \mathbf{t}(i)\mathbf{i}_k^{\intercal}(i)}\Big)$$

$$\text{Subject to :}$$

$$\text{C1} : t_v(i) \in \{0, 1\}, \ \forall v$$

$$\text{C2} : r_v(i) \in \{0, 1\}, \ \forall v$$

$$\text{C3} : s_v(i) \in \{0, 1\}, \ \forall v$$

$$\text{C4} : s_v(i) + r_v(i) + s_v(i) = 1, \ \forall v, \tag{28}$$

where $\mu_k, \forall k$ is fixed. The solution of this problem is given in the following theorem.

Theorem 3: The optimal values of the vectors $\mathbf{t}(i)$, $\mathbf{r}(i)$, and $\mathbf{s}(i)$ which maximize the boundary of the rate region of the considered network comprised of HD nodes, found as the solution of (28), is also given by Algorithm 1 where lines 17-18 in Algorithm 1 need to be removed and where $\gamma_{j,k}(i)$ is set to $\gamma_{j,k}(i) = \infty, \forall j = k$ and $\forall i$ in the weighted connectivity matrix $\mathbf{G}(i)$.

Proof: Please refer to Appendix C for the proof. ■

Remark 4: For the case when the network is comprised of both FD and HD nodes, Theorem 3 needs to be applied only to the HD nodes in order to obtain the optimal centralized D-TDD scheme for this case

V. Rate Allocation Based on Rate Demands

The nodes in a network have different rate demands based on the application they employ. In this section, we propose a scheme that allocates resources to the network nodes based on the rate demand of the network nodes. To this end, in the following, we assume that the central processor has access to the rate demands of the network nodes.

Rate allocation can be done using a prioritized rate allocation policy, where some nodes have a higher priority compared to others, and thereby, should be served preferentially. For example, some nodes are paying more to the network operator compared to the other nodes in exchange for higher data rates. In this policy, nodes with lower priority are served only when higher priority nodes are served acceptably. On the other hand, nodes that have the same priority level should be served by a fair rate allocation scheme that allocates resources proportional to the node needs.

In the optimal centralized D-TDD scheme given in Theorem 2, the average received rate of user k can be controlled via the constant $0 \leq \mu_k \leq 1, \forall k$. By varying μ_k from zero to one, the average received rate of user k can be increased from zero to the maximum possible rate. Thereby, by optimizing the value of $\mu_k, \forall k$, we can establish a rate allocation scheme among the

This article has been accepted for publication in a future issue of this journal, but has not been fully edited. Content may change prior to final publication. Citation information: DOI 10.1109/TWC.2020.3022990, IEEE Transactions on Wireless Communications

users which allocates resources based on the rate demand of the nodes. In the following, we propose a practical centralized D-TDD scheme for rate allocation in real-time by adjusting the values of $\boldsymbol{\mu} = [\mu_1,\ \mu_2,\ ...,\ \mu_K]$.

A. Proposed Rate Allocation Scheme based on Rate Demands

The average received rate at node k obtained using the proposed optimal centralized D-TDD scheme is given by

$$\bar{R}_k(\boldsymbol{\mu}) = \lim_{T\to\infty} \frac{1}{T} \sum_{i=1}^{T} R_k^*(i, \boldsymbol{\mu}), \tag{29}$$

where $R_k^*(i, \mu_k)$ is the maximum received rate at node k in the time slot i, obtained by Algorithm 1 for fixed $\boldsymbol{\mu}$.

Let $\boldsymbol{\tau} = [\tau_1,\ \tau_2,\ ...,\ \tau_K]$, where $\tau_k \geq 0$ be a vector of the rate demands of the nodes and let $\boldsymbol{\alpha} = [\alpha_1,\ \alpha_2,\ ...,\ \alpha_K]$ be the priority level vector of the nodes, where $0 \leq \alpha_k \leq 1$ and $\sum_{k=1}^{N} \alpha_k = 1$. The priority level vector, α_k, determines the importance of user k such that the higher the value of α_k, the higher the priority of the k-th node.

In order to achieve rate allocations according to the rate demands in $\boldsymbol{\tau}$ and the priority levels in $\boldsymbol{\alpha}$, we aim to minimize the weighted squared difference between the average received rate $\bar{R}_k(\boldsymbol{\mu})$ and the rate demand, given by $\tau_k, \forall k$, i.e., to make the weighted sum squared error, $\sum_{k=1}^{N} \alpha_k \left(\bar{R}_k(\boldsymbol{\mu}) - \tau_k\right)^2$, as smallest as possible. Note that there may not be enough network resource to make the weighted sum squared error to be equal to zero. However, the higher α_k is, more network resources need to be allocated to node k in order to increase its rate and bring $\bar{R}_k(\boldsymbol{\mu})$ close to τ_k.

Using $\boldsymbol{\tau}$ and $\boldsymbol{\alpha}$, we devise the following rate-allocation problem

$$\begin{aligned} &\underset{\boldsymbol{\mu}}{\text{Minimize:}} \sum_{k=1}^{N} \alpha_k \left(\bar{R}_k(\boldsymbol{\mu}) - \tau_k\right)^2 \\ &\text{Subject to :} \\ &\qquad \text{C1} : 0 \leq \mu_k \leq 1,\ \forall k \\ &\qquad \text{C1} : \sum_{k=1}^{N} \mu_k = 1. \end{aligned} \tag{30}$$

The optimization problem in (30) belongs to a family of a well investigated optimization problems in [33], which do not have closed form solutions. Hence, we propose the following heuristic solution of (30) by setting $\boldsymbol{\mu}$ to $\boldsymbol{\mu} = \boldsymbol{\mu}^e(i)$, where each element of $\boldsymbol{\mu}^e(i)$ is obtained as

$$\mu_k^e(i+1) = \mu_k^e(i) + \delta_k(i)\alpha_k \left[\bar{R}_k^e(i, \boldsymbol{\mu}^e(i)) - \tau_k\right], \tag{31}$$

where $\delta_k(i)$, $\forall k$, can be some properly chosen monotonically decaying function of i with $\delta_k(1) < 1$, such as $\frac{1}{2i}$. Note that after updating $\mu_k^e(i), \forall k$, values, we should normalize them to bring $\mu_k^e(i), \forall k$ in the range ($0 \leq \mu_k \leq 1$). To this end, we apply the following normalization method

$$\mu_k^e(i+1) = \frac{\mu_k^e(i+1)}{\sum_{k=1}^{N} \mu_k^e(i+1)}, \forall k. \tag{32}$$

In (31), $\bar{R}_k^e(i, \boldsymbol{\mu}^e(i))$ is the real time estimation of $\bar{R}_k(\boldsymbol{\mu})$, which is given by

$$\begin{aligned} \bar{R}_k^e(i, \boldsymbol{\mu}^e(i)) = \frac{i-1}{i} \bar{R}_k^e(i-1, \mu_k^e(i-1)) \\ + \frac{1}{i} R_k^*(i, \boldsymbol{\mu}^e(i)). \end{aligned} \tag{33}$$

VI. Simulation and Numerical Results

In this section, we provide numerical results where we compare the proposed optimal centralized D-TDD scheme with benchmark centralized D-TDD schemes found in the literature. All of the presented results in this section are generated for Rayleigh fading by numerical evaluation of the derived results and are confirmed by Monte Carlo simulations.

The Network: In all numerical examples, we use a network covering an area of $\rho \times \rho\ m^2$. In this area, we place 50 pairs of nodes randomly as follows. We randomly place one node of each pair in the considered area and then the paired node is placed by choosing an angle uniformly at random from 0° to 360° and choosing a distance uniformly at random from χ=10 m to 100 m, from the first node. For a given pair of two nodes, we assume that only the link between the paired nodes is desired and all other links act as interference links. The channel gain corresponding to the each link is assumed to have Rayleigh fading, where the mean of $\gamma_{j,k}(i)$ is calculated using the standard path-loss model [34] using (1), where $f_c = 1.9$ GHz, and $\beta = 3.6$. In addition, the average SI suppression varies from 110 dB to 130 dB.

Benchmark Scheme 1 (Conventional scheme): This benchmark is the TDD scheme used in current wireless networks. The network nodes are divided into two groups, denoted by A and B. In odd time slots, nodes in group A send information to the desired nodes in group B. Then, in the even time slots, nodes in group B send information to the desired nodes in group A. With this approach there is no interference between the nodes within group A and within group B since the transmissions are synchronized. However, there are interferences from the nodes in group A to the nodes in group B, and vice versa.

Benchmark Scheme 2 (Interference spins scheme): The interference spins scheme, proposed in [27], has been considered as the second benchmark scheme.

Benchmark Scheme 3 (Conventional FD scheme): This benchmark is the TDD scheme used in a wireless networks with FD nodes. The network nodes are divided into two groups, denoted by A and B. In all the time slots, nodes in group A send information to the desired nodes in group B, and also nodes in group B send information to the desired nodes in group A. The SI suppression is set to 110 dB.

A. Numerical Results

In Fig. 2, we show the sum-rates achieved using the proposed scheme for different SI suppression levels and the benchmark schemes as a function of the transmission power at the nodes, $P_j = P, \forall j$. This example is for an area of 1000*1000 m^2, where μ_k is fixed to $\mu_k = \frac{1}{k}, \forall k$. As can be seen from Fig. 2, for the low transmit power region, where noise is dominant, all schemes achieve a similar sum-rate. However, increasing the transmit power causes the overall interference to increase, in which case

This article has been accepted for publication in a future issue of this journal, but has not been fully edited. Content may change prior to final publication. Citation information: DOI 10.1109/TWC.2020.3022990, IEEE Transactions on Wireless Communications

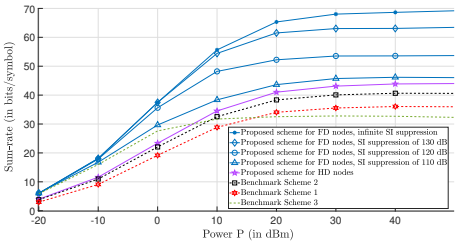

Fig. 2. Sum-rate vs. transmit power $P_j = P, \forall j$ of the proposed schemes and the benchmark schemes for ρ=1000 m.

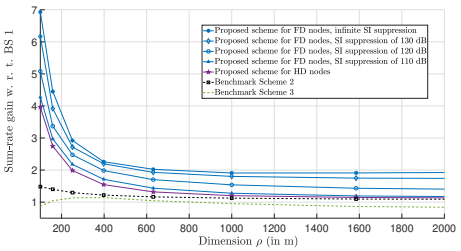

Fig. 3. Sum-rate vs. dimension D of the proposed schemes and the benchmark schemes for $P_j = 20$ dBm, $\forall j$.

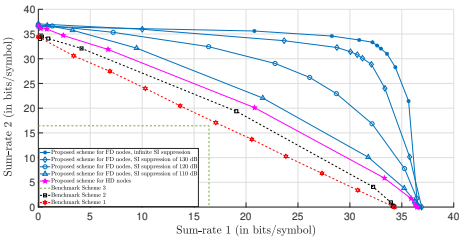

Fig. 4. Sum-rate 1 vs. sum-rate 2 of the proposed schemes and the benchmark schemes for $P_j = 20$ dBm, $\forall j$, ρ=1000 m.

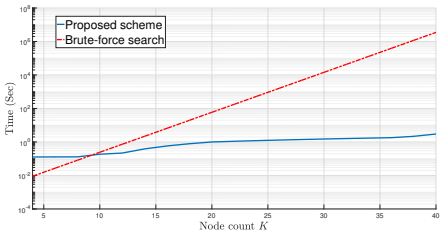

Fig. 5. Complexity vs. node count of the proposed schemes and the benchmark scheme for $P_j = 20$ dBm, $\forall j$, and ρ=1000 m.

the optimal centralized D-TDD scheme achieves a large gain over the considered benchmark schemes. The benchmark schemes show limited performance since in the high power region they can not avoid the interference as effective as the proposed scheme.

In Fig. 3, the sum-rates gain with respect to (w. r. t.) Benchmark Scheme 1 (BS 1) is presented for different schemes as a function of the dimension of the considered area, ρ. We assume that the transmit power is fixed to $P_j = 20$ dBm, $\forall j$, and $\mu_k = \frac{1}{K}, \forall k$. Since the nodes are placed randomly in an area of $\rho \times \rho$ m^2, for large ρ, the links become more separated and the interference has a weeker effect. As a result, all of the schemes have close sum-rate results. However, decreasing the dimension, ρ, causes the overall interference to increase, which leads to the optimal centralized D-TDD scheme to have a considerable gain over the benchmark schemes.

In Fig. 4, we show the rate region achieved using the optimal centralized D-TDD scheme for two different group of nodes, where all the nodes that belong in each group have the same values of μ. Let μ_1 be assigned to the first group and μ_2 to the second group of nodes. By varying the value of μ_1 from zero to one, and setting $\mu_2 = 1 - \mu_1$, as well as aggregating the achieved rates for each group we can get the rate region of the network of the two groups. In this example, the transmit power is fixed to $P_j = 20$ dBm, $\forall j$, and the area dimension is 1000×1000 m^2. As shown in Fig. 4, the proposed scheme with HD nodes has more than 15% improvement in the rate region area compared to the benchmark schemes. More importantly, the proposed scheme for FD nodes with SI suppression of 110 dB performs approximately four times better then Benchmark Scheme 3, in addition to outperforming the other benchmark schemes as well, which is a huge gain and a promising result for using FD nodes.

In Fig. 5, we present the total time required by the optimal algorithm presented in Algorithm 1 to obtain the solution as a function of the number of nodes in the network. The computation time of each algorithm is measured by starting a timer at the moment when the corresponding algorithm is started and then stopping the timer at the moment when the corresponding algorithm provides the final output. For comparison purpose, we also present the total time required by a general brute-force search algorithm to search over all the possible solutions in order to to find the optimal one. However, for the brute-force simulation, we could not run the brute-force algorithm for more that 25 nodes since the computation time was too big. To obtain the computation time of the brute-force algorithm beyond 25 nodes we did interpolation on the curve based on the curve up to 25 nodes. We set the power at the nodes to $P_j = 20$ dBm, $\forall j$, and the area to 1000×1000 m^2. As it can be seen from Fig. 5, the brute-force search algorithm's computation time increases exponentially, however, the computation time with the proposed algorithm increases linearly, since the equations from (23) to (27), which are the basis of the proposed algorithm, are straightforward calculations since the expressions are given in closed form and they do not depend on any hidden function or loop routines.

In Fig. 6, we illustrate the rate achieved using the proposed

This article has been accepted for publication in a future issue of this journal, but has not been fully edited. Content may change prior to final publication. Citation information: DOI 10.1109/TWC.2020.3022990, IEEE Transactions on Wireless Communications

scheme applying the rate allocation scheme for $N = 10$, as a function of node number index. Moreover, we assume that the transmit power is fixed to $P_j = 20$ dBm, $\forall j$, the dimension is ρ=1000 m, and the SI suppression is 110 dB. We have investigated two cases where in both cases the users have same priority, i.e., $\alpha_k = 0.1, \forall k$. However, in one case data demand by users (right plot) is set to $\tau_k = \frac{k}{2}, \forall k$, and in the other the data demand by users (left plot) is set to $\tau_k = k, \forall k$. As can be seen in the right plot of the Fig. 6, the rate allocation scheme is able to successfully answer the data demanded by users. However, in the case of the left plot of Fig. 6, the rate allocation scheme was not able to answer the rates demand of the nodes due to capacity limits. Regardless, it successfully managed to hold the average received rates as close as possible to the demanded rates.

VII. Conclusion

In this paper, we devised the optimal centralized D-TDD scheme for a wireless network comprised of K FD and/or HD nodes, which maximizes the rate region of the network. The proposed centralized D-TDD scheme makes an optimal decision of which node should receive, transmit, simultaneously receive and transmit, or be silent in each time slot. In addition, we proposed a rate allocation scheme that allocates data rates to the nodes according to the user data demands. We have shown that the proposed optimal centralized D-TDD scheme has significant gains over existing centralized D-TDD schemes.

Appendix

A. Proof of Theorem 1

The signal received at node k is given by

$$\begin{aligned} y_k(i) =& r_k(i)\Bigg(\sum_{v\in\mathcal{K}_d}[t_v(i)+f_v(i)]\sqrt{P_v g_{v,k}(i)}\mathbf{s}_v(i) \\ &+\sum_{v\in\mathcal{K}_u}[t_v(i)+f_v(i)]\sqrt{P_v g_{v,k}(i)}\mathbf{s}_v(i)\Bigg) \\ &+ f_k(i)\Bigg(\sum_{v\in\mathcal{K}_d}[t_v(i)+f_v(i)]\sqrt{P_v g_{v,k}(i)}\mathbf{s}_v(i) \\ &+\sum_{v\in\mathcal{K}_u}[t_v(i)+f_v(i)]\sqrt{P_v g_{v,k}(i)}\mathbf{s}_v(i)\Bigg)+n_k(i) \end{aligned} \tag{34}$$

where $\mathcal{K}_d$ and $\mathcal{K}_u$ are the sets of desired and undesired nodes, respectively and $\mathbf{s}_v(i)$ is the transmitted codeword from node v. Assuming the transmission rates of the desired nodes are adjusted such that the receiving node can perform successive interference cancellation of the desired codewords, the rate received at node k from all the desired nodes is given by

$$\begin{aligned} R_k(i) =& \log_2\Big(1 \\ &+\frac{[r_k(i)+f_k(i)]\sum_{v\in\mathcal{K}_d}[t_v(i)+f_v(i)]P_v g_{v,k}(i)}{\sigma_k^2+[r_k(i)+f_k(i)]\sum_{v\in\mathcal{K}_u}[t_v(i)+f_v(i)]P_v g_{v,k}(i)}\Big), \end{aligned} \tag{35}$$

which can be simplified to

$$\begin{aligned} R_k(i) =& \log_2\Big(1 \\ &+\frac{[r_k(i)+f_k(i)]\sum_{v\in\mathcal{K}_d}[t_v(i)+f_v(i)]P_v g_{v,k}(i)}{\sigma_k^2+\sum_{v\in\mathcal{K}_u}[t_v(i)+f_v(i)]P_v g_{v,k}(i)}\Big). \end{aligned} \tag{36}$$

By substituting $\sum_{v\in\mathcal{K}_d}P_v g_{v,k}(i) = [\mathbf{t}(i)+\mathbf{f}(i)]\,\mathbf{d}_k^{\intercal}(i)$ and $\sum_{v\in\mathcal{K}_u}P_v g_{v,k}(i)=[\mathbf{t}(i)+\mathbf{f}(i)]\,\mathbf{i}_k^{\intercal}(i)$ into (36), and assuming that $\sigma_k^2 = 1$, we obtain the rate $R_k(i)$ as in (18). This completes the proof.

B. Proof of Theorem 2

Using the vector $\mathbf{t}(i)$ and the matrix $\mathbf{Q}$, we can obtain the other vectors, $\mathbf{r}(i)$, $\mathbf{f}(i)$, and $\mathbf{s}(i)$. Specially, if $t_x(i) = 0$, $t_k(i) = 1$, and the (x,k) element of $\mathbf{Q}$ is equal to one, then, $r_x(i) = 1$. If $t_x(i) = 0$, $t_k(i) = 0$, and (x,k) element of $\mathbf{Q}$ is equal to one, then, $s_x(i) = 1$. If $t_x(i) = 1$, $t_k(i) = 1$, and (x,k) element of $\mathbf{Q}$ is equal to one, then, $f_x(i) = 1$ and we set $t_x(i) = 0$. Finally, if $t_x(i) = 1$, $t_k(i) = 0$, and (x,k) element of $\mathbf{Q}$ is equal to one, then, $t_x(i)$ is given by (22).

Since the values of $\mathbf{t}(i)$ are sufficient, we simplify the optimization problem in (21) as

$$\begin{aligned} &\underset{t(i),\forall i}{\text{Maximize:}}\ \lim_{T\to\infty}\frac{1}{T}\sum_{i=1}^{T}\sum_{k=1}^{N}\mu_k\log_2\left(1+\frac{\mathbf{t}(i)\mathbf{d}_k^{\intercal}(i)}{1+\mathbf{t}(i)\mathbf{i}_k^{\intercal}(i)}\right) \\ &\text{Subject to :} \\ &\qquad \text{C1}: t_v(i)\in\{0,1\},\ \forall v. \end{aligned} \tag{37}$$

To obtain the solution of (37), we first transform the non-convex objective function in (37) into an equivalent objective function. To this end, let us define $A_k(i)$ and $B_k(i)$ as the numerator and denominator values to simplify the notation, where

$$A_k(i) = \mathbf{t}(i)\mathbf{d}_k^{\intercal}(i), \tag{38}$$

$$B_k(i) = 1+\mathbf{t}(i)\mathbf{i}_k^{\intercal}(i). \tag{39}$$

Now, we relax constraint C1 in (21) such that $0\le t_v(i)\le 1$, $0\le r_v(i)\le 1$, and $0\le t_v(i)+r_v(i)\le 1$, $\forall v$, respectively, and rewrite (21) as

$$\begin{aligned} &\underset{t(i),\forall i}{\text{Maximize:}}\ \lim_{T\to\infty}\frac{1}{T}\sum_{i=1}^{T}\sum_{k=1}^{N}\mu_k\log_2\left(1+\frac{A_k(i)}{B_k(i)}\right) \\ &\text{Subject to :} \\ &\qquad \text{C1}: 0\le t_v(i)\le 1,\ \forall v. \end{aligned} \tag{40}$$

Since the solutions of the relaxed convex problem is such that $t_v(i)$ takes the limiting values 0 or 1, and not the values between 0 and 1, the relaxed convex problem is equivalent to the original problem.

Using Proposition 1 in [35], we transform the objective

This article has been accepted for publication in a future issue of this journal, but has not been fully edited. Content may change prior to final publication. Citation information: DOI 10.1109/TWC.2020.3022990, IEEE Transactions on Wireless Communications

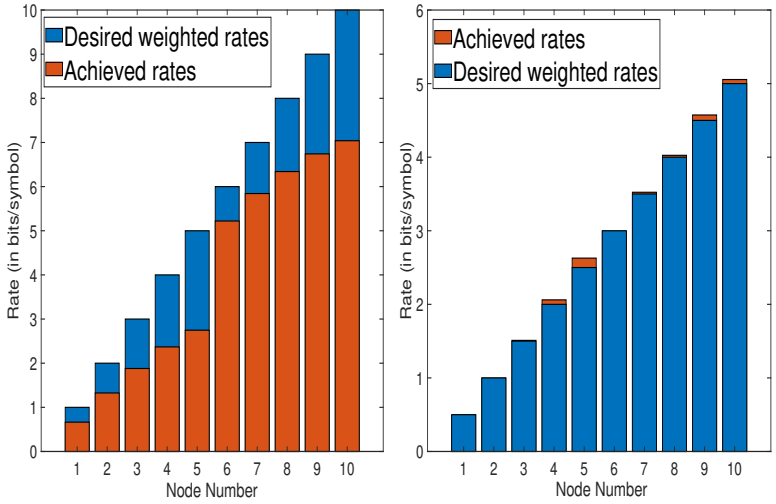

Fig. 6. Rate vs. node number of the proposed scheme applying rate allocation scheme with under-capacity data demand (right), and with over-capacity data demand (left), $P_j = 20$ dBm, $\forall j$. SI=110 dB, and ρ=1000 m.

function in (40) into an equivalent form as

$$\underset{t(i),w(i),\forall i}{\text{Maximize:}} \quad \lim_{T\to\infty}\frac{1}{T}\sum_{i=1}^{T}\sum_{k=1}^{N}\mu_k \log_2\left(\frac{|w_k(i)|^2}{|\sqrt{A_k(i)}-w_k(i)|^2+B_k(i)}\right)$$
$$\text{Subject to :}$$
$$\text{C1}: 0 \le t_v(i) \le 1, \ \forall v, \tag{41}$$

where the vector $\mathbf{w}(i) = \{w_1(i), w_2(i), ..., w_N(i)\}$ is a scaling factor vector, given by

$$w_k(i) = \frac{A_k(i)+B_k(i)}{\sqrt{A_k(i)}}. \tag{42}$$

It has been shown in Proposition 1 in [35] that the optimization problem in (41) is equivalent to the optimization problem in (40) when the scaling factor $\mathbf{w}(i)$ is optimized using (42), i.e., both (41) and (40) have the same global solution when $\mathbf{w}(i) = \mathbf{W^{opt}}(i)$ is selected optimally. When $\mathbf{w}(i)$ is obtained from (42), the optimization problem in (41) can be written as an optimization of $\mathbf{t}(i)$ as

$$\underset{t(i),\forall i}{\text{Maximize:}} \quad \lim_{T\to\infty}\frac{1}{T}\sum_{i=1}^{T}\sum_{k=1}^{N}\mu_k\Bigg(\log_2\left(|w_k^{opt}(i)|^2\right) - \log_2\left(|\sqrt{A_k(i)}-w_k^{opt}(i)|^2+B_k(i)\right)\Bigg)$$
$$\text{Subject to :}$$
$$\text{C1}: 0 \le t_v(i) \le 1, \ \forall v. \tag{43}$$

However, the optimization problem in (43) is still non-convex [36]. Hence, we define an additional scaling factors vector, $\mathbf{l}(i) = \{l_1(i), l_2(i), ..., l_N(i)\}$, and rewrite (43) as

$$\underset{t(i),l(i),\forall i}{\text{Maximize:}} \quad \lim_{T\to\infty}\frac{1}{T}\sum_{i=1}^{T}\sum_{k=1}^{N}\mu_k\Bigg(\log_2\left(|w_k^{opt}(i)|^2\right) + \log_2(l_k(i)) - \frac{l_k(i)}{\ln 2}\left(|\sqrt{A_k(i)}-w_k^{opt}(i)|^2+B_k(i)\right)\Bigg)$$
$$\text{Subject to :}$$
$$\text{C1}: 0 \le t_v(i) \le 1, \ \forall v, \tag{44}$$

where clearly (44) is a concave function of $\mathbf{l}(i)$. Furthermore, the optimum $\mathbf{l}(i)$ can be calculated by taking the derivative from the objective function in (44) with respect to $\mathbf{l}(i)$ and then setting the result to zero, which results in

$$l_k(i) = \frac{1}{\left(|\sqrt{A_k(i)}-w_k^{opt}(i)|^2+B_k(i)\right)}. \tag{45}$$

The optimization problem in (44) has the same solution as the main optimization problem in (43), when $\mathbf{w}(i)$ and $\mathbf{l}(i)$ are chosen using (42) and (45), respectively. As a result, our problem

This article has been accepted for publication in a future issue of this journal, but has not been fully edited. Content may change prior to final publication. Citation information: DOI 10.1109/TWC.2020.3022990, IEEE Transactions on Wireless Communications

now is

$$\underset{t(i),\forall i}{\text{Maximize:}} \lim_{T\to\infty}\frac{1}{T}\sum_{i=1}^{T}\sum_{k=1}^{N}\mu_k\Bigg(\log_2\left(|w_k^{opt}(i)|^2\right) + \log_2(l_k^{opt}(i)) - \frac{l_k^{opt}(i)}{\ln 2}\left(|\sqrt{A_k(i)}-w_k^{opt}(i)|^2+B_k(i)\right)\Bigg)$$

$$\text{Subject to :}\quad \text{C1}: 0\le t_v(i)\le 1,\ \forall v. \tag{46}$$

We now use the Lagrangian to solve (46). Thereby, we obtain

$$\mathcal{L}=\lim_{T\to\infty}\frac{1}{T}\sum_{i=1}^{T}\sum_{k=1}^{N}\frac{\mu_k l_k^{opt}(i)}{\ln 2}\left(|\sqrt{A_k(i)}-w_k^{opt}(i)|^2+B_k(i)\right) - \sum_{v=1}^{N}\lambda_1^v(i)t_v(i)-\sum_{v=1}^{N}\lambda_2^v(i)\left(1-t_v(i)\right), \tag{47}$$

where $\lambda_1^v(i)\ge 0$ and $\lambda_2^v(i)\ge 0$, $\forall v$, are the Lagrangian multipliers. By differentiating $\mathcal{L}$ in (47) with respect to $t_x(i)$, $\forall x$, we obtain

$$\frac{d\mathcal{L}}{dt_x(i)}=\sum_{k=1}^{N}\frac{\mu_k l_k^{opt}(i)}{\ln 2}\left[d_{x,k}(i)\left(1-\frac{w_k^{opt}(i)}{\sqrt{A_k(i)}}\right)+i_{x,k}(i)\right] - \lambda_1^x(i)+\lambda_2^x(i). \tag{48}$$

Finally, equivalenting the results in (48) to zero, $\frac{d\mathcal{L}}{dt_x(i)}=0$, gives us the necessary equations to acquire optimum $t_x(i)$, $\forall x$, as

$$\sum_{k=1}^{N}\frac{\mu_k l_k^{opt}(i)}{\ln 2}\left[d_{x,k}(i)\left(1-\frac{w_k^{opt}(i)}{\sqrt{A_k(i)}}\right)+i_{x,k}(i)\right] - \lambda_1^x(i)+\lambda_2^x(i)=0,\forall i. \tag{49}$$

Let's first see that $t_v(i)$ cannot take values between 0 and 1. Specifically, if $t_v(i)$ takes values between 0 and 1, then $\lambda_1^x(i)$ and $\lambda_2^x(i)$ in (49) have to satisfy $\lambda_1^x(i)=0$ and $\lambda_2^x(i)=0$ due to the complementary slackness in the KKT conditions. Now, if we set $\lambda_1^x(i)=0$ and $\lambda_2^x(i)=0$ in (49), the equality in (49) becomes

$$\sum_{k=1}^{N}\frac{\mu_k l_k^{opt}(i)}{\ln 2}\left[d_{x,k}(i)\left(1-\frac{w_k^{opt}(i)}{\sqrt{A_k(i)}}\right)+i_{x,k}(i)\right]=0,\forall i. \tag{50}$$

However, the above equality cannot hold $\forall i$ since the values of $d_{x,k}(i)$, $l_k^{opt}(i)$, $w_k^{opt}(i)$, $A_k(i)$, and $i_{x,k}(i)$ depend and change with the fading, and therefore it is impossible for these variables to take values such that the above equality holds $\forall i$. Hence, $t_v(i)$ can take the value 0 or the value 1, but not values between 0 and 1.

In order to find the condition for specifying the value of one or zero to each $t_x(i)$, $\forall x$, we set $t_x(i)=0$ in (49) which leads $\lambda_2^x(i)=0$ (by complementary slackness in KKT condition), as a result the condition for choosing $t_x(i)=0$ is acquired as

$$\sum_{k=1}^{N}\frac{\mu_k l_k^{opt}(i)}{\ln 2}\left[d_{x,k}(i)\left(1-\frac{w_k^{opt}(i)}{\sqrt{\sum_{v=1,v\neq x}^{N}t_v(i)d_{v,k}(i)}}\right)+i_{x,k}(i)\right]=\lambda_1^x(i),\forall v,i. \tag{51}$$

By knowing that $\lambda_1^x(i)\ge 0$, we obtain the optimal state selection scheme in Theorem 2. This completes the proof.

C. Proof of Theorem 3

The main diagonal elements of $\mathbf{G}(i)$ model the SI channel of each node. Hence, by setting the values of the main diagonal of $\mathbf{G}(i)$ to infinite, we make the simultaneous reception and transmissions for the FD nodes impossible to be selected and thereby make the FD nodes into HD nodes. As a result, in the proposed centralized D-TDD scheme in Algorithm 1, the nodes will either be transmitting, receiving, or be silent. Hence, the proposed scheme in Algorithm 1 is the optimal centralized D-TDD scheme for a wireless network comprised of HD nodes when the main diagonal of the $\mathbf{G}(i)$ are set to infinity.

REFERENCES

[1] M. M. Razlighi, N. Zlatanov, and P. Popovski, "Optimal centralized dynamic-TDD scheduling scheme for a general network of half-duplex nodes," in *Prof. IEEE Wireless Commun. Netw. Conf.*, Marrakech, Morocco, April 2019, pp. 1–6.

[2] H. Holma and A. Toskala, *LTE for UMTS: Evolution to LTE-Advanced*. Wiley, 2011.

[3] "Further Advancements for E-UTRA Physical Layer Aspects," Tech. Rep., document TR 36.814, Release 9, v9.0.0, 3GPP, Mar. 2010.

[4] T. Ding, M. Ding, G. Mao, Z. Lin, A. Y. Zomaya, and D. López-Pérez, "Performance analysis of dense small cell networks with dynamic TDD," *IEEE Trans. Veh. Technol.*, vol. 67, no. 10, pp. 9816–9830, Oct 2018.

[5] J. Liu, S. Han, W. Liu, and C. Yang, "The value of full-duplex for cellular networks: A hybrid duplex-based study," *IEEE Trans. Commun.*, vol. 65, no. 12, pp. 5559–5573, Dec 2017.

[6] M. Ding, D. López-Pérez, R. Xue, A. V. Vasilakos, and W. Chen, "On dynamic time-division-duplex transmissions for small-cell networks," *IEEE Trans. Veh. Technol.*, vol. 65, no. 11, pp. 8933–8951, Nov 2016.

[7] H. Haas and S. McLaughlin, "A dynamic channel assignment algorithm for a hybrid TDMA/CDMA-TDD interface using the novel ts-opposing technique," *IEEE J. Select. Areas Commun.*, vol. 19, no. 10, pp. 1831–1846, Oct 2001.

[8] F. R. V. Guimarães, G. Fodor, W. C. Freitas, and Y. C. B. Silva, "Pricing-based distributed beamforming for dynamic time division duplexing systems," *IEEE Trans. Veh. Technol.*, vol. 67, no. 4, pp. 3145–3157, April 2018.

[9] W. Jeong and M. Kavehrad, "Cochannel interference reduction in dynamic-TDD fixed wireless applications, using time slot allocation algorithms," *IEEE Trans. Commun.*, vol. 50, no. 10, pp. 1627–1636, Oct 2002.

[10] H. Sun, M. Wildemeersch, M. Sheng, and T. Q. S. Quek, "D2D enhanced heterogeneous cellular networks with dynamic TDD," *IEEE Trans. Wireless Commun.*, vol. 14, no. 8, pp. 4204–4218, Aug 2015.

[11] J. Li, A. Huang, H. Shan, H. H. Yang, and T. Q. S. Quek, "Analysis of packet throughput in small cell networks under clustered dynamic TDD," *IEEE Trans. Wireless Commun.*, vol. 17, no. 9, pp. 5729–5742, Sep. 2018.

[12] M. M. Razlighi, N. Zlatanov, and P. Popovski, "On distributed dynamic-TDD schemes for base stations with decoupled uplink-downlink transmissions," in *Prof. IEEE Int. Conf. on Commun. Workshops*, Kansas City, MO, USA, May 2018, pp. 1–6.

[13] E. de Olivindo Cavalcante, G. Fodor, Y. C. B. Silva, and W. C. Freitas, "Distributed beamforming in dynamic TDD MIMO networks with BS to BS interference constraints," *IEEE Wireless Commun. Lett.*, vol. 7, no. 5, pp. 788–791, Oct 2018.

[14] E. d. O. Cavalcante, G. Fodor, Y. C. B. Silva, and W. C. Freitas, "Bidirectional sum-power minimization beamforming in dynamic TDD MIMO networks," *IEEE Trans. Veh. Technol.*, vol. 68, no. 10, pp. 9988–10 002, Oct 2019.

[15] R. Yin, Z. Zhang, G. Yu, Y. Zhang, and Y. Xu, "Power allocation for relay-assisted TDD cellular system with dynamic frequency reuse," *IEEE Trans. Wireless Commun.*, vol. 11, no. 7, pp. 2424–2435, July 2012.

[16] G. Liu, F. Yu, H. Ji, V. Leung, and X. Li, "In-band full-duplex relaying: A survey, research issues and challenges," *IEEE Commun. Surveys Tutorials*, vol. 17, no. 2, pp. 500–524, Secondquarter 2015.

[17] A. A. Dowhuszko, O. Tirkkonen, J. Karjalainen, T. Henttonen, and J. Pirskanen, "A decentralized cooperative uplink/downlink adaptation scheme for TDD small cell networks," in *Prof. IEEE 24th Annu. Int. Symp. on Personal, Indoor, and Mobile Radio Commun.*, London, United Kingdom, Sept 2013, pp. 1682–1687.

[18] B. Yu, L. Yang, H. Ishii, and S. Mukherjee, "Dynamic TDD support in macrocell-assisted small cell architecture," *IEEE J. Select. Areas Commun.*, vol. 33, no. 6, pp. 1201–1213, June 2015.

[19] R. Veronesi, V. Tralli, J. Zander, and M. Zorzi, "Distributed dynamic resource allocation for multicell SDMA packet access net," *IEEE Trans. on Wireless Commun.*, vol. 5, no. 10, pp. 2772–2783, Oct 2006.

[20] I. Spyropoulos and J. R. Zeidler, "Supporting asymmetric traffic in a TDD/CDMA cellular network via interference-aware dynamic channel allocation and space-time LMMSE joint detection," *IEEE Trans. Veh. Technol.*, vol. 58, no. 2, pp. 744–759, Feb 2009.

[21] Y. Yu and G. B. Giannakis, "Opportunistic medium access for wireless networking adapted to decentralized CSI," *IEEE Trans. on Wireless Commun.*, vol. 5, no. 6, pp. 1445–1455, June 2006.

[22] V. Venkatasubramanian, M. Hesse, P. Marsch, and M. Maternia, "On the performance gain of flexible UL/DL TDD with centralized and decentralized resource allocation in dense 5G deployments," in *Prof. IEEE 25th Annu. Int. Symp. on Personal, Indoor, and Mobile Radio Commun.*, Washington, DC, USA, Sept 2014, pp. 1840–1845.

[23] R. Wang and V. K. N. Lau, "Robust optimal cross-layer designs for TDD-OFDMA systems with imperfect CSIT and unknown interference: State-space approach based on 1-bit ACK/NAK feedbacks," *IEEE Trans. on Commun.*, vol. 56, no. 5, pp. 754–761, May 2008.

[24] A. Łukowa and V. Venkatasubramanian, "Centralized UL/DL resource allocation for flexible TDD systems with interference cancellation," *IEEE Trans. Veh. Technol.*, vol. 68, no. 3, pp. 2443–2458, March 2019.

[25] E. Hossain and V. K. Bhargava, "Link-level traffic scheduling for providing predictive QoS in wireless multimedia networks," *IEEE Trans. on Mult.*, vol. 6, no. 1, pp. 199–217, Feb 2004.

[26] K. Lee, Y. Park, M. Na, H. Wang, and D. Hong, "Aligned reverse frame structure for interference mitigation in dynamic TDD systems," *IEEE Trans. Wireless Commun.*, vol. 16, no. 10, pp. 6967–6978, Oct 2017.

[27] P. Popovski, O. Simeone, J. J. Nielsen, and C. Stefanovic, "Interference spins: Scheduling of multiple interfering two-way wireless links," *IEEE Commun. Lett.*, vol. 19, no. 3, pp. 387–390, March 2015.

[28] S. Lagen, A. Agustin, and J. Vidal, "Joint user scheduling, precoder design, and transmit direction selection in MIMO TDD small cell networks," *IEEE Trans. Wireless Commun.*, vol. 16, no. 4, pp. 2434–2449, April 2017.

[29] S. Sekander, H. Tabassum, and E. Hossain, "Decoupled uplink-downlink user association in multi-tier full-duplex cellular networks: A two-sided matching game," *IEEE Trans. on Comput.*, vol. 16, no. 10, pp. 2778–2791, Oct 2017.

[30] S. Goyal, P. Liu, and S. S. Panwar, "User selection and power allocation in full-duplex multicell networks," *IEEE Trans. Veh. Technol.*, vol. 66, no. 3, pp. 2408–2422, March 2017.

[31] T. Cover and A. El Gamal, "Capacity theorems for the relay channel," *IEEE Trans. Inf. Theory*, vol. 25, pp. 572–584, Sep. 1979.

[32] V. R. Cadambe and S. A. Jafar, "Interference alignment and spatial degrees of freedom for the K user interference channel," in *Prof. IEEE Int. Conf. on Commun.*, Beijing · China, May 2008, pp. 971–975.

[33] C. T. Kelley, *Iterative Methods for Optimization*. Society for Industrial and Applied Mathematics, 1999. [Online]. Available: https://epubs.siam.org/doi/abs/10.1137/1.9781611970920

[34] D. Nguyen, L. N. Tran, P. Pirinen, and M. Latva-aho, "On the spectral efficiency of full-duplex small cell wireless systems," *IEEE Trans. Wireless Commun.*, vol. 13, no. 9, pp. 4896–4910, Sept 2014.

[35] H. Al-Shatri, X. Li, R. S. Ganesan, A. Klein, and T. Weber, "Maximizing the sum rate in cellular networks using multiconvex optimization," *IEEE Trans. Wireless Commun.*, vol. 15, no. 5, pp. 3199–3211, May 2016.

[36] J. Conway, *Functions of One Complex Variable*. Springer, 1978, vol. 1.

Mohsen Mohammadkhani Razlighi (S'17) was born in Tehran, Iran, in 1987. He received his B.S. degrees in electrical engineering from University of Zanjan in 2010, and M.S. degrees in Telecommunication engineering from Sharif University of Technology in 2012. Currently, he is working toward his Ph.D. degree at the Monash University, Melbourne, Australia. His research interests include information theory, and machine learning and wireless communications.

Nikola Zlatanov (S'06, M'15) was born in Macedonia. He received the Dipl.Ing. and Master degree in electrical engineering from Ss. Cyril and Methodius University, Skopje, Macedonia in 2007 and 2010, respectively, and his PhD degree from the University of British Columbia (UBC) in Vancouver, Canada in 2015. He is currently a Lecturer (US equivalent to Assistant Professor) in the Department of Electrical and Computer Systems Engineering (ECSE) at Monash University in Melbourne, Australia. His current research interests include wireless communications, information theory, and machine learning. Dr. Zlatanov received several scholarships/awards/grants for his work including UBC's Four Year Doctoral Fellowship in 2010, UBC's Killam Doctoral Scholarship and Macedonia's Young Scientist of the Year in 2011, the Vanier Canada Graduate Scholarship in 2012, best journal paper award from the German Information Technology Society (ITG) in 2014, best conference paper award at ICNC in 2016, ARC Discovery Project and ARC Discovery Early Career Researcher Award in 2018.

Shiva Raj Pokhrel (M'19) is a Lecturer of Mobile Computing at Deakin University, Geelong, Australia. He received the B.E./M.E. degree in 2007/2013 from Pokhara University, Nepal and PhD degree in 2017 from Swinburne University of Technology, Australia. He was a research fellow at the University of Melbourne and a network engineer at Nepal Telecom (2007-2014). His research interests include multi-connectivity, machine learning, industry 4.0 automation, blockchain modeling, optimization, recommender systems, 6G, cloud computing, dynamics control, Internet of Things and and cyber-physical systems as well as their applications in smart manufacturing, autonomous vehicles and cities. He serves/served as the Workshop Chair/Publicity Co-Chair for several IEEE/ACM conferences including IEEE INFOCOM, IEEE GLOBECOM, IEEE ICC, ACM MobiCom, and more. He was a recipient of the prestigious Marie Skłodowska-Curie grant Fellowship in 2017.

Petar Popovski (S'97,A'98,M'04,SM'10,F'16) is a Professor Aalborg University, where he heads the research section on Connectivity. He received his Dipl.-Ing and M. Sc. degrees in communication engineering from the University of Sts. Cyril and Methodius in Skopje and the Ph.D. degree from Aalborg University in 2005. He is a Fellow of the IEEE. He received an ERC Consolidator Grant (2015), the Danish Elite Researcher award (2016), IEEE Fred W. Ellersick prize (2016), IEEE Stephen O. Rice prize (2018) and Technical Achievement Award from the IEEE Technical Committee on Smart Grid Communications (2019). He is currently a Member at Large at the Board of Governors in IEEE Communication Society. Prof. Popovski is a Steering Committee Member of IEEE SmartGridComm and IEEE TRANSACTIONS ON GREEN COMMUNICATIONS AND NETWORKING. He previously served as a Steering Committee Member of the IEEE INTERNET OF THINGS JOURNAL. He is currently an Area Editor of the IEEE TRANSACTIONS ON WIRELESS COMMUNICATIONS. Prof. Popovski was the General Chair for IEEE SmartGridComm 2018 and IEEE Communication Theory Workshop 2019. His research interests are in the area of wireless communication and communication theory.

Chapter 5

Conclusion and Future Works

In this chapter, we provide conclusions, and we discuss selected future works.

5.1 Conclusion

The contribution of this thesis chapters to the optimal adaptive reception-transmission scheduling in general networks is as following:

- In Chapter 2 , we proposed three buffer-aided relaying schemes with adaptive reception-transmission at the FD relay for the two-hop FD relay channel with SI for the cases of continuous-rate transmission with adaptive-power allocation, continuous-rate transmission with fixed-power allocation, and discrete-rate transmission, respectively. The proposed schemes is expected to be used in the deployment of FD relays which would provide support to HD BSs. In particular, the idea is to deploy FD relays around HD BSs, which will relay information from the HD BSs to users that are at significant distances from the base stations.
- In Chapter 3, we proposed a distributed D-TFDD scheme for unknown ICI. Using the proposed D-TFDD scheme, in a given frequency band, the BS adaptively selects to either communicate with U1 or with U2 in a given time slot based on the qualities of the BS-U1 and BS-U2 channels without ICI knowledge such that the BS-U1 and BS-U2 throughput region is maximized.

In particular, this invention can help flexible physical layer design for 5G networks.

- In Chapter 4, we devised the optimal centralized D-TDD scheme for a wireless network comprised of K FD and/or HD nodes, which maximizes the rate region of the network. The proposed centralized D-TDD scheme makes an optimal decision of which node should receive, transmit, simultaneously receive and transmit, or be silent in each time slot. In addition, we proposed a rate allocation scheme that allocates data rates to the nodes according to the user data demands. Knowing the performance of the optimal centralized D-TDD scheme is highly valuable since it serves as an upper bound and thus an (unattainable) benchmark for any practical TDD scheme.

5.2 Future Works

Some of the research directions are listed below:

- Chapter 3 investigates a distributed resource scheduling scheme, and Chapter 4 investigates a centralized resource scheduling scheme. This means there is room for a research to come up with a combined solution to take advantage of both schemes. This can be done by having edge processing in order to decrease the amount of information to be exchanged by the central node.

- Work in Chapter 4 does not include nodes with interference alignment capability, and it is interesting to investigate a case where the nodes also can align themselves relative to interference.

Bibliography

[1] T. Cover and A. El Gamal, "Capacity theorems for the relay channel," *IEEE Trans. Inf. Theory*, vol. 25, pp. 572–584, Sep. 1979. → page 2

[2] N. Zlatanov, V. Jamali, and R. Schober, "On the capacity of the two-hop half-duplex relay channel," in *Proc. of the IEEE Global Telecomm. Conf. (Globecom)*, San Diego, Dec. 2015. → page 2

[3] A. Host-Madsen and J. Zhang, "Capacity bounds and power allocation for wireless relay channels," *IEEE Trans. Inf. Theory*, vol. 51, pp. 2020 –2040, Jun. 2005. → page 2

[4] N. Zlatanov, R. Schober, and P. Popovski, "Buffer-aided relaying with adaptive link selection," *IEEE J. Select. Areas Commun.*, vol. 31, no. 8, pp. 1530–1542, Aug. 2013. → page 2

[5] S. M. Kim and M. Bengtsson, "Virtual full-duplex buffer-aided relaying in the presence of inter-relay interference," *IEEE Trans. Wireless Commun.*, vol. 15, no. 4, pp. 2966–2980, April 2016. → page 2

[6] N. Zlatanov, E. Sippel, V. Jamali, and R. Schober, "Capacity of the gaussian two-hop full-duplex relay channel with residual self-interference," *IEEE Trans. on Commun.*, vol. 65, no. 3, pp. 1005–1021, March 2017. → page 2

[7] H. Holma and A. Toskala, *LTE for UMTS: Evolution to LTE-Advanced*. Wiley, 2011. → page 3

[8] "Further advancements for E-UTRA physical layer aspects," Tech. Rep., document TR 36.814, Release 9, v9.0.0, 3GPP, Mar. 2010. → page 3

[9] A. K. Gupta, M. N. Kulkarni, E. Visotsky, F. W. Vook, A. Ghosh, J. G. Andrews, and R. W. Heath, "Rate analysis and feasibility of dynamic TDD in 5G cellular systems," in *2016 IEEE Int. Conf. on Commun. (ICC)*, May 2016, pp. 1–6. → page 3

[10] Z. Shen, A. Khoryaev, E. Eriksson, and X. Pan, "Dynamic uplink-downlink configuration and interference management in TD-LTE," *IEEE Commun. Mag.*, vol. 50, no. 11, pp. 51–59, November 2012. → pages 3, 5

[11] S. Adireddy and L. Tong, "Exploiting decentralized channel state information for random access," *IEEE Transactions on Information Theory*, vol. 51, no. 2, pp. 537–561, Feb 2005. → page 3

[12] S. Lagen, A. Agustin, and J. Vidal, "Joint user scheduling, precoder design, and transmit direction selection in mimo tdd small cell networks," *IEEE Transactions on Wireless Communications*, vol. 16, no. 4, pp. 2434–2449, April 2017. → pages 3, 5

[13] K. Lee, Y. Park, M. Na, H. Wang, and D. Hong, "Aligned reverse frame structure for interference mitigation in dynamic tdd systems," *IEEE Transactions on Wireless Communications*, vol. 16, no. 10, pp. 6967–6978, Oct 2017. → pages 3, 5

[14] H. Haas and S. McLaughlin, "A dynamic channel assignment algorithm for a hybrid tdma/cdma-tdd interface using the novel ts-opposing technique," *IEEE Journal on Selected Areas in Communications*, vol. 19, no. 10, pp. 1831–1846, Oct 2001.

[15] C. Yoon and D. H. Cho, "Energy efficient beamforming and power allocation in dynamic tdd based c-ran system," *IEEE Communications Letters*, vol. 19, no. 10, pp. 1806–1809, Oct 2015.

[16] P. Popovski, O. Simeone, J. J. Nielsen, and C. Stefanovic, "Interference spins: Scheduling of multiple interfering two-way wireless links," *IEEE Communications Letters*, vol. 19, no. 3, pp. 387–390, March 2015. → page 5

[17] K. Sivarajah and H. S. Al-Raweshidy, "Dynamic channel allocation for ongoing calls in utra tdd system," *Electronics Letters*, vol. 40, no. 19, pp. 1197–1198, Sept 2004.

[18] C. H. Chiang, W. Liao, T. Liu, I. K. Chan, and H. L. Chao, "Adaptive downlink and uplink channel split ratio determination for tcp-based best effort traffic in tdd-based wimax networks," *IEEE Journal on Selected Areas in Communications*, vol. 27, no. 2, pp. 182–190, February 2009.

[19] J. Huang, K. Qi, Z. Xu, and C. Yang, "Hybrid full and half duplex networking," in *2016 IEEE/CIC International Conference on Communications in China (ICCC)*, July 2016, pp. 1–6.

[20] J. Liu, S. Han, W. Liu, and C. Yang, "The value of full-duplex for cellular networks: A hybrid duplex-based study," *IEEE Transactions on Communications*, vol. 65, no. 12, pp. 5559–5573, Dec 2017.

[21] S. Goyal, P. Liu, and S. S. Panwar, "User selection and power allocation in full-duplex multicell networks," *IEEE Transactions on Vehicular Technology*, vol. 66, no. 3, pp. 2408–2422, March 2017. → page 5

[22] K. Smiljkovikj, P. Popovski, and L. Gavrilovska, "Analysis of the decoupled access for downlink and uplink in wireless heterogeneous networks," *IEEE Wireless Commun. Lett.*, vol. 4, no. 2, pp. 173–176, April 2015. → page 3

[23] *Key Technologies for 5G Wireless Systems*. Cambridge University Press, 2017. → page 4

[24] B. Yu, S. Mukherjee, H. Ishii, and L. Yang, "Dynamic tdd support in the lte-b enhanced local area architecture," in *2012 IEEE Globecom Workshops*, Dec 2012, pp. 585–591. → page 5

[25] A. A. Dowhuszko, O. Tirkkonen, J. Karjalainen, T. Henttonen, and J. Pirskanen, "A decentralized cooperative uplink/downlink adaptation scheme for tdd small cell networks," in *2013 IEEE 24th Annual International Symposium on Personal, Indoor, and Mobile Radio Communications (PIMRC)*, Sept 2013, pp. 1682–1687.

[26] M. S. ElBamby, M. Bennis, W. Saad, and M. Latva-aho, "Dynamic uplink-downlink optimization in tdd-based small cell networks," in *2014 11th International Symposium on Wireless Communications Systems (ISWCS)*, Aug 2014, pp. 939–944.

[27] D. Zhu and M. Lei, "Cluster-based dynamic dl/ul reconfiguration method in centralized ran tdd with trellis exploration algorithm," in *2013 IEEE Wireless Communications and Networking Conference (WCNC)*, April 2013, pp. 3758–3763.

[28] V. Venkatasubramanian, M. Hesse, P. Marsch, and M. Maternia, "On the performance gain of flexible ul/dl tdd with centralized and decentralized resource allocation in dense 5g deployments," in *2014 IEEE 25th Annual International Symposium on Personal, Indoor, and Mobile Radio Communication (PIMRC)*, Sep. 2014, pp. 1840–1845. → page 5

[29] A. Łukowa and V. Venkatasubramanian, "Centralized ul/dl resource allocation for flexible tdd systems with interference cancellation," *IEEE*

Transactions on Vehicular Technology, vol. 68, no. 3, pp. 2443–2458, March 2019. → page 5

[30] E. Hossain and V. K. Bhargava, "Link-level traffic scheduling for providing predictive qos in wireless multimedia networks," *IEEE Transactions on Multimedia*, vol. 6, no. 1, pp. 199–217, Feb 2004.

[31] E. d. O. Cavalcante, G. Fodor, Y. C. B. Silva, and W. C. Freitas, "Bidirectional sum-power minimization beamforming in dynamic tdd mimo networks," *IEEE Transactions on Vehicular Technology*, vol. 68, no. 10, pp. 9988–10 002, Oct 2019. → page 5

[32] S. Sekander, H. Tabassum, and E. Hossain, "Decoupled uplink-downlink user association in multi-tier full-duplex cellular networks: A two-sided matching game," *IEEE Transactions on Mobile Computing*, vol. 16, no. 10, pp. 2778–2791, Oct 2017. → page 5